International Standard

ISO 10828

First edition
2024-04

Worm gears — Worm profiles and gear mesh geometry

Engrenage à vis cylindriques — Géométrie des profils de vis et de l'engrènement

Reference number
ISO 10828:2024(en)

ISO copyright office
CP 401 • Ch. de Blandonnet 8
CH-1214 Vernier, Geneva
Phone: +41 22 749 01 11
Email: copyright@iso.org
Website: www.iso.org

Published in Switzerland

Contents

Page

Foreword

ISO (the International Organization for Standardization) is a worldwide federation of national standards bodies (ISO member bodies). The work of preparing International Standards is normally carried out through ISO technical committees. Each member body interested in a subject for which a technical committee has been established has the right to be represented on that committee. International organizations, governmental and non-governmental, in liaison with ISO, also take part in the work. ISO collaborates closely with the International Electrotechnical Commission (IEC) on all matters of electrotechnical standardization.

The procedures used to develop this document and those intended for its further maintenance are described in the ISO/IEC Directives, Part 1. In particular, the different approval criteria needed for the different types of ISO document should be noted. This document was drafted in accordance with the editorial rules of the ISO/IEC Directives, Part 2 (see www.iso.org/directives).

ISO draws attention to the possibility that the implementation of this document may involve the use of (a) patent(s). ISO takes no position concerning the evidence, validity or applicability of any claimed patent rights in respect thereof. As of the date of publication of this document, ISO had not received notice of (a) patent(s) which may be required to implement this document. However, implementers are cautioned that this may not represent the latest information, which may be obtained from the patent database available at www.iso.org/patents. ISO shall not be held responsible for identifying any or all such patent rights.

Any trade name used in this document is information given for the convenience of users and does not constitute an endorsement.

For an explanation of the voluntary nature of standards, the meaning of ISO specific terms and expressions related to conformity assessment, as well as information about ISO's adherence to the World Trade Organization (WTO) principles in the Technical Barriers to Trade (TBT), see www.iso.org/iso/foreword.html.

This document was prepared by Technical Committee ISO/TC 60, *Gears,* Subcommittee SC 1, *Nomenclature and wormgearing*.

This first edition of ISO 10828 cancels and replaces the second edition of ISO/TR 10828:2015.

The main changes are as follows:

— conversion from a Technical Report to an International Standard and implementation of necessary editorial changes;

— incorporation of a new Annex H on interface for geometry for involute worms defined as cylindrical gear with ISO 21771-1.

Any feedback or questions on this document should be directed to the user's national standards body. A complete listing of these bodies can be found at www.iso.org/members.html

Introduction

This document includes the formulation for the geometrical dimensions of the worm and worm wheel, and that for the determination of gear mesh geometry (path of contact, zone and lines of contact) with the details to determine the non-dimensional parameters used to apply load capacity calculations (radius of curvature, sliding velocities). Thread forms of the worms of worm gear pairs are commonly related to the following machining processes:

— the type of machining process (turning, milling, grinding, metal forming);

— the shapes of edges or surfaces of the cutting tools used;

— the tool position relative to an axial plane of the worm;

— where relevant, the diameters of disc type tools (grinding wheel diameter).

The calculations developed in this document are relatively complex as they involved primary and secondary derivatives of mathematical expression. In order to facilitate the writing of equations, the numerators in the left part of formulae are often omitted; this is why several formulae have special symbols and are not written in a mathematical way:

Example in Formula (B.12) $\frac{d}{dy_G}\alpha_G(y_G)$ is written $\mathrm{d}\alpha_G(y_G)$

Example in Formula (B.14) $\frac{d^2}{dy_G{}^2}\alpha_G(y_G)$ is written $\mathrm{d}2\alpha_G(y_G)$

In this document, the figures show a generic representation of worm profile types A, I, N, K, C. For the influence of different worm profile types, see Annex E.

This document introduces all the aspects concerning the gear mesh geometry to define conjugate worm wheel, path of contact, lines of contact and other associated geometrical characteristics.

Worm gears — Worm profiles and gear mesh geometry

1 Scope

This document describes the thread profiles of the five most common worm profile types and provides formulae of their axial profiles.

The five worm profile types covered in this document are designated by the letters A, C, I, K and N.

This document provides the formulae to calculate the path of contact, the conjugate profile of the worm wheel, the lines of contact, the radius of curvature and the velocities at points of contact. The application of those formulae to calculate parameters used in load capacity calculations are provided in 11.11.

2 Normative references

The following documents are referred to in the text in such a way that some or all of their content constitutes requirements of this document. For dated references, only the edition cited applies. For undated references, the latest edition of the referenced document (including any amendments) applies.

ISO 701, *International gear notation — Symbols for geometrical data*

ISO 1122-2, *Vocabulary of gear terms — Part 2: Definitions related to worm gear geometry*

3 Terms and definitions

For the purposes of this document, the terms and definitions given in ISO 701 and ISO 1122-2 and the following apply.

ISO and IEC maintain terminology databases for use in standardization at the following addresses:

— ISO Online browsing platform: available at https://www.iso.org/obp

— IEC Electropedia: available at https://www.electropedia.org/

3.1
mid plane of worm wheel
plane perpendicular to its datum axis containing the centre of virtual major torus radius generating tooth flanks

Note 1 to entry: See Figure 26.

Note 2 to entry: It can be axially located by measuring the position of inflection point along the helix of the cylinder of the worm wheel defined by the measurement diameter for worm wheel. In hobbed worm wheel, the number of flutes can influence the tooth flank surface and consequently the mid plane detection.

3.2
axial plane of worm
plane containing the line of axis of the worm defined by its datum axis

Note 1 to entry: Diameters can be measured in this plane, but thread surfaces would require a theoretical sharpened edge measurement probe or correction in order to keep the contact point between the probe and the flank in this plane.

4 Symbols and abbreviated terms

Table 1 to Table 3 provide the symbols, the indices and the descriptions used in this document.

NOTE First and second derivatives symbols are not listed in Table 1 and Table 2.

Table 1 — Symbols for worm gears

Symbols	Description	Units	Figure numbers	Formula numbers
A	distance from the worm axis to virtual point of the cutter (see Reference [4])	mm	A.4	—
a	centre distance	mm	5	42 and 43
a_0	refers to the worm/tool centre distance (length of the common perpendicular to the worm/tool axes)	mm	22	55
a_1 to a_4	coefficients for A, I and N profile	—		See Table 5
b_1	facewidth of worm	mm		24
b_{2H}	effective wheel facewidth	mm	5	40
b_{2R}	wheel rim width	mm	5	—
$b_{\phi 2}$	face end chamfer depth	mm	5	—
c_1,c_2	tip clearance	mm	—	47 and 48
d_{a1}	worm tip diameter	mm	1	14
d_{a2}	worm wheel tip diameter	mm	4	36
d_{b1}	base diameter of involute helicoid (for profile type I)	mm	—	22
d_{e2}	worm wheel outside diameter	mm	—	38
d_{e2max}	maximum worm wheel outside diameter	mm	—	39
d_{e2min}	minimum worm wheel outside diameter	mm	—	38
d_{f1}	worm root diameter	mm	1	15
d_{f2}	worm wheel root diameter	mm	4	35
d_{Fa1}	worm tip form diameter	mm	3	—
d_{Fa2}	worm wheel tip form diameter	mm	6	—
d_{Ff1}	worm root form diameter	mm	3	—
d_{Ff2}	worm wheel root form diameter	mm	6	—
d_{m1}	worm reference diameter	mm	1	10
d_{m2}	worm wheel reference diameter	mm	4	25
d_{Na1}	active worm tip form diameter	mm	6	—
d_{Na2}	active worm wheel tip form diameter	mm	6	—
d_{Nf1}	active worm root form diameter	mm	6	—
d_{Nf2}	active worm wheel root form diameter	mm	6	—
d_{w1}	worm pitch diameter	mm	—	45
d_{w2}	worm wheel pitch diameter	mm	7	44
e_{mx1}	worm reference tooth space width in axial section	mm	1	17
e_{n1}	worm normal tooth space width in normal section	mm	—	19
e_{m2}	worm wheel tooth space width in mid plane section	mm	—	28
h_1	worm tooth depth	mm	1	11
h_2	worm wheel tooth depth	mm	—	33
h_{am1}	worm tooth reference addendum in axial section	mm	1	12
h_{am2}	worm wheel tooth reference addendum in mid plane section	mm	5	31
h^*_{am1}	worm tooth reference addendum coefficient in axial section	—	—	31

Table 1 *(continued)*

Symbols	Description	Units	Figure numbers	Formula numbers
h^*_{am2}	worm wheel tooth reference addendum coefficient in mid plane section	—	—	32
h_{e2}	worm wheel tooth external addendum	mm	—	34
h_{fm1}	worm tooth reference dedendum in axial section	mm	1	13
h_{fm2}	worm wheel tooth reference dedendum in mid plane section	mm	—	32
h^*_{fm1}	worm tooth reference dedendum coefficient in axial section	—	1	13
h^*_{fm2}	worm wheel tooth reference dedendum coefficient in mid plane section	—	—	32
h_{k1}	radial height of chamfer (of worm)	mm	3	—
h_{k2}	radial height of chamfer (of worm wheel)	mm	7	—
j_x	axial backlash	mm	—	28
m_n	normal module	mm	—	9
m_{x1}	axial module	mm	—	2 and G.1
n_1	rotational speed of the worm	rpm	—	144
p_{bn1}	normal pitch on base cylinder (for profile type I)	mm	—	23
p_{n1}	normal pitch	mm	—	8
p_{t2}	transverse pitch	mm	—	27
p_{x1}	axial pitch	mm	1	1
p_{z1}	lead (of worm)	mm	—	3
p_{zu1}	unit lead (lead of worm per radian)	mm/rd	—	4
q_1	diameter quotient	mm	—	5
R_{Ga}	outside radius of the grinding wheel (for profile type C and K)	mm	22	—
R_{Gm}	nominal or mean radius of the grinding wheel (for profile type C and K)	mm	22	56
r_{g2}	worm wheel throat form radius	mm	5	41
r_{b1}	base radius for involute profile (for profile type I)	mm	A.4 and A.5	22
r'_{b1}	base radius of a notional base circle (for profile type N)	mm	A.4 and A.5	—
r_{k1}	tip radius (of worm)	mm	3	—
r_{k2}	tip radius (of worm wheel)	mm	7	—
r_T	radius at cusp	mm	34	—
s_{m2}	tooth thickness at the reference diameter of the worm wheel	mm	4	28
s_K	rim thickness	mm	16	—
s_{mx1}	worm thread thickness in axial section	mm	1	16
s^*_{mx1}	worm thread thickness in axial section coefficient	—	—	—
s_{n1}	normal worm thread thickness in normal section	mm	—	18
u	gear ratio	—	—	46
x_2	worm wheel profile shift coefficient	—	—	30
x_{Gm}	thickness of grinding wheel at nominal radius	mm	22 and B.2	B.9
z_1	number of threads in worm	—	—	—
z_2	number of teeth in worm wheel	—	—	—
α_{0n}	tool normal pressure angle	°		20
α_{0t}	tool transverse pressure angle for profile types A and I	°		20
α_n	normal pressure angle	°	—	20
β_{m1}	reference helix angle of worm	°	—	7

Table 1 *(continued)*

Symbols	Description	Units	Figure numbers	Formula numbers
γ_{m1}	reference lead angle of worm	°	—	6
γ_{b1}	base lead angle of worm thread (for profile type I)	°	A.1	21
γ'_{b1}	base lead angle of the notional base helix (for profile type N)	°	A.4 and A.5	—
ϕ_2	face end chamfer angle	°	5	—
ρ_{Gm}	radius of curvature of grinding wheel (for profile type C)	—	—	—
ω_{w1}	angular velocity of the worm	rad/s	—	144
ω_{w2}	angular velocity of the worm wheel	rad/s	—	146

In calculation, when a radius is derived, the symbol *d* for diameter shall be replaced by *r* for radius.

Table 2 — Subscripts for worm gears

Symbols	Description
0	cutting tool
1	worm
2	wheel
G	grinding wheel

Table 3 — Coordinate of remarkable points (units are mm for length and degrees for angles)

Symbols	Description	Figure numbers	Formula numbers
$\vec{b_D}(y_p, D)$	normal vector to an offset plane	—	140
c_1, $c_2(y_G)$, $c_3(y_G)$, $\varepsilon(y_G)$	parameters to determine generated point by the grinding wheel	—	59 to 62
$x_G(y_G)$, y_G, $\alpha_G(y_G)$	coordinates of a point on the tool flank when the origin is at the point of intersection of the tool axis and the tool median plane, with the x-axis as the tool spindle axis and the abscissa on the trace of the median plane for profile C and K	22	Table 8
$x_x(y_r)$, $y_x(y_r)$, $\alpha_x(y_r)$	coordinates of axial profile and axial pressure angle for A, I, N worm profiles	25	49, 50, 54
$x_x(y_G)$, $y_x(y_G)$, $\alpha_x(y_G)$	coordinates of axial profile and axial pressure angle for K and C worm profiles	25	67, 68, 78
$x_D(y_p, D)$, $y_D(y_p, D)$, $\alpha_D(y_p, D)$, $\delta_D(y_p, D)$	coordinates of worm profile and pressure angle of worm profile in an offset plane, projection angle from axial profile	27	80, 81, 82, 86
$x'_D(y_p, D)$, $y_{lD}(y_p, D)$	coordinates of worm profile with origin at pitch point	27	90, 81, 82
$x_{lD}(y_p, D)$, $y_{lD}(y_p, D)$	coordinates of path of contact in an offset plane with origin on pitch axis	27	91, 92
$xR_D(y_p, D)$, $yR_D(y_p, D)$ $r_{M2D}(y_p, D)$, $\vartheta_D(y_p, D)$	coordinates of conjugate worm wheel profile of the worm in an offset plane with origin on worm wheel axis and polar coordinates	29	96, 97
$xT_D(r_{t2D}, D)$, $yT_D(r_{t2D}, D)$	coordinates of trochoid profile of the worm wheel profile in an offset plane with origin on worm wheel axis	30	101, 102
$x_D(ycusp, D)$, $y_D(ycusp, D)$	coordinates of cusp point in an offset plane with origin on pitch axis	—	—
$C_{eq1D}(y_p, D)$	curvature for the worm at a point in an offset plane	—	103, 110

Table 3 *(continued)*

Symbols	Description	Figure numbers	Formula numbers
$C_{eq2D}(y_p, D)$	curvature for the worm wheel at a point in an offset plane	31	111
$R_{eqD}(y_p, D)$	equivalent radius of curvature in an offset plane	—	113
$r_{a2D}(D)$	radius of worm wheel conjugate to point B, tip of the worm profile in the offset plane D	28 and 34	10.6.2
$r_{e2D}(D)$	outside radius of the worm wheel in the offset plane D	—	98
$r_{f2D}(D)$	root radius of the worm wheel in the offset plane D	—	99
$r_{wD}(D)$	radius of cylinder crossing the pitch point of in an offset plane D	—	87
$\overrightarrow{M_1(y_p, D)}$	coordinate of a point of contact for the worm	—	126
$\overrightarrow{M_2(y_p, D)}$	coordinate of a point of contact for the worm wheel	—	127, 149
$\overrightarrow{TN1_{cont}(y_p, D)}$	tangent unit vector to conjugate profile in the offset plane D	—	134
$\overrightarrow{n_D(y_p, D)}$	normal vector to the worm and worm wheel profile in an offset plane	—	139
$\overrightarrow{\text{Normal}Nxy(y_p, D)}$	normal unit vector to the lines of contact at common point of contact	—	124
$\overrightarrow{\text{NORMAL}(y_p, D)}$	normal unit vector to the lines of contact	—	122
$\text{Req}(y_p, D)$, $\text{Req}_1(y_p, D)$	radius of curvature along the line the contact	—	143, 141
$\overrightarrow{TD1(y_p, D)}$, $\overrightarrow{TD2(y_p, D)}$	normalized unit vectors of the common tangent plane at point of contact between the tooth flanks	—	117, 121
$\overrightarrow{t_D(y_p, D)}$	tangent vector to the worm and worm wheel profile in an offset plane	—	138
$\overrightarrow{V_1(y_p, D)}$	velocity of a point of the thread of the worm	—	146
$\overrightarrow{V_2(y_p, D)}$	velocity of a point of the tooth flank of the worm wheel	—	150
$V_{cDn}(y_p, D)$	velocity at the contact point along the path of contact	—	160
$V_{SUMn}(y_p, D)$	sum of velocities at the point of contact for method B in ISO/TS 14521:2020	—	163
$\delta_{DI}(D)$	angle of the projection of the pitch point of the offset plane D in the axial plane	°	88
$\Delta x_D(D)$	axial translation for the projection of the pitch point of the offset plane D in the axial plane	—	89
$\overrightarrow{\omega_1}$	angular velocity vector of the worm	—	145
$\overrightarrow{\omega_2}$	angular velocity vector of the worm wheel	—	148

5 Formulae for calculation of dimensions

5.1 Parameters for a cylindrical worm

5.1.1 Axial pitch

Axial pitch is given by Formula (1), (see Figure 1):

$$p_{x1} = \pi \cdot m_{x1} \tag{1}$$

5.1.2 Axial module

Axial module is given by Formula (2):

$$m_{x1} = \frac{p_{x1}}{\pi} \tag{2}$$

5.1.3 Lead

Lead is given by Formula (3), (see Figure 1):

$$p_{z1} = z_1 \cdot p_{x1} \tag{3}$$

5.1.4 Unit lead

Unit lead is given by Formula (4):

$$p_{zu1} = \frac{p_{z1}}{2 \cdot \pi} \tag{4}$$

5.1.5 Diameter quotient

Diameter quotient is given by Formula (5):

$$q_1 = \frac{d_{m1}}{m_{x1}} \tag{5}$$

5.1.6 Reference lead angle

Reference angle is given by Formula (6):

$$\tan \gamma_{m1} = \frac{m_{x1} \cdot z_1}{d_{m1}} = \frac{z_1}{q_1} \tag{6}$$

5.1.7 Reference helix angle

Reference helix angle is given by Formula (7):

$$\beta_{m1} = 90° - \gamma_{m1} \tag{7}$$

5.1.8 Normal pitch on reference cylinder

Normal pitch on reference cylinder is given by Formula (8):

$$p_{n1} = p_{x1} \cdot \cos \gamma_{m1} \tag{8}$$

5.1.9 Normal module

Normal module is given by Formula (9):

$$m_n = m_{x1} \cdot \cos\gamma_{m1} \tag{9}$$

5.1.10 Reference diameter

Reference diameter given by Formula (10):

$$d_{m1} = q_1 \cdot m_{x1} \tag{10}$$

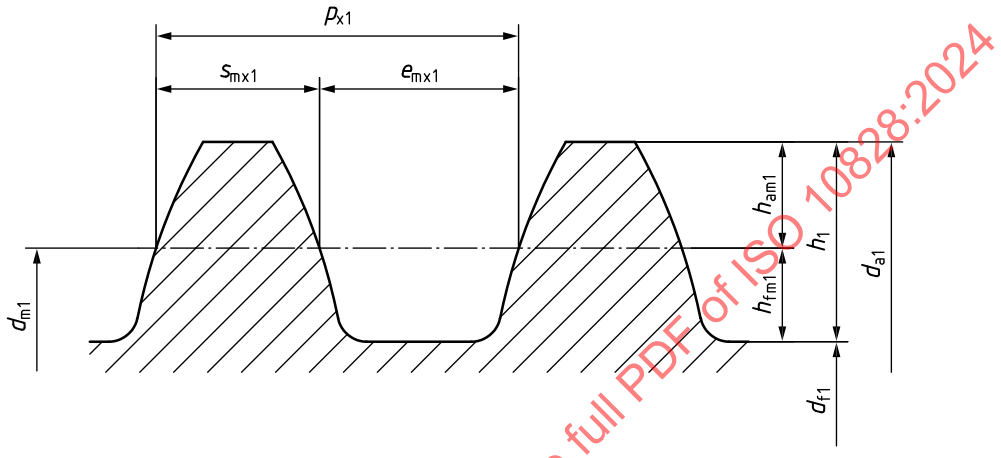

Figure 1 — Axial parameters for worm

5.1.11 Reference tooth depth

Reference tooth depth is given by Formula (11), (see Figure 1):

$$h_1 = h_{am1} + h_{fm1} = \frac{1}{2} \cdot (d_{a1} - d_{f1}) \tag{11}$$

5.1.12 Reference addendum

Reference addendum is given by Formula (12), (see Figure 1):

$$h_{am1} = h^*_{am1} \cdot m_{x1} = \frac{1}{2} \cdot (d_{a1} - d_{m1}) \tag{12}$$

where h^*_{am1} is the addendum coefficient; normally $h^*_{am1} = 1$.

5.1.13 Reference dedendum

Reference dedendum is given by Formula (13), (see Figure 1):

$$h_{fm1} = h^*_{fm1} \cdot m_{x1} = \frac{1}{2} \cdot (d_{m1} - d_{f1}) \tag{13}$$

where h^*_{fm1} = dedendum coefficient; generally, 1,1 < h^*_{fm1} < 1,3, the recommended value is 1,2.

5.1.14 Tip diameter

Tip diameter is given by Formula (14), (see Figure 1):

$$d_{a1} = d_{m1} + 2 \cdot h_{am1} \tag{14}$$

5.1.15 Root diameter

Root diameter is given by Formula (15), (see Figure 1):

$$d_{f1} = d_{m1} - 2 \cdot h_{fm1} \tag{15}$$

5.1.16 Thread thickness coefficient s^*_{mx1}

A recommended value is $s^*_{mx1} = 0{,}5$

In general practice, this coefficient is very often less than 0,5 when there is a wish to increase the worm wheel thread thickness to extend durability against wear of worm wheel.

5.1.17 Reference thread thickness in the axial section

Reference thread thickness in the axial section is given by Formula (16), (see Figure 1):

$$s_{mx1} = s^*_{mx1} \cdot p_{x1} \tag{16}$$

5.1.18 Reference space width in the axial section

Reference space width in the axial section is given by Formula (17), (see Figure 1):

$$e_{mx1} = p_{x1} - s_{mx1} \tag{17}$$

5.1.19 Normal thread thickness

Normal thread thickness is given by Formula (18):

$$s_{n1} = s_{mx1} \cdot \cos\gamma_{m1} \tag{18}$$

5.1.20 Normal space width

Normal space width is given by Formula (19):

$$e_{n1} = e_{mx1} \cdot \cos\gamma_{m1} \tag{19}$$

5.1.21 Profile flank form

It is specified by a letter:

A is the envelope of straight line in the axial section;

N is the envelope of straight line in the normal section of the space width;

I is the involute helicoid (the envelope of straight line in a plane tangent to the base cylinder);

K is a milled helicoid by double cone form;

C is a milled helicoid by circular convex form.

5.1.22 Normal pressure angle

For A worm profile type:

Normal pressure angle is given by Formula (20):

$$\tan\alpha_{\mathrm{n}} = \tan\alpha_{0\mathrm{t}} \cdot \cos\gamma_{\mathrm{m1}} \tag{20}$$

For other worm profile types, $\alpha_{\mathrm{n}} = \alpha_{0\mathrm{n}}$ where $\alpha_{0\mathrm{n}}$ is defined in 7.3 for I worm profile type, in 7.4 for N worm profile type, in 7.6 for K worm profile type and 7.7 for C worm profile type.

5.1.23 Base lead angle for profile type I

Base lead angle for profile type is given by Formula (21):

$$\cos\gamma_{\mathrm{b1}} = \cos\gamma_{\mathrm{m1}} \cdot \cos\alpha_{0\mathrm{n}} \tag{21}$$

5.1.24 Base diameter for profile type I

Base diameter for profile type is given by Formula (22):

$$d_{\mathrm{b1}} = d_{\mathrm{m1}} \cdot \frac{\tan\gamma_{\mathrm{m1}}}{\tan\gamma_{\mathrm{b1}}} = \frac{m_{\mathrm{x1}} \cdot z_1}{\tan\gamma_{\mathrm{b1}}} \tag{22}$$

For profile type I, when the root diameter is lower than the base diameter, the diameter of start of active profile (SAP) shall be greater than d_{b1}.

5.1.25 Normal pitch on base cylinder

Normal pitch on base cylinder is given by Formula (23):

$$p_{\mathrm{bn1}} = p_{\mathrm{x1}} \cdot \cos\gamma_{\mathrm{b1}} \tag{23}$$

5.1.26 Worm face width

Worm face width is given by Formula (24):

$$b_1 \geq \sqrt{(d_{e2})^2 - (2 \cdot a - d_{\mathrm{a1}})^2} \tag{24}$$

5.1.27 Right-hand helix and left-hand helix

The flank direction is right-handed if the flank line describes a right-hand helix and left-handed if the flank line describes a left-hand helix. See Figure 2.

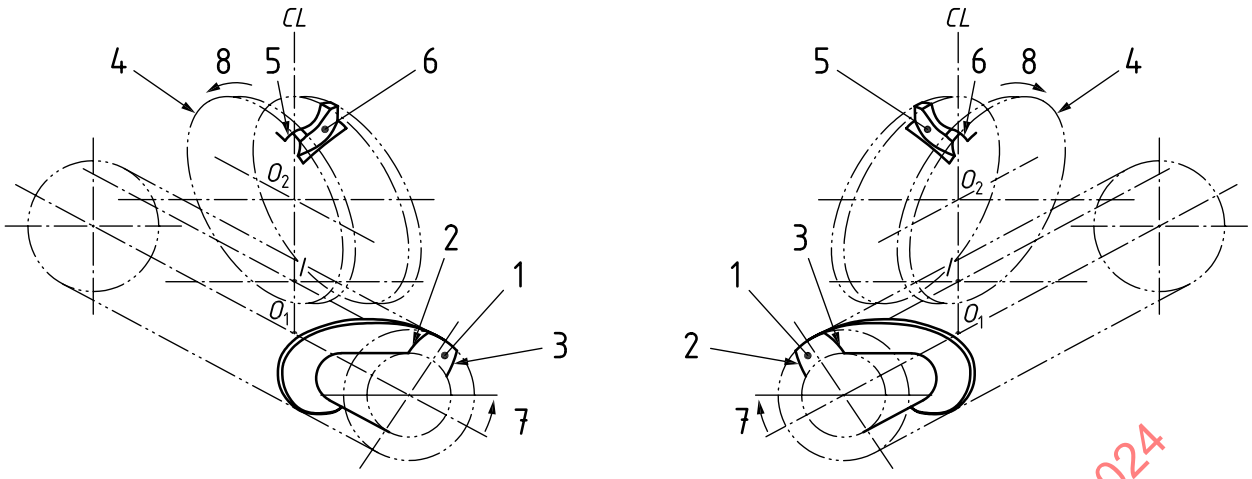

a) Left-hand worm gear set **b) Right-hand worm gear set**

Key

1	selected reference face of worm	5	left flank (LF) of worm wheel
2	left flank (LF) of worm	6	right flank (RF) of worm wheel
3	right flank (RF) of worm	7	rotating direction of worm wheel
4	selected reference face of worm wheel	8	rotating direction of worm

Figure 2 — Direction of helix and flank conventions

5.1.28 Right flank and left flank

The right flank (or left flank) is the tooth flank that an observer sees on the right-hand (or left-hand) side when viewing the selected reference face of a tooth when it is pointing upwards. This definition applies to both worms and worm wheels, see Figure 2.

Right flank parameters are indicated by the subscript R and left flank parameters by the subscript L.

5.1.29 Flank definition

The flank direction is right-handed if the flank line describes a right-hand helix and left-handed if the flank line describes a left-hand helix. See Figure 9.

5.1.30 Root form and tip form diameter for worm

The root form diameter, d_{Ff1}, is the start of the portion of the worm profile (A, I, N, K, or C). For a worm, it is the diameter of the intersection of the flank with the root fillet or root radius (taking into account undercut if necessary). See Figure 3.

The tip form diameter is d_{Fa1}, is the end of the portion of the worm profile (A, I, N, K, or C). For a worm, it is the diameter of the intersection of the flank with the tip chamfer or tip radius when existing.

With direct transition between the nominal helicoid profile and the top land of the tooth, the tip form diameter is equal to the tip diameter (d_{Fa1}=d_{a1}). In the case of tip rounding or tip chamfering, tip form diameter and tip diameter differ by double the height of chamfer or rounding h_{k1} then to study gear mesh geometry in Clauses 10 and 11, tip diameter d_{a1} shall be replaced by form diameter d_{Fa1}.

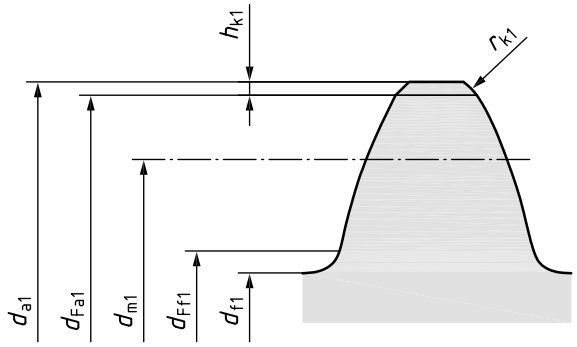

Figure 3 — Root form and tip form diameter for worm

5.2 Parameters for a worm wheel

5.2.1 General

Figure 4 shows parameters for worm wheel and Figure 7 shows pitch and reference diameters for worm gear set.

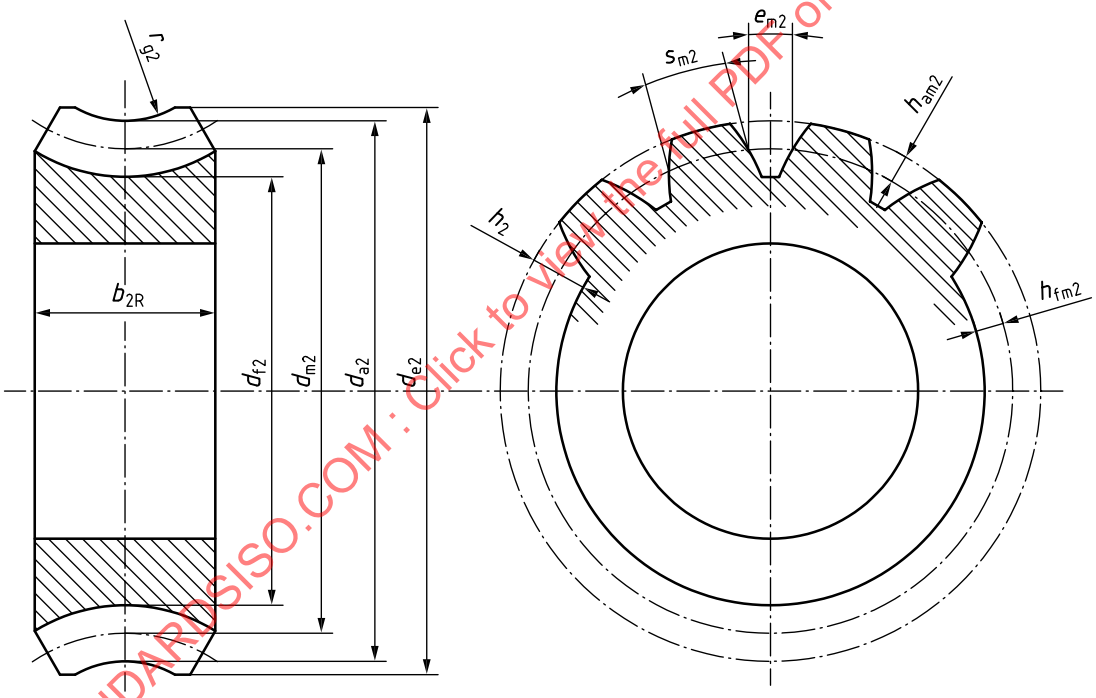

Figure 4 — Parameters for worm wheel

5.2.2 Reference diameter

Reference diameter is given by Formulae (25) and (26), (see Figures 4 and 5):

$$d_{m2} = d_{w2} + 2 \cdot x_2 \cdot m_{x1} \tag{25}$$

or

$$d_{m2} = 2 \cdot a - d_{m1} \tag{26}$$

5.2.3 Transverse pitch

Transverse pitch is given by Formula (27):

$$p_{t2} = p_{x1} \tag{27}$$

5.2.4 Transverse tooth thickness at reference diameter

This value can be calculated only for a worm wheel without profile shift from Formula (28), (see Figure 4):

$$s_{m2} = e_{mx1} - j_x \tag{28}$$

where j_x = axial backlash.

5.2.5 Space width at reference diameter

This value can be calculated only for a worm wheel without profile shift from Formula (29), (see Figure 4):

$$e_{m2} = p_{x1} - s_{m2} \tag{29}$$

5.2.6 Profile shift coefficient

Profile shift coefficient is given by Formula (30), (see Figure 6):

$$x_2 = \frac{2 \cdot a - d_{m1} - m_{x1} \cdot z_2}{2 \cdot m_{x1}} \tag{30}$$

5.2.7 Tooth reference addendum

Tooth reference addendum is given by Formula (31):

$$h_{am2} = m_{x1} \cdot h^*_{am2} = \frac{1}{2} \cdot (d_{a2} - d_{m2}) \tag{31}$$

where h^*_{am2} is the tooth reference addendum coefficient; h^*_{am2} = 1 (normally).

5.2.8 Tooth reference dedendum

Tooth reference dedendum is given by Formula (32):

$$h_{fm2} = m_{x1} \cdot h^*_{fm2} = \frac{1}{2} \cdot (d_{m2} - d_{f2}) \tag{32}$$

where h^*_{fm2} is the tooth reference dedendum coefficient; generally 1,1 < h^*_{fm2} < 1,3, the recommended value is 1,2.

5.2.9 Tooth depth

Tooth depth is given by Formula (33):

$$h_2 = h_{am2} + h_{fm2} \tag{33}$$

5.2.10 Outside addendum

Outside addendum is given by Formula (34), (see Figure 4):

$$h_{e2} = \frac{1}{2} \cdot (d_{e2} - d_{a2}) \tag{34}$$

Generally: $0,4 \leq \frac{h_{e2}}{m_{x1}} \leq 1,5$ Normally $h_{e2} / m_{x1} = 0,5$

5.2.11 Root diameter

Root diameter is given by Formula (35), (see Figure 4):

$$d_{f2} = d_{m2} - 2 \cdot h_{fm2} \tag{35}$$

5.2.12 Tip diameter

Tip diameter is given by Formula (36), (see Figure 4):

$$d_{a2} = d_{m2} + 2 \cdot h_{am2} \tag{36}$$

5.2.13 Outside diameter

Outside diameter is given by Formula (37), (see Figure 4):

$$d_{e2} = d_{a2} + 2 \cdot h_{e2} \tag{37}$$

NOTE For min/max values see 5.2.14.

5.2.14 Minimum and maximum outside diameter

Generally, minimum and maximum outside diameters are given by Formulae (38) and (39):

$$d_{e2min} = d_{a2} + 0,8 \cdot m_{x1} \tag{38}$$

$$d_{e2max} = d_{a2} + 3 \cdot m_{x1} \tag{39}$$

5.2.15 Worm wheel face width

Worm wheel face width is given by Formula (40), (see Figures 4 and 6):

$$b_{2H} \leq \sqrt{(2 \cdot a - d_{f2})^2 - (2 \cdot a - d_{e2})^2} \tag{40}$$

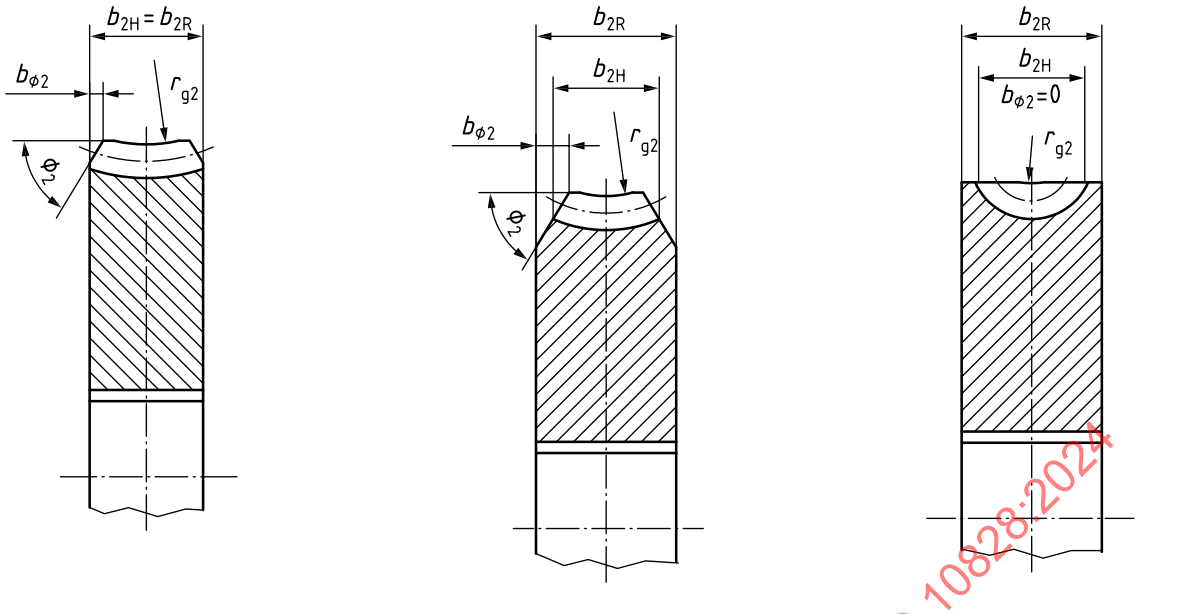

a) Worm wheel with full face width limited by face/lateral chamfers

b) Worm wheel with full face larger than tooth face width

c) Worm wheel with full face without face/lateral chamfer

NOTE c) represents the geometrical conditions where b_{2H} reaches its maximum value.

Figure 5 — Worm wheel face width

5.2.16 Throat form radius

Throat form radius is given by Formula (41), (see Figure 4):

$$r_{g2} \geq a - \frac{d_{a2}}{2} \tag{41}$$

5.2.17 Root form and tip diameter for worm wheel

The root form diameter, d_{Ff2}, is the start of the portion of the worm wheel conjugate to worm profile type (A, I, N, K or C). For a worm wheel, it is the diameter of the intersection of the flank with the root fillet or trochoid (considering undercut if necessary). See Figure 5.

The tip form diameter is d_{Fa2}, is the end of the portion of the worm wheel conjugate to worm profile type (A, I, N, K or C). For a worm wheel, it is the diameter of the intersection of the flank with the tip chamfer or tip radius when existing.

With direct transition between the worm wheel conjugate flank to worm profile type and the top land of the tooth, the tip form diameter is equal to the tip diameter (d_{Fa2}=d_{a2}). In the case of tip rounding or tip chamfering, tip form diameter and tip diameter differ by double the height of chamfer or rounding; h_{k2}, then to study gear mesh geometry in Clauses 10 and 11, tip diameter d_{a2} shall be replaced by form diameter d_{Fa2}.

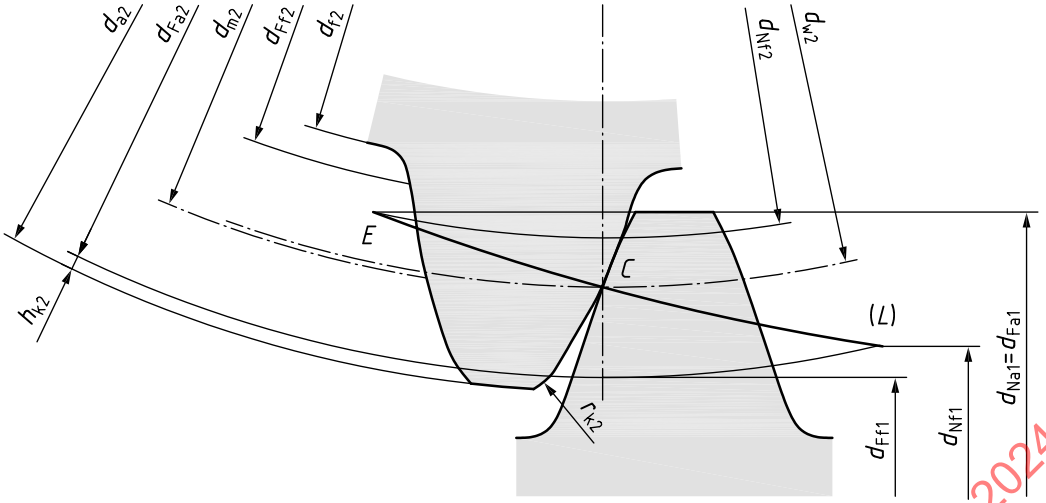

Key

(*L*) path of contact
C pitch point
E end point of meshing

Figure 6 — Root form and tip form diameter for worm wheel

5.3 Meshing parameters

5.3.1 Centre distance

Centre distance is given by Formulae (42) or (43), (see Figure 7):

$$a = 0{,}5 \cdot (d_{m1} + d_{m2}) = 0{,}5 \cdot (d_{w1} + d_{w2}) \tag{42}$$

NOTE In case of crossed axis gear composed of two involute cylindrical helical gears with parameters defined according to ISO 21771-1:—[1], Annex H provides an interface to convert those parameters with the convention used in this document.

or

$$a = m_{x1} \cdot [0{,}5 \cdot (q_1 + z_2) + x_2] \tag{43}$$

1) Under preparation. Stage at the time of publication: ISO/DIS 21771-1.2:2024.

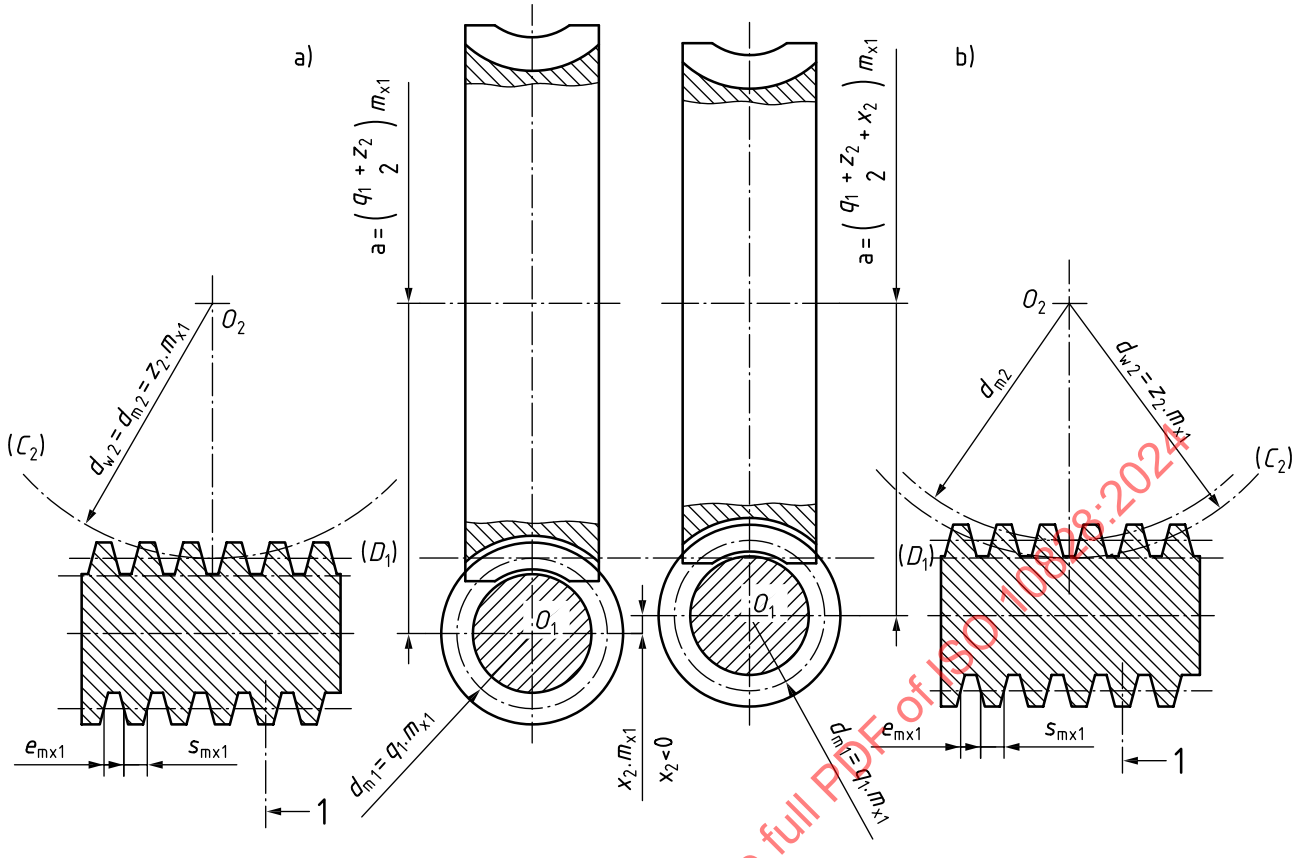

Key

1 symmetrical axis of the thread

NOTE 1 The profile shift coefficient x_2 is negative.

NOTE 2 On both parts a) and b), the worm is the same. On part a) (left), the profile shift coefficient equal zero and on part b) (right) the profile shift coefficient is negative.

Figure 7 — Pitch and reference diameters for worm gear set

5.3.2 Pitch diameter of worm wheel

Pitch diameter of worm wheel is given by Formula (44), (see Figure 7):

$$d_{w2} = z_2 \cdot m_{x1} \tag{44}$$

5.3.3 Pitch diameter of worm

Pitch diameter of worm is given by Formula (45), (see Figure 7):

$$d_{w1} = 2 \cdot a - d_{w2} \tag{45}$$

5.3.4 Worm gear ratio

Worm gear ration is given by Formula (46):

$$u = \frac{z_2}{z_1} \tag{46}$$

5.3.5 Contact ratio

The calculation of the contact ratio is defined in 11.6.

5.3.6 Tip clearance

Tip clearances are given by Formulae (47) and (48):

$$c_1 = a - 0{,}5 \cdot (d_{a2} + d_{f1}) \tag{47}$$

$$c_2 = a - 0{,}5 \cdot (d_{a1} + d_{f2}) \tag{48}$$

5.3.7 Start of active profile (SAP) and end of active profile (EAP) diameters for worm and worm wheel

In a defined gear pair, the active tip diameter, d_{Na}, of a gear can be governed either by its tip form diameter, d_{Fa} or by the start of conjugate profile of its mate (i.e. d_{Nf} or d_{Ff}). The SAP, (active root) diameter, d_{Nf}, can be governed either by the diameter of start of the portion of the worm profile type (A, I, N, K or C) or by the tip form diameter of its mate. The active area of the flank extends from the active tip diameter to the active root diameter and so is dependent on the characteristics of both gears and the centre distance. See Figure 8.

NOTE In some cases (e.g. low-pressure angle) the conjugate action of profiles can be limited by a cusp (see point E in Figure 8). In such case, the active lengths of profile are shortened; the EAP is below the tip form diameter of the worm and the SAP on the worm wheel is above the usual one (see Figure 8 and 10.6.3).

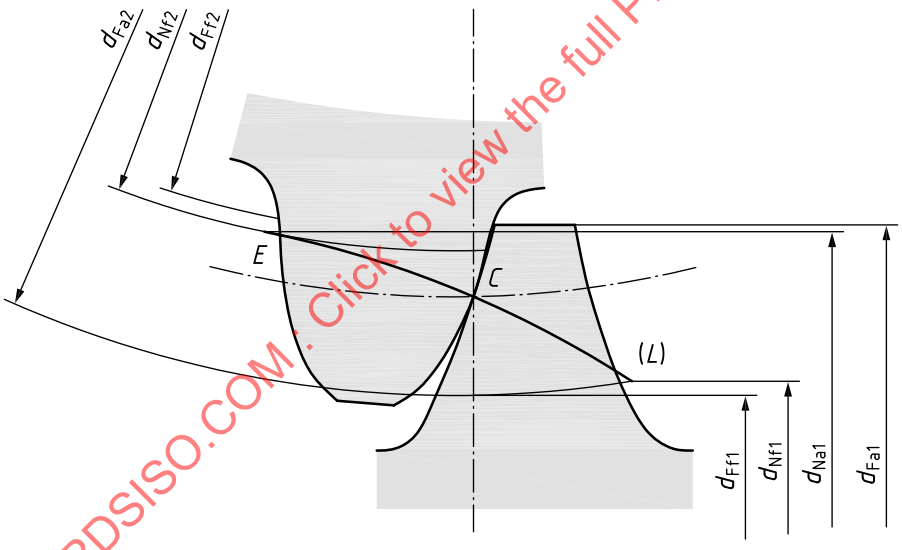

Key

(L) path of contact
C pitch point
E end point of meshing

Figure 8 — Diameters and worm wheel evaluation height for profile in mid plane

6 Generalities on worm profile types

6.1 Worm profile types, see Table 4

Table 4 — Worm profile types

Profile type	Description
A Profile type	straight sided axial profile
C Profile type	concave axial profile formed by machining with a convex circular profile disc type cutter or grinding wheel
I Profile type	involute helicoid, straight generatrix in base tangent planes
N Profile type	straight profiles in normal plane of thread space width helix
K Profile type	milled helicoid generated by biconical grinding wheel or milling cutter, convex profiles in axial planes

6.2 Conventions relative to the formulae of this document

6.2.1 The worm threads are right-handed.

The formulae in this document define the coordinates of the flank of the axial profile of worm, located on the left when looking in the plane XOY of Figure 9. This is the right flank of the worm according to Figure 2.

A symmetric profile to the right flank relative to a perpendicular axis to the worm axis shall be drawn to obtain the left flank.

6.2.2 The worm and wheel pairs operate as speed reducing gears with directions of rotation as shown in Figure 9, thus the worm thread right flanks contact the wheel tooth left flanks. These are the flanks studied in this report.

6.2.3 The worm wheel is above the worm.

6.2.4 With the origin O, the reference axes X Y Z, are mutually perpendicular (see Figure 9):

— OX the worm axis coincides with the X axis;

— OY the common perpendicular to the worm and wheel axes coincides with the Y axis;

— OZ to complete the direct coordinate system.

A point is defined by its x, y, z coordinates. The following subscripts are used:

— x refers to the X-Y axial plane;

— D refers to an offset plane;

— n refers to the normal plane;

— t refers to a transverse plane.

6.2.5 If the worm is driving, the worm gear set is a reducer. If the worm wheel is driving, the worm gear set is an increaser.

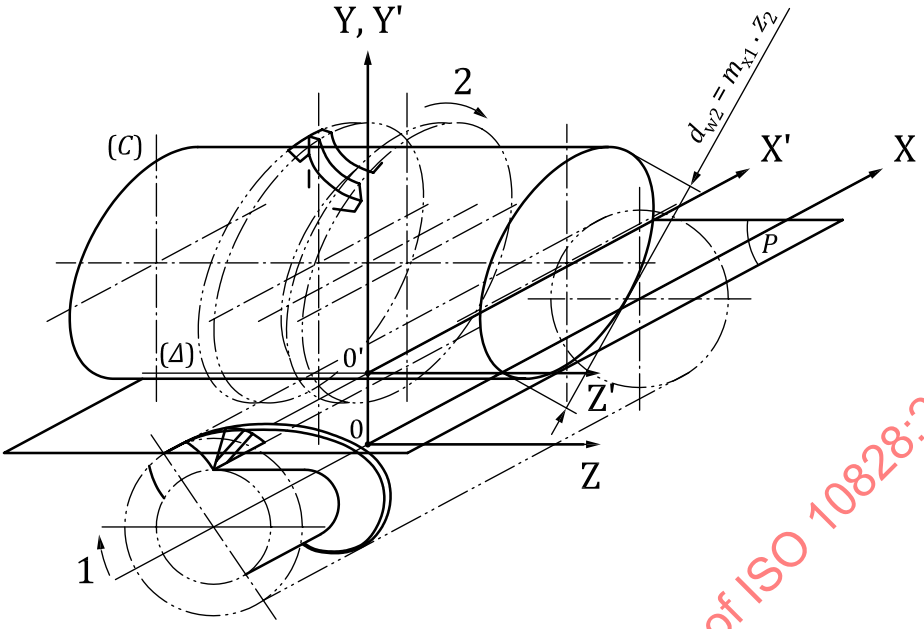

Key

1 direction of rotation of the worm

2 direction of rotation of the worm wheel

(Δ) pitch axis – common tangent between pitch surfaces of worm and worm wheel

(C) pitch cylinder of the worm wheel – diameter d_{w2}

P pitch plane of the worm – distance from the axis of the worm equal to $d_{w1}/2$

NOTE For the clarity of drawing, only one thread for worm is represented.

Figure 9 — Conventions used in formulae

7 Definition of profile types

7.1 General

There are two kinds of worm profile types:

— Profile types A, I, N are generated by a helical movement of a straight line in the space. The formulae of the axial profile are a direct function according to the radius of the worm. In that case, gear mesh in an offset plane uses two parameters: y_r which is the radius of the worm and D which is the distance of the offset plane.

— Profile types K and C are generated by a helical movement of a grinding wheel with a certain profile (see Figure 22) in the space. The generated flanks on the worm are the envelope of the grinding wheel. Each point of the worm profile is generated by a point of the grinding wheel. The formulae of the axial profile are not a direct function according to the radius of the grinding wheel profile. In that case, gear mesh in an offset plane uses two parameters: y_r which is the radius of the grinding wheel and D which is the distance of the offset plane. In those cases, the calculations are more complex.

The differences between these five profile types are shown in Annex D. In complement, Annex G provides an informative calculation method to link the main geometric parameters of the gear set with the tooling parameters.

7.2 A worm profile type

7.2.1 Geometrical definition

The worm flanks with A profile type are generated as envelopes of straight lines in axial planes which are inclined at a constant angle: $\frac{\grave{A}}{2} - \alpha_{ot}$ to the axis (see Figure 10). This line as it is moved with simultaneous rotation about and translation along the axis X, defines the worm thread flank (see Figure 10). The form of which is commonly described as an Archimedean helix.

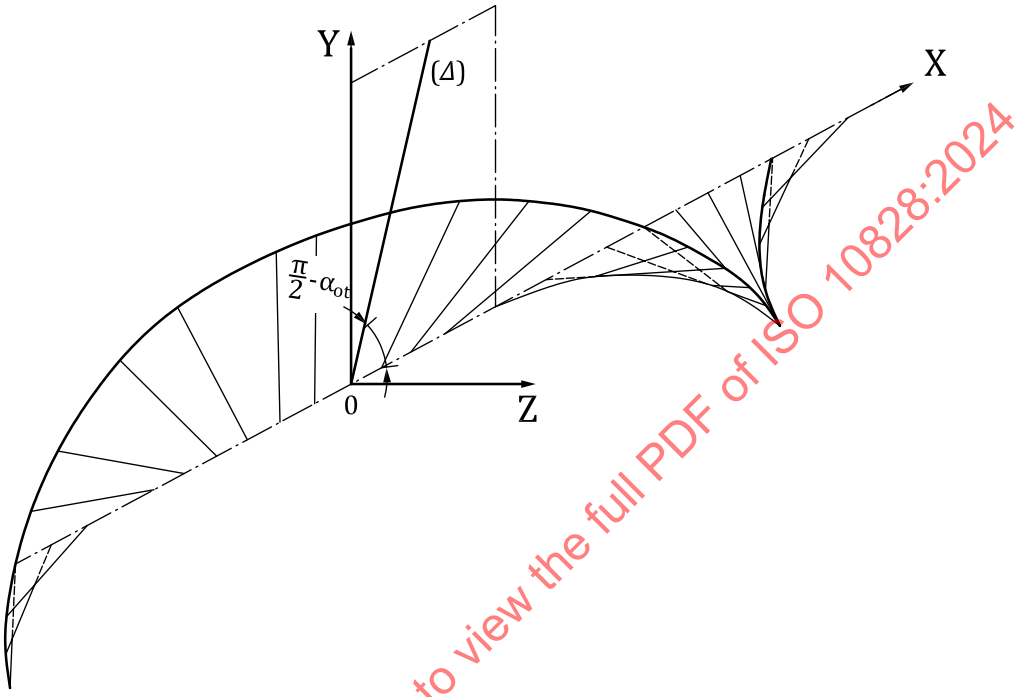

Figure 10 — A Profile type - Theoretical generation

7.2.2 Machining methods

The straight generatrix is always crossing the worm axis; the flank of thread in an axial plane is always a straight line; so machining methods should ensure to generate this straight axial flank.

The threads can be cut on a lathe with a tool having straight edges, the cutting plane of which lies in an axial plane of the worm [see Figure 11 a)].

Both flanks of a thread space can be machined simultaneously by using a tool of trapezoidal form.

Another method, which is an inversion of the process of cutting a helical gear with a rack cutter, involves the use of an involute shaper to produce the desired rectilinear rack profile in an axial plane of the worm. The cutting face shall lie in that axial plane [see Figure 11 b)].

The pitch circle of the shaper shall roll without slip on the datum line of the rack profile. This coincides with a straight line generatrix of the worm pitch cylinder.

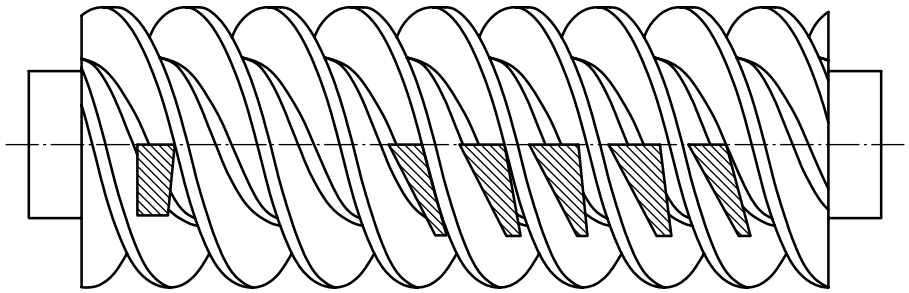

a) Profile type A generation by two methods

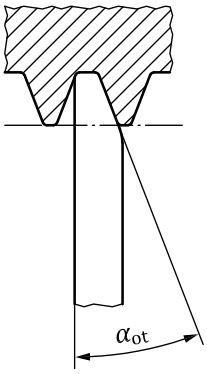

b) Partial projection view in axial plane of the worm of tool of trapezoidal form

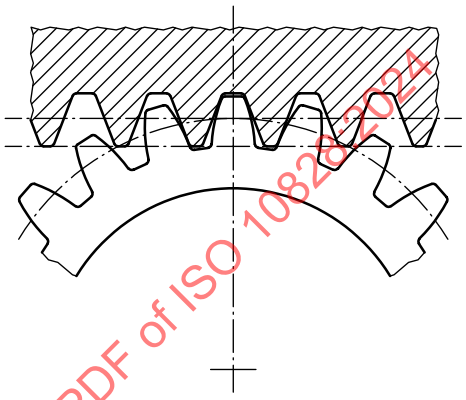

c) Partial projection view in axial plane of the worm of involute shaper

Figure 11 — A Profile type - Machining methods

An A Profile type is equivalent to a straight line in an axial plane.

The development of the formulae for the axial profile of A worm profile type is shown in Annex A, A.2.

7.3 I worm profile type

7.3.1 Geometrical definition

The worm flank with I profile type is an involute helicoidal surface. The form of which can be generated by a line (Δ) which is tangent to the base helix (H) lying on the base cylinder of the worm, and is moving along (H). (H) is concentric with the worm axis (see Figure 12).

A transverse profile (in a normal plane to the worm axis) of a flank is an involute to a circle.

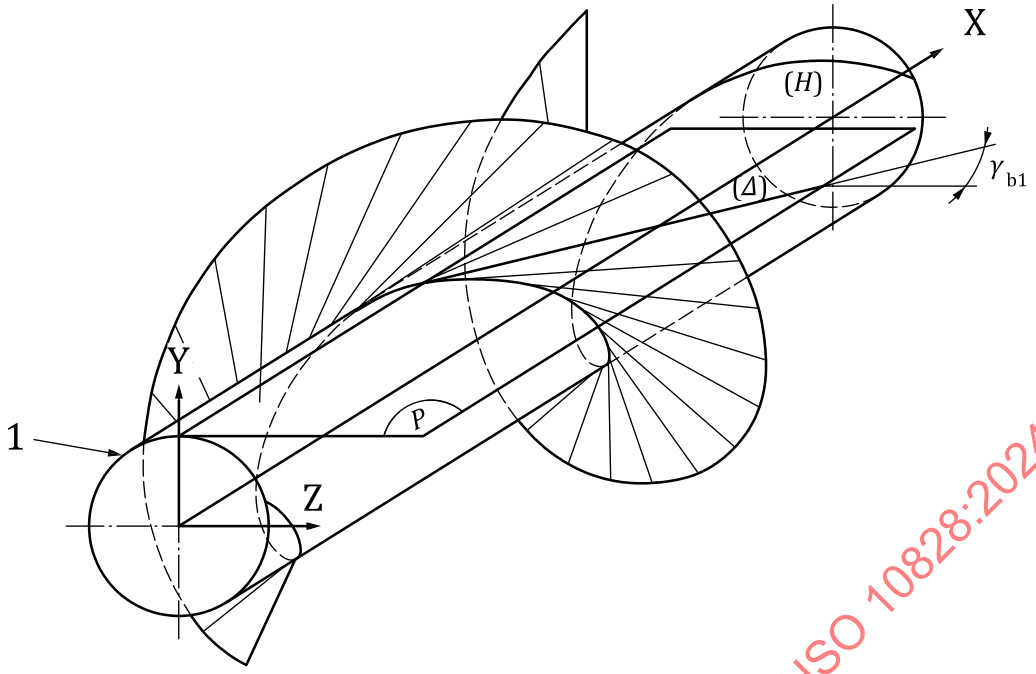

Key

1 base cylinder of the worm

Figure 12 — I Profile type - Theoretical generation

7.3.2 Machining methods

The straight generatrix is always tangential to the base helix in a plane which is tangential to the base cylinder, so the flank of the worm is a straight line in an offset plane which is tangential to the base cylinder. Machining methods should ensure this straight offset profile.

The involute helicoidal flanks of the threads can be generated by turning on a lathe using a knife tool with its straight edge aligned with the base tangent generatrix in a plane tangential to the base cylinder.

In order to machine both flanks of a thread simultaneously, one left hand tool in one plane and one right hand tool in another plane as described in Figure 13 shall be set.

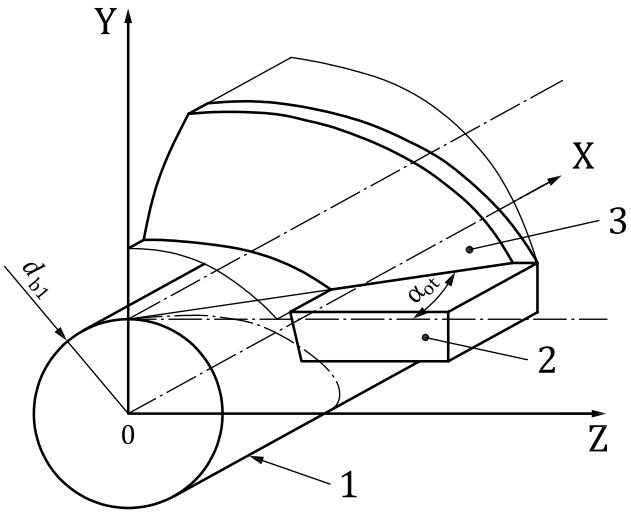

Key

1 base cylinder

2 cutting tool

3 generatrix

NOTE $\alpha_{0t} = \gamma_{b1}$

Figure 13 — I Profile type - Machining method with a lathe

The worm flanks can be machined by milling or grinding using the plane side face of a disc type milling cutter or grinding wheel. The cutting face shall be aligned either

— with its axis parallel to the X-Z plane and the base tangent generatrix of the flank in the cutting face (see Figure 14), or

— with the reference helix of the worm and in a plane perpendicular to the reference helix set to the normal pressure angle α_{0n} (see Figure 15).

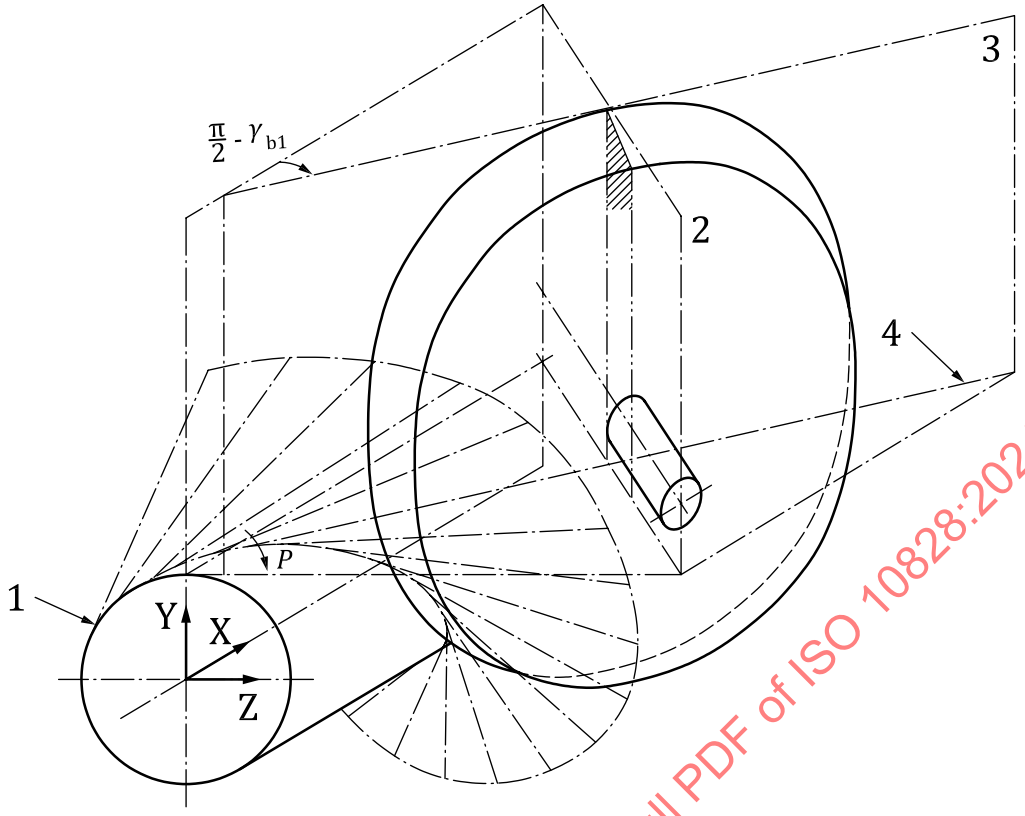

Key

1 base cylinder
2 grinding wheel (with flat active face)
3 action plane of the grinding wheel
4 generatrix
P plane tangent to the base circle containing the generatrix

Figure 14 — I Profile type - Machining method by grinding (solution 1)

In the set-up of alignment in Figure 15, the cutting face has the advantage to extend near the thread root.

In the set-up of method of Figure 14, the cutter/grinding-wheel spindle shall be raised so that the cutter/wheel periphery is tangent to the point of intersection of the base tangent generatrix with the root cylinder of the worm.

Both methods require that the mounting of the worm in the milling/grinding machine be reversed between machining right and left flanks.

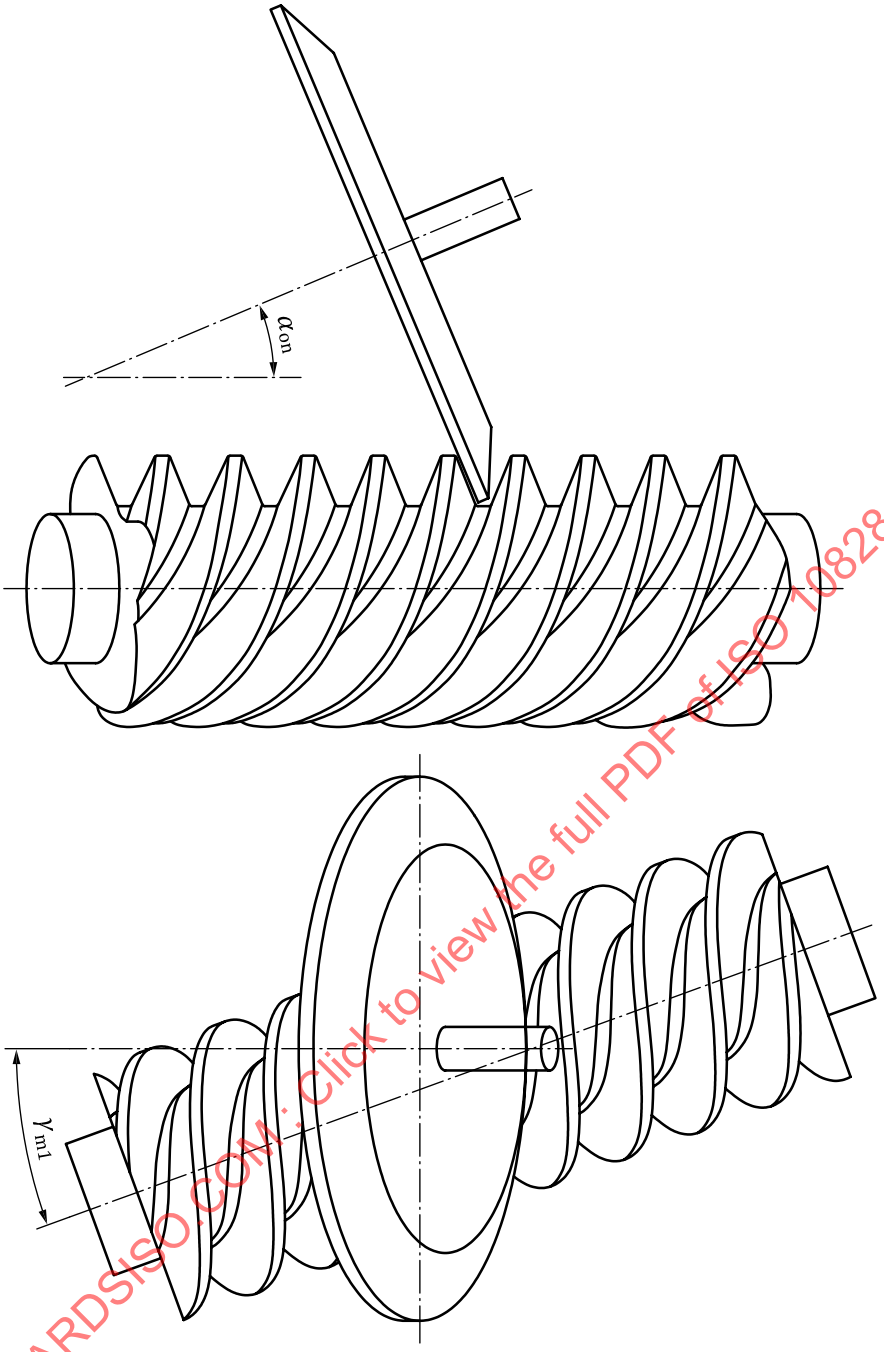

Figure 15 — I Profile type - Machining method by grinding (solution 2)

I profile type is slightly convex in an axial plane.

The development of the formulae for the axial profile of I worm profile type is shown in Annex A, A.3.

7.4 N worm profile type

7.4.1 Geometrical definition

The worm flank with N profile type is formed by a straight line generatrix (Δ) which lies in a plane normal to the reference helix (H_1); crossing (M) which is a common point of intersection of a vector radius, the generatrix (Δ) and the reference helix H. The angle α between (Δ) and the radius vector at M point is constant.

The flank envelope is formed by the generatrix (Δ), due to the helicoidal movement of the vector radius carrying the point M which describes the reference helix (see Figure 12).

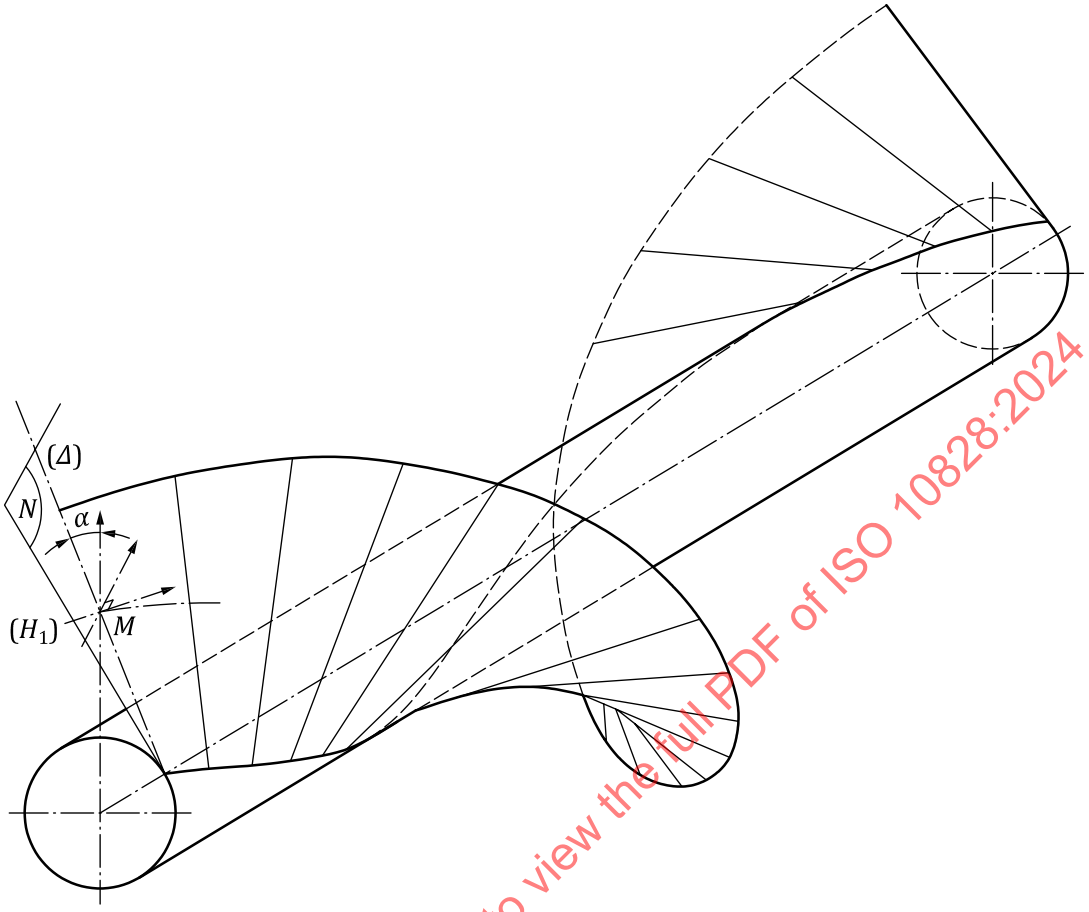

Figure 16 — N Profile type - Theoretical generation

7.4.2 Machining methods

The threads can be cut in a lathe with a tool having trapezoidal form having edges in the cutting plane which match the profile of the thread space in a plane normal to the reference helix of the thread space.

This is equivalent to placing the tool as for threads with A profile type, then to rotate it around an axis matching its symmetrical axis up to an angle equal to the reference lead angle γ_{m1} (see Figure 17).

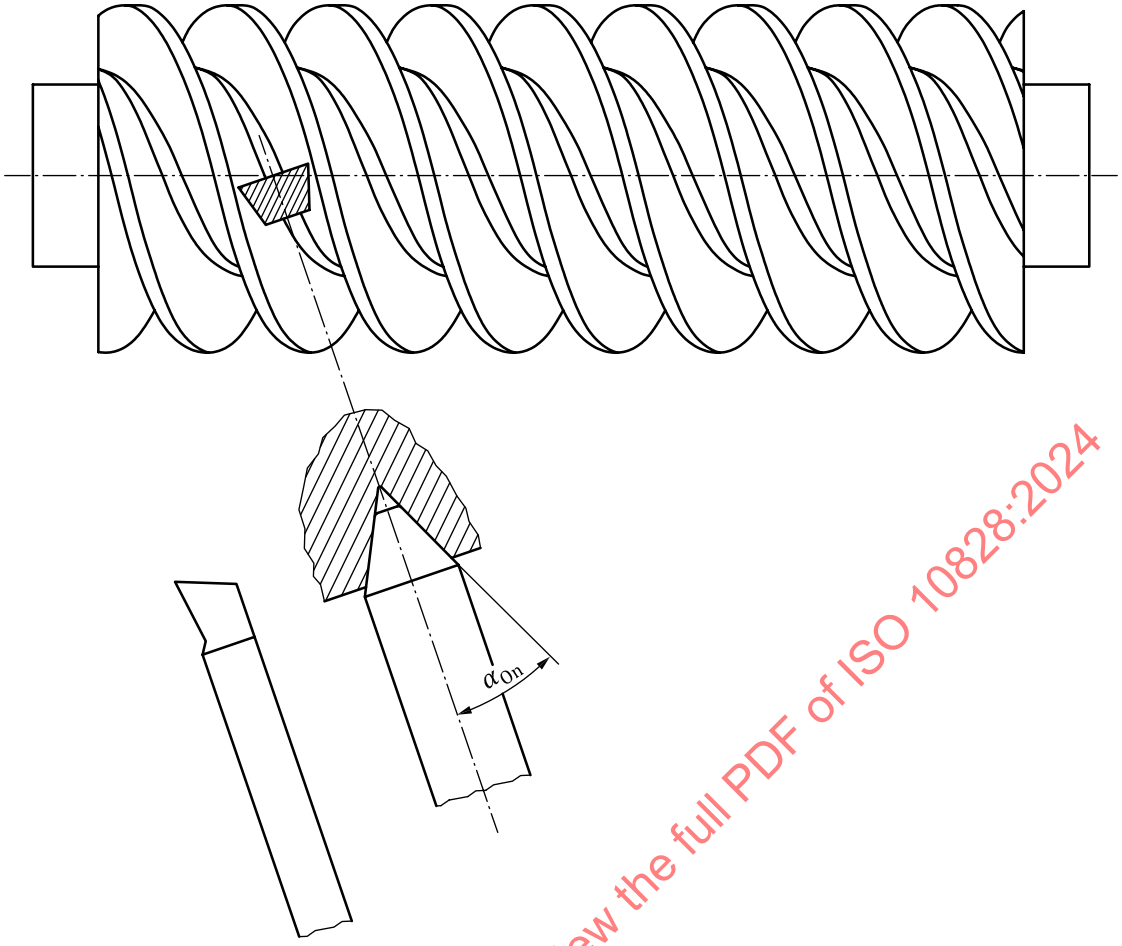

Figure 17 — N Profile type - Machining methods

Type N profiles are slightly concave in an axial plane.

The development of the formulae for the axial profile of N worm profile type is shown in Annex A, A.4.

7.5 General formulae for A, I and N profile types

Formulae (49) to (54) shall be used to obtain the axial profile for A, I, N profile types.

The general formula of the axial profile of the worm for A, I, N profiles can be given by Formula (49) and Formula (50) with x_x as the axial abscissa of the axial profile point function of the radius of the circle y_r at this point:

$$x_x(y_r) = a_1 \cdot \arctan\left(\frac{\sqrt{y_r^2 - a_2^2}}{a_2}\right) + a_3 \cdot \sqrt{y_r^2 - a_2^2} + a_4 \tag{49}$$

$$y_x(y_r) = y_r \tag{50}$$

The values for the coefficients are given in Table 5.

Table 5 — Coefficients a_1 to a_4 for A, I and N profile types

Coefficients	Profile types		
	A Profile	I Profile	N Profile
a_1	$a_{1A} = 0$	$a_{1I} = -p_{zu1}$	$a_{1N} = p_{zu1}$
a_2	$a_{2A} = 0$	$a_{2I} = r_{b1}$	$a_{2N} = \frac{A \cdot \sin(\gamma_{m1}) \cdot \tan(\alpha_{0n})}{\sqrt{1 + (\sin(\gamma_{m1}) \cdot \tan(\alpha_{0n}))^2}}$ $A = r_{ml} - \frac{s_{mx1} \cdot \cos(\gamma_{m1})}{2 \cdot \tan(\alpha_{0n})}$
a_3	$a_{3A} = \frac{\tan(\alpha_n)}{\cos(\gamma_{m1})}$	$a_{3I} = \tan(\gamma_{b1})$	$a_{3N} = \frac{a_{2N}}{A \cdot \tan(\gamma_{m1})}$
a_4	0	0	0

In Formula (49), a_4 coefficient allows to translate the axial profile and to set it up at the correct position needed in the calculation.

To set up axial profile at the pitch point in the mid plane the a_4 coefficient shall be determined by the application of the general Formula (51) for the pitch radius r_{w1}.

$$a_4 = -x_x(r_{w1}) = -a_1 \cdot \arctan\left(\frac{\sqrt{{r_{w1}}^2 - a_2^2}}{a_2}\right) - a_3 \cdot \sqrt{{r_{w1}}^2 - a_2^2} \tag{51}$$

In complement to the coordinate of the axial point, it is possible to define at this point the axial pressure angle at the y_r circle which is defined by the derivate of x_x function according to y_r, as given by Formulae (52) to (54):

$$dx_x(y_r) = \left(\frac{a_1 \cdot a_2}{y_r} + a_3 \cdot y_r\right) \cdot \frac{1}{\sqrt{y_r^2 - a_2^2}} \tag{52}$$

$$d y_x(y_r) = 1 \tag{53}$$

$$\tan\alpha_x(y_r) = \frac{d x_x(y_r)}{d y_x(y_r)} \tag{54}$$

7.6 K worm profile type

7.6.1 Geometrical definition and method

Unlike those of A, I and N profile types, the worm flanks with K profile type do not have straight line generatrixes. The thread spaces of K worm profile type are generated with a biconical grinding wheel or disc type milling cutter having straight cone generatrixes (see Figure 18).

The common perpendicular to the tool spindle and worm axes lies in the line (Δ) of intersection of the median plane (M) of the tool and a transverse plane of the worm (R). The angle between the two planes is equal to the worm reference lead angle of the worm γ_{m1}.The straight generatrix of each tool cone and the median plane of the tool forms an angle equal to the normal pressure angle α_{0n} of the tool.

The worm is turned uniformly with simultaneous axial translation of threads so that a point on the common perpendicular, distant r_{m1} (r_{m1}: reference radius of worm) from the worm axis, describes the reference helix.

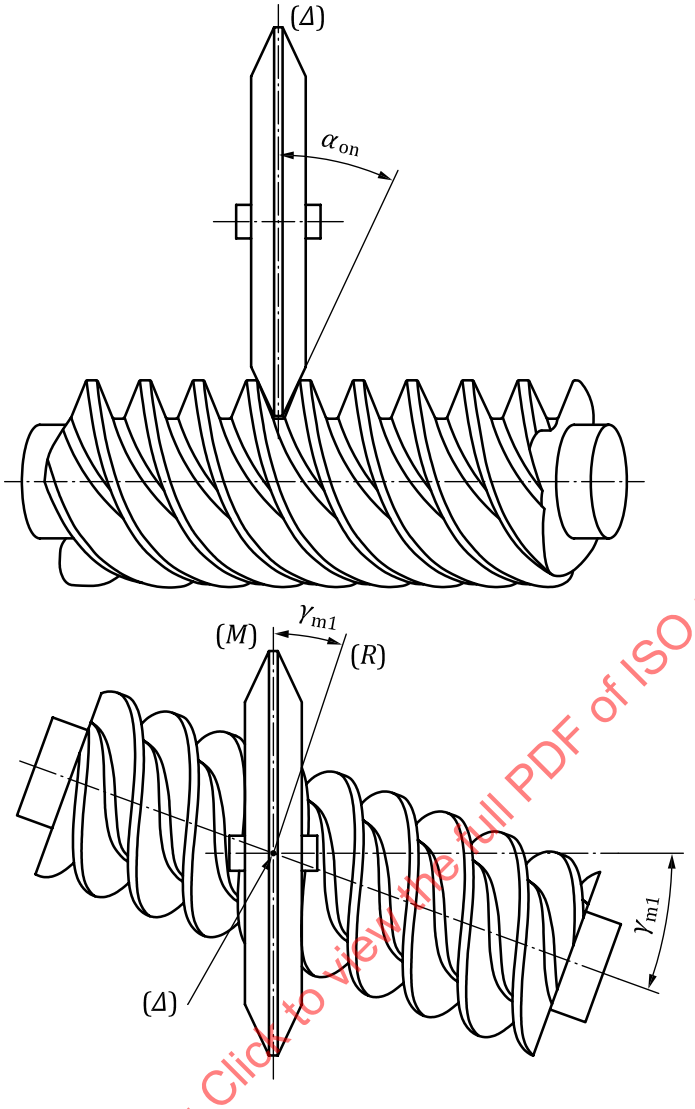

Figure 18 — Profile K - Machining method

The helicoidal flanks of the worm are generated by the conical sides of the tool and the profile form is influenced by the change of helix angle with change of thread height and points on the tool flanks which contact the worm threads lie on a curve and not on any one cone generatrix (see Figure 19).

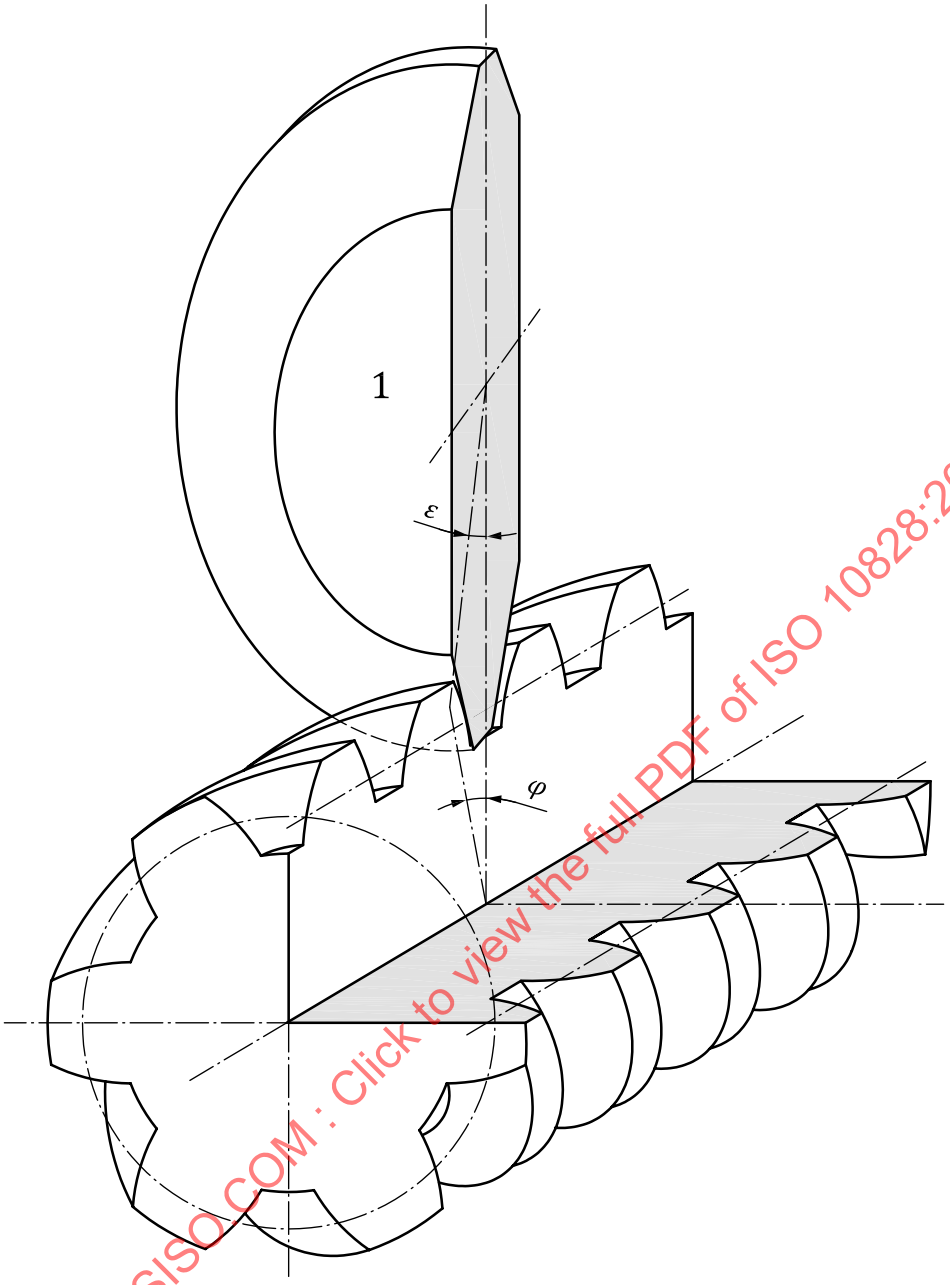

Key

1 grinding wheel

Figure 19 — Profile K - System of coordinates

Like I profile type, K profile type is convex in axial planes.

The development of the formulae for the axial profile of grinding wheel for K worm profile type is shown in Annex B, B.1.

7.7 C worm profile type

7.7.1 Geometrical definition

Unlike those of A, I and N profile types, the worm flanks with C profile type do not have straight line generatrixes.

Like worms with K profile type, the thread spaces of worms with C profile type are generated with a grinding wheel or disc type milling cutter. In order to produce the concave thread C worm profile type, the tool has a cutting profile consisting of convex circular arcs. Figure 20 shows a tool and worm with the system of coordinates for the worm (x, y, z) and for the tool (x_G, y_G, z_G).

The length of the line of centres a_0 (the common perpendicular to the worm and tool axes x_G and x) varies with the tool diameter. The angle between the projections of these axes (x, x_G) onto a plane perpendicular to the line of centres is usually equal to the reference lead angle of worm γ_{m1}. Figure 21 shows partially the tool. The four-tool dimensions which determine the thread form of the worm are: the profile radius ρ_{Gm}, the mean radius R_{Gm} of the tool profile, the tool pressure angle α_{0n} and the tool thickness (equal to 2 times x_{Gm}).

The process of generating the worm C profiles is the same as for K profile type (see 7.6).

The thread flank profile form varies a little with a change of tool diameter.

However, in contrast to thread with K profile type, thread with C profile type can be adjusted to compensate change of tool diameter by modifying the radius ρ_{Gm} and the angle α_{0n} of the tool.

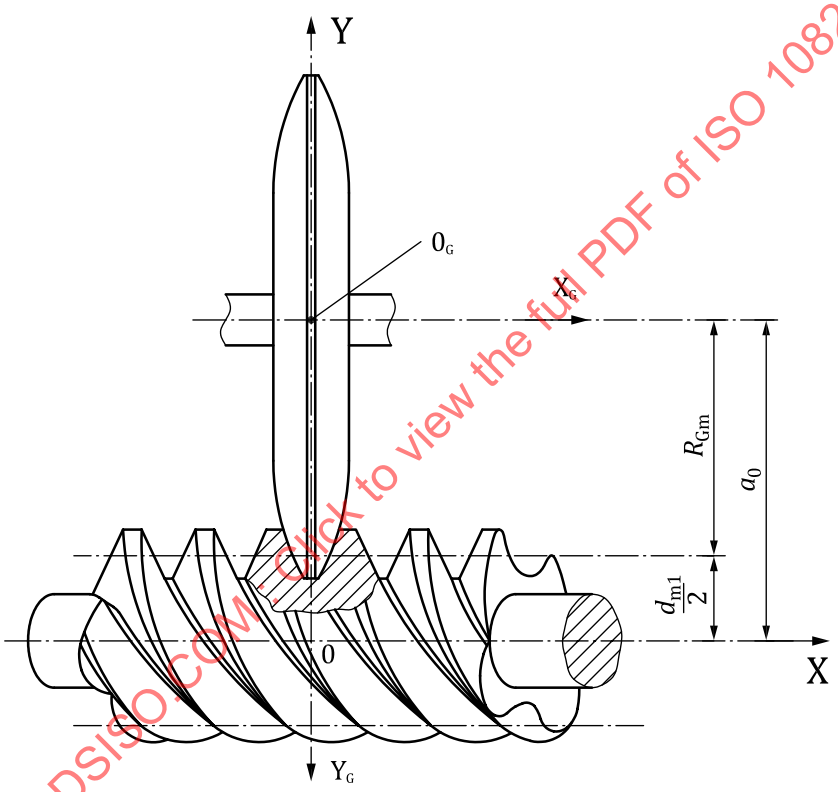

Figure 20 — K and C Profile types - System of coordinates

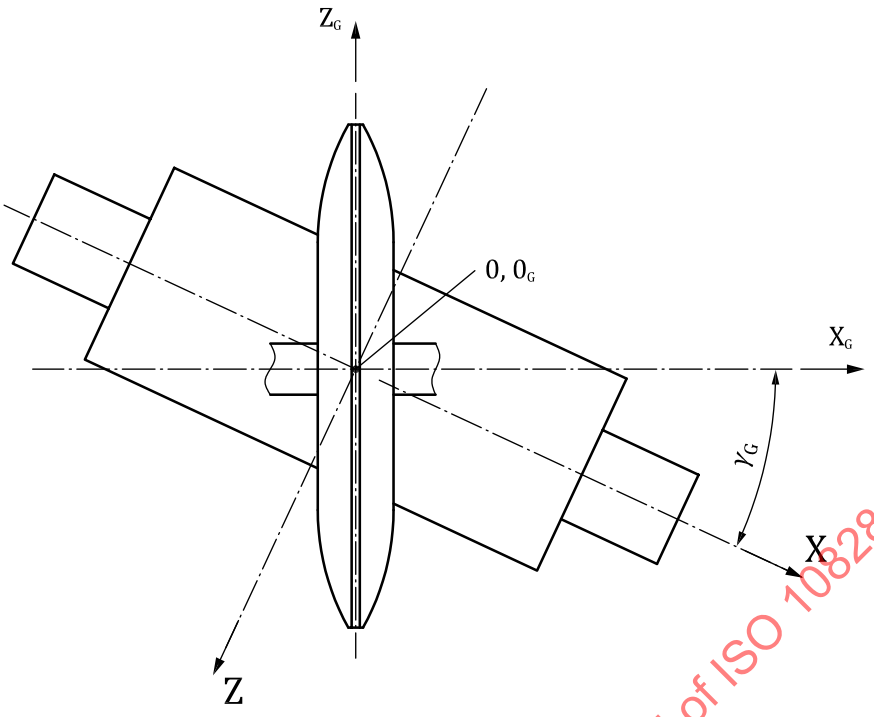

a) System of coordinate

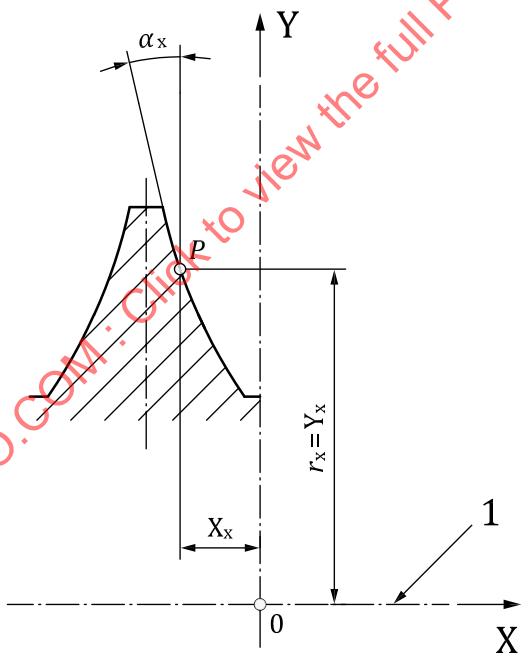

b) Axial section of the worm

Key

γ_G γ_{m1}

1 worm axis

Figure 21 — C Profile type

C profile type is concave in an axial plane.

The development of the formulae for the axial profile of grinding wheel for C worm profile type is shown in Annex B, B.2.

7.7.2 General formulae for C and K profiles

For C and K profiles, the parameter of the profile is the Y-circle radius y_G at a point on the profile of the grinding wheel which generates a point of the profile of the worm which shall be projected along its own helix in the axial plane of worm to obtain the axial profile point. Table 6 gives the parameters to establish common formulae for both profile types.

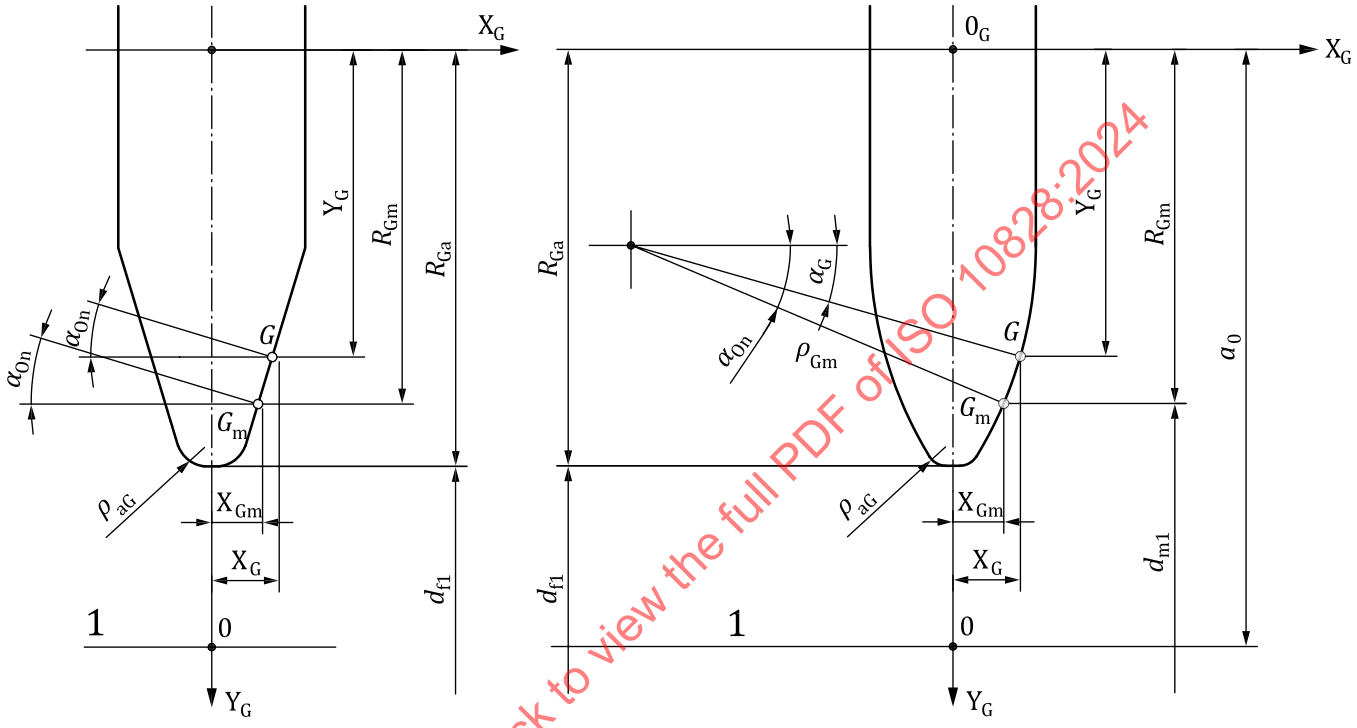

a) K Profile type **b) C Profile type**

Key

1 worm axis

Figure 22 — Parameter of grinding wheel

Table 6 — Parameters for profile grinding wheel

	K Profile type	C Profile type
Pressure angle at a point of axial profile of the grinding wheel	$\alpha_G(y_G)=\alpha_{0n}$	$\alpha_G(y_G)=\arcsin\left(\sin(\alpha_{0n})-\frac{R_{Gm}-y_G}{\rho_{Gm}}\right)$
Abscissa at a point of axial profile of the grinding wheel	$x_G(y_G)=x_{Gm}-\tan(\alpha_{0n})\cdot(y_G-R_{Gm})$	$x_G(y_G)=x_{Gm}+\rho_{Gm}\cdot(\cos(\alpha_G(y_G))-\cos(\alpha_{0n}))$
Radius at a point of axial profile of the grinding wheel	y_G	y_G
		ρ_{Gm}: Radius of curvature of the grinding wheel

With:

Centre distance for grinding is given by Formula (55):

$$a_{0n} = R_{Ga} + \frac{d_{f1}}{2} \tag{55}$$

with R_{Ga} as the outside radius of the grinding wheel

Nominal radius of the grinding wheel is given by Formulae (56) and (57):

$$R_{Gm} = a_{0n} - \frac{d_{m1}}{2} \tag{56}$$

$$x\mathrm{Gm} = \frac{(\pi \cdot m_{x1} - s_{mx1}) \cdot \cos(\gamma_{m1})}{2} \tag{57}$$

7.7.2.1 Formula for the point generated on the worm

Formula (58) shows the mesh condition of point G on the tool with a worm surface:

$$c_1 \cdot \sin(\varepsilon_G(y_G)) + c_2(y_G) \cdot \cos(\varepsilon_G(y_G)) - c_3(y_G)) = 0 \tag{58}$$

where $\varepsilon_G(y_G)$ is the rotation angle of the tool and c_i, given by Formulae (59) to (61):

$$c_1 = a_0 \cdot \cos(\gamma_{m1}) + p_{zu1} \cdot \sin(\gamma_{m1}) \tag{59}$$

$$c_2(y_G) = \sin(\gamma_{m1}) \cdot \left(x_G(y_G) - \frac{y_G}{\tan(\alpha_G(y_G))} \right) \tag{60}$$

$$c_3(y_G) = \left(-\frac{1}{\tan(\alpha_G(y_G))} \right) \cdot (a_0 \cdot \sin(\gamma_{m1}) - p_{zu1} \cdot \cos(\gamma_{m1})) \tag{61}$$

NOTE By default, the inclination of the grinding wheel is equal to the lead angle.

From these formulae $\varepsilon_G(y_G)$ is calculated as in Formula (62):

$$\varepsilon_G(y_G) = \arcsin\left(\frac{c_3(y_G)}{\sqrt{c_1^2 + c_2(y_G)^2}} \right) - \arctan\left(\frac{c_2(y_G)}{c_1} \right) \tag{62}$$

Then the point on the worm surface generated by the point G is shown by Formulae (63) to (68):

$$xc_{uw}(y_G) = x_G(y_G) \cdot \cos(\gamma_{m1}) - y_G \cdot \sin(\varepsilon_G(y_G)) \cdot \sin(\gamma_{m1}) \tag{63}$$

$$yc_{uw}(y_G) = a_0 - y_G \cdot \cos(\varepsilon_G(y_G)) \tag{64}$$

$$zc_{uw}(y_G) = -x_G(y_G) \cdot \sin(\gamma_{m1}) - y_G \cdot \cos(\gamma_{m1}) \cdot \sin(\varepsilon_G(y_G)) \tag{65}$$

7.7.2.2 Point of the worm thread flank surface in the axial plane

Point of the worm thread flank surface in the axial plane is defined by Formulae (66) to (68):

$$\varphi_x(y_G) = \arctan\left(\frac{zc_{uw}(y_G)}{yc_{uw}(y_G)} \right) \tag{66}$$

$$x_x(y_G) = xc_{uw}(y_G) - p_{zu1} \cdot \varphi_x(y_G) \quad (67)$$

$$y_x(y_G) = \frac{yc_{uw}(y_G)}{\cos(\varphi_x(y_G))} \quad (68)$$

7.7.2.3 Pressure angle of the C/K profiles

7.7.2.3.1 First derivatives of $c_2(y_G)$ and $c_3(y_G)$

First derivative of $c_1(y_G)$ and $c_2(y_G)$ are given by Formulae (69) and (70):

$$dc_2(y_G) = \left(dx_G(y_G) + \frac{1}{dx_G(y_G)} - \frac{y_G}{dx_G(y_G)^2} \cdot d2x_G(y_G) \right) \cdot \sin(\gamma_{m1}) \quad (69)$$

$$dc_3(y_G) = \left(\frac{-a_0 \cdot \sin(\gamma_{m1}) + p_{zu1} \cdot \cos(\gamma_{m1})}{dx_G(y_G)^2} \cdot d2x_G(y_G) \right) \quad (70)$$

7.7.2.3.2 First derivative of $\varepsilon_G(y_G)$

First derivative of $\varepsilon_G(y_G)$ is given by Formula (71):

$$d\varepsilon_G(y_G) = \frac{dc_3(y_G)}{\left(c_1^2 + c_2(y_G)^2 - c_3(y_G)^2\right)^{\frac{1}{2}}} - \frac{c_3(y_G) \cdot c_2(y_G) \cdot dc_2(y_G)}{\left(c_1^2 + c_2(y_G)^2\right) \cdot \left(c_1^2 + c_2(y_G)^2 - c_3(y_G)^2\right)^{\frac{1}{2}}} - \frac{dc_2(y_G) \cdot c_1}{c_1^2 + c_2(y_G)^2} \quad (71)$$

7.7.2.3.3 First derivative of point generated by the grinding wheel

First derivative of point generated by the grinding wheel is given by Formulae (72) to (74):

$$dxc_{uw}(y_G) = dx_G(y_G) \cdot \cos(\gamma_{m1}) - (\sin(\varepsilon_G(y_G)) + y_G \cdot \cos(\varepsilon_G(y_G)) \cdot d\varepsilon_G(y_G)) \cdot \sin(\gamma_{m1}) \quad (72)$$

$$dyc_{uw}(y_G) = -\cos(\varepsilon_G(y_G)) + y_G \cdot \sin(\varepsilon_G(y_G)) \cdot d\varepsilon_G(y_G) \quad (73)$$

$$dzc_{uw}(y_G) = -(dx_G(y_G) \cdot \sin(\gamma_{m1})) - [\sin(\varepsilon_G(y_G)) + y_G \cdot \cos(\varepsilon_G(y_G)) \cdot (d\varepsilon_G(y_G))] \cdot \cos(\gamma_{m1}) \quad (74)$$

7.7.2.3.4 First derivative of point generated by the grinding wheel projected in the axial plane of the worm

First derivative of point generated by the grinding wheel projected in the axial plane of the worm is given by Formulae (75) to (77):

$$d\varphi_x(y_G) = \frac{dzc_{uw}(y_G) \cdot yc_{uw}(y_G) - zc_{uw}(y_G) \cdot dyc_{uw}(y_G)}{yc_{uw}(y_G)^2 + zc_{uw}(y_G)^2} \quad (75)$$

$$dx_x(y_G) = dxc_{uw}(y_G) - p_{zu1} \cdot d\varphi_x(y_G) \quad (76)$$

$$dy_x(y_G) = \frac{dyc_{uw}(y_G)}{\cos(\varphi_x(y_G))} + \frac{yc_{uw}(y_G)}{\cos(\varphi_x(y_G))^2} \cdot \sin(\varphi_x(y_G)) \cdot d\varphi_x(y_G) \quad (77)$$

7.7.2.3.5 Pressure angle of the C and K profile types in axial plane

Pressure angle in the axial plane of the worm for a point generated by the grinding wheel, for C and K profile types is given by Formula (78):

$$\tan\alpha_x(y_G)=\frac{\mathrm{d}x_x(y_G)}{\mathrm{d}y_x(y_G)} \tag{78}$$

7.8 General formula of the axial profile

7.8.1 General

In this document the axial profile of the worm is considered with general formulae $x_x(y_p)$, $y_x(y_p)$, $\tan\alpha_x(y_p)$ as a function of a parameter y_p, with

— $y_p = y_r$, radius of the worm for A, I, N profiles, and

— $y_p = y_G$ for radius of the worm for C and K profiles.

7.8.2 Derivative of pressure angle for all profile types

Derivative of pressure angle for all profile types is given by Formula (79):

$$\mathrm{d}\tan\alpha_x(y_G)=\frac{\mathrm{d}2x_x(y_G)}{\mathrm{d}y_x(y_G)}-\frac{\mathrm{d}x_x(y_G)\cdot\mathrm{d}2x_x(y_G)}{\mathrm{d}y_x(y_G)^2} \tag{79}$$

For the calculation of second derivative of x_x, y_x, see Annex A for A, I, N profile types and Annex B for C and K profiles.

NOTE Formula (79) applies to any profile of disc type tool.

7.9 Algorithm to initialize the calculation

The first step is to initialize the calculation by the input of geometric parameters:

— of the worm: z_1, γ_{m1}, m_{x1}, α_n, profile type, d_{f1}, d_1, c_1^*, s_{mx1}^* and only for K profile type R_{Ga} and C profile type R_{Ga}, ρ_{Gm};

— of the worm wheel: z_2, b_{2H}, x_2, c_1^*, c_2^*, d_{e2}.

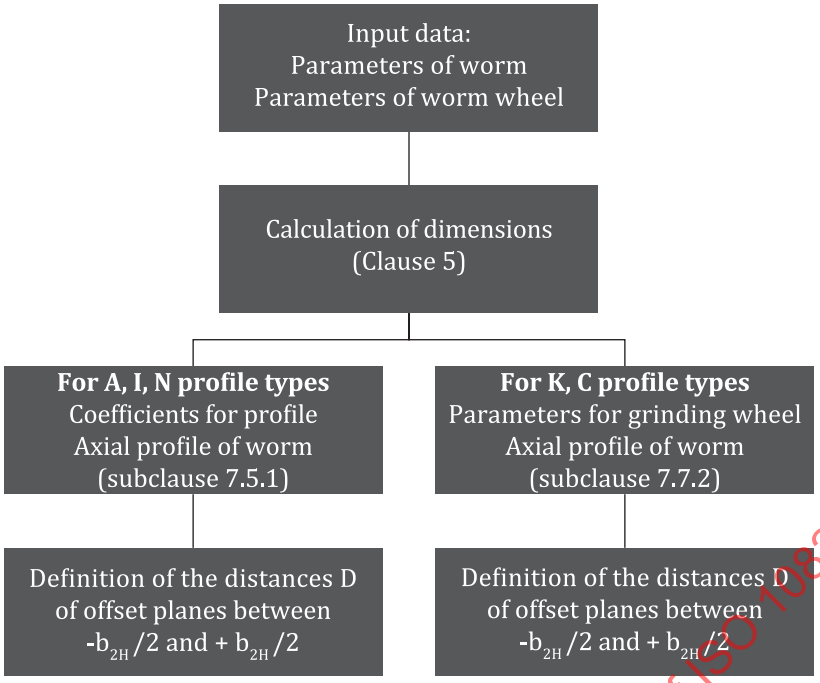

Figure 23 — Algorithm to initialize the calculation

Note The worm gear mesh is split in an odd number of offset planes, N_{plane}, equally spaced by a value of $b_{2H}/(N_{plane}$ -1). The offset planes are noted D_i.

The algorithm is continued in 11.4.

8 Useful section planes

8.1 General

The useful sections to study worm gear geometry are defined by planes shown in Figure 24.

8.2 Axial plane and axial section

The axial plane is the plane containing the worm axis and the X and Y axes of the coordinate system (see plane X in Figure 24). It provides an axial section of the worm used to define the axial profile of the worm in plane X.

For the gear pair, it provides a transverse section of the worm wheel in the mid-plane of the worm wheel, to define the mid-plane profile of the worm wheel.

8.3 Offset plane and offset section

An offset plane of the worm is a plane parallel to the X-Y plane at an offset distance D (Z axis) (see plane D in Figure 24). It provides an offset section of the worm used to define the offset profile of the worm in plane D.

A point in the offset plane is determined by the point of intersection between this offset plane and the helix through a referenced point x, y, in the axial X-Y plane.

For the gear pair, it provides a transverse section of the worm wheel in the offset plane of the worm wheel, to define the offset profile of the worm wheel in plane D.

Offset planes are very important to study worm gear mesh.

8.4 Transverse plane and transverse section

A transverse plane of the worm is a plane which is perpendicular to the axis of the worm (see plane R in Figure 24). It provides a transverse section of the worm used to define the transverse profile of the worm in plane R.

8.5 Normal plane and normal section

A normal plane of the worm is defined as a plane which is perpendicular to the reference helix (on the reference diameter) crossing the axis of symmetry of the complete axial profile of the concerned thread (left and right flank) (see plane N in Figure 24). It provides a normal section of the worm used to define the normal profile of the worm in plane N.

NOTE The section of the worm by a plane normal to the reference helix (on the reference diameter) crossing the axis of symmetry of the complete axial space-width profile of the worm thread is not equivalent to the normal section of the worm. It is called normal space width section and is used as a basis to define the profile of the cutting tool to generate the teeth of the conjugate worm wheel.

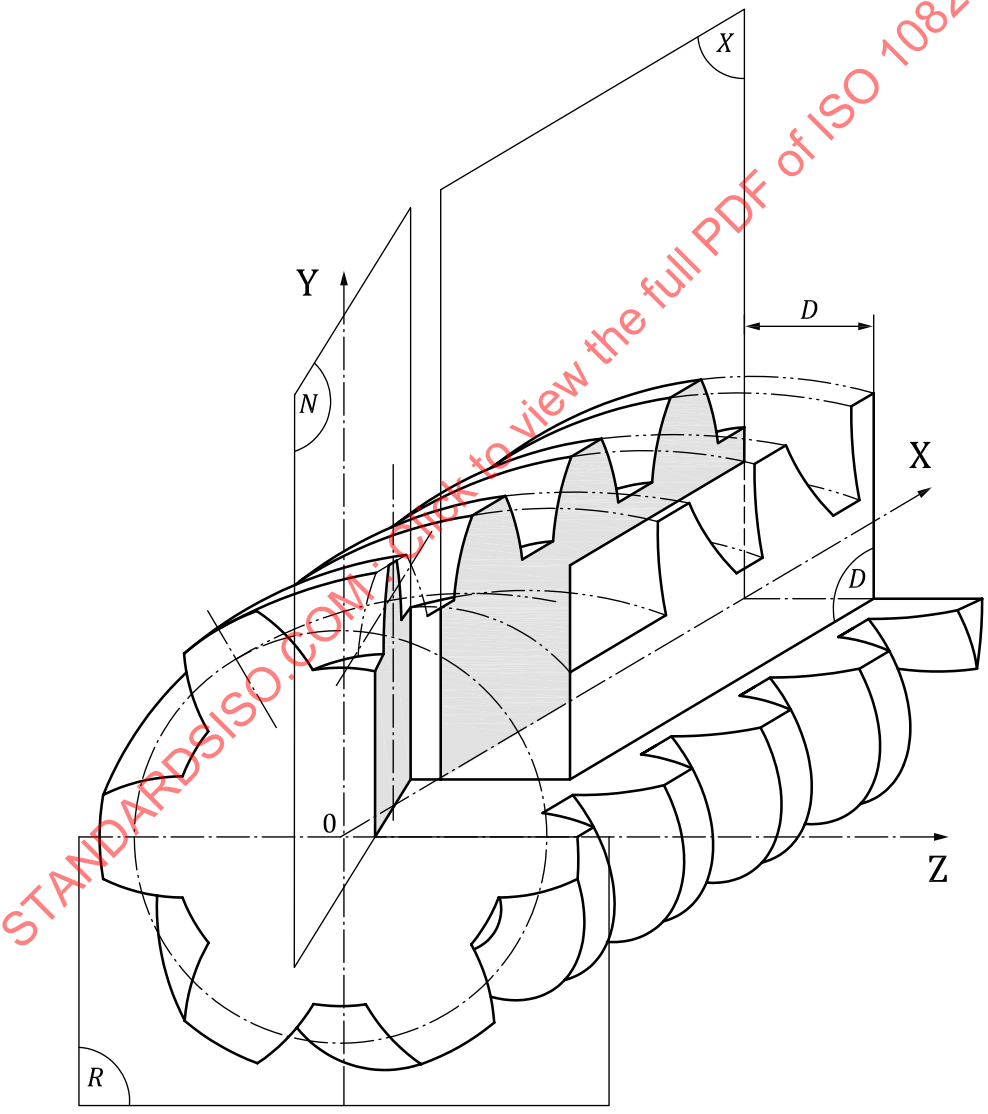

Figure 24 — Section planes

8.6 Point of the worm surface in an offset plane: offset profile of worm

By definition, the worm wheel is conjugate to the worm. The profile of the worm is defined in an axial plane, and it is projected in offset planes (see Figure 25) in order to study the gear mesh of the worm gear set.

The distance between the axial plane of the worm and an offset plane is defined by distance *D*. *D* can be positive or negative along the Z axis.

The coordinates of point (M_D) in an offset plane and on the helix curve, which pass the point (M_x) in the plane, are shown as follows:

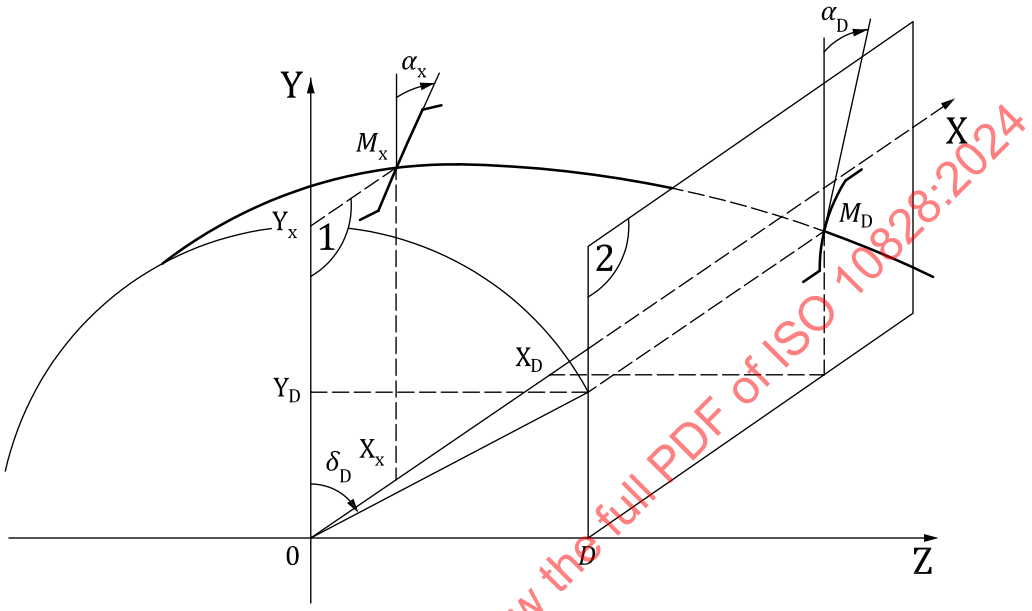

Key

1 axial plane (O, X, Y)

2 offset plane

Figure 25 — Relationship between axial profile and the profile in an offset plane

For a given axial point of worm surface, the corresponding point x_D and y_D on the same helix in an offset plane *D*, is obtained with the angle δ_D in the transverse plane (Y,Z), with Formulae (80) to (82). See 7.8.1 for the definition of y_p.

$$\delta_D(y_p, D) = \arcsin\left(\frac{D}{y_x(y_p)}\right) \tag{80}$$

$$x_D(y_p, D) = x_x(y_p) + p_{zu1} \cdot \delta_D(y_p, D) \tag{81}$$

$$y_D(y_p, D) = y_x(y_p) \cdot \cos\left(\delta_D(y_p, D)\right) = y_x(y_p) \cdot \sqrt{1 - \frac{D^2}{y_x(y_p)^2}} = \sqrt{y_x(y_p)^2 - D^2} \tag{82}$$

First derivatives of rack profile Formulae (83) to (86):

With the derivatives according to y_p:

$$d\delta_D(y_p,D)=\frac{-D}{y_x(y_p)^2}\cdot\frac{dy_x(y_p)}{\sqrt{1-\frac{D^2}{y_x(y_p)^2}}}=\frac{-D}{y_x(y_p)^2}\cdot\frac{dy_x(y_p)}{\cos(\delta_D(y_p,D))}=\frac{-D}{y_x(y_p)\cdot y_D(y_p,D)}\cdot dy_x(y_p) \quad (83)$$

$$dx_D(y_p,D)=dx_x(y_p)+p_{zu1}\cdot d\delta_D(y_p,D)=\left[\tan\alpha_x(y_p)-\frac{p_{zu1}\cdot D}{y_x(y_p)\cdot y_D(y_p,D)}\right]\cdot dy_x(y_p) \quad (84)$$

$$dy_D(y_p,D)=\frac{d}{dy_p}\left(\sqrt{y_x(y_p)^2-D^2}\right)=\frac{y_x(y_p)}{\sqrt{y_x(y_p)^2-D^2}}\cdot dy_x(y_p)=\frac{y_x(y_p)}{y_D(y_p,D)}\cdot dy_x(y_p)=\frac{dy_x(y_p)}{\cos(\delta_D(y_p,D))}$$

$$dy_D(y_p,D)=\frac{d}{dy_p}\left(\sqrt{y_x(y_p)^2-D^2}\right)=\frac{y_x(y_p)}{\sqrt{y_x(y_p)^2-D^2}}\cdot dy_x(y_p)=\frac{y_x(y_p)}{y_D(y_p,D)}\cdot dy_x(y_p) \quad (85)$$

And it results that the pressure angle of the axial projected point is given by Formula (86):

$$\tan\alpha_D(y_p,D)=\frac{dx_D(y_p,D)}{dy_D(y_p,D)}=\frac{\left[\tan\alpha_x(y_p)-\frac{p_{zu1}\cdot D}{y_x(y_p)\cdot y_D(y_p,D)}\right]\cdot dy_x(y_p)}{\frac{y_x(y_p)}{y_D(y_p,D)}\cdot dy_x(y_p)} \quad (86)$$

$$=\left[\frac{y_D(y_p,D)}{y_x(y_p)}.\tan\alpha_x(y_p)-\frac{p_{zu1}\cdot D}{y_x(y_p)^2}\right]=\cos(\delta_D(y_p,D))\cdot\tan\alpha_x(y_p)-\frac{p_{zu1}\cdot D}{y_x(y_p)^2}$$

9 Pitch surfaces

When studying worm gear geometry, the first step is to define the main parameters of the worm gear set (see Clause 5), and to select the profile type of the worm:

— For the worm:
  — number of threads on worm;
  — diameter quotient;
  — axial module;
  — normal pressure angle;
  — thread thickness;
  — rotational speed of the worm (rpm);
  — worm profile;
  — outside diameter of the grinding wheel for K and C profile;
  — radius of curvature of the grinding wheel for C profile.
— For the worm wheel:
  — number of teeth on worm wheel;
  — profile shift coefficient;
  — face width of worm wheel;

— outside addendum coefficient;

— bottom clearance coefficient;

— In complement addendum and dedendum, coefficients can be defined if they are not equal to the proposed values of Clause 5.

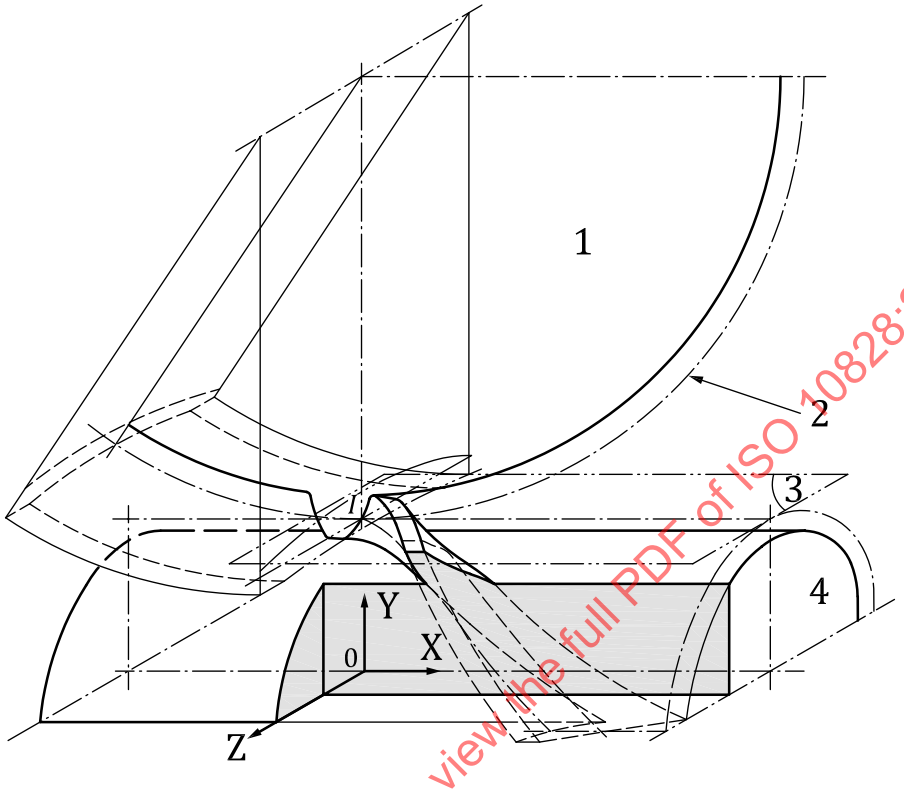

Key

1 mid plane of worm wheel
2 pitch circle in the offset plane
3 pitch plane
4 worm

NOTE Definition of axes (by default, a right-hand driving worm is considered).

Figure 26 — Definition of pitch surfaces

The axis to study the gear mesh (see Figure 26) are (0, X, Y, Z), with OX as the axis of the worm, OY along the centre line in the mid plane of worm wheel. The Z axis is used to define the distance D of each offset plane according to the mid plane.

Right flanks of right-hand helix worm threads are considered, as the worm is driving, and the worm wheel driven.

The pitch surface of the worm is a plane parallel to the axis of the worm and the axis of the wheel with a distance to the axis of the worm equal to the half of pitch diameter $d_{w1}/2$ (see 5.3.3).

The pitch cylinder of the worm wheel is defined with the pitch diameter d_{w2} (see 5.3.2).

The pitch cylinder of the wheel is rolling without sliding on the pitch plane of the worm.

The common tangent between the two-pitch surfaces is called pitch axis; it is also the instantaneous axis of rotation.

10 Conjugate worm wheel profile

10.1 General

For all the calculations in Clauses 10 to 12, the origin of the abscissa of the profile in an offset plane D shall be defined on the pitch line PL which is the intersection of pitch plan and offset plane (see Figure 27) with transformation Formulae (87) to (89):

$$r_{wD}(D)=\sqrt{D^2+\left(\frac{d_{w1}}{2}\right)^2} \tag{87}$$

$$\delta_{DI}(D)=\delta_D(r_{wD},D)=\arcsin\left(\frac{D}{y_x(r_{wD}(D))}\right) \tag{88}$$

$$\Delta x_D(D)=x_x(r_{wD}(D))+p_{zu1}\cdot\delta_{DI}(D) \tag{89}$$

As the projection of the axial plane in an offset plane is done along the helix, consequently each offset profile, obtained with Formulae (71) to (82), shall be translated by a value $\Delta x_D(D)$ in order that each offset profile crosses the pitch axis (see the last paragraph of Clause 9). For the following calculations, the values defined in Clauses 10 and 11 shall be determined.

This translation is given by Formula (90):

$$x'_D(y_P,D)=x_D(y_P,D)-\Delta x_D(D) \tag{90}$$

10.2 Path of contact

The path of contact in an offset plane is the line along which the contact point between the flank of the worm and the conjugate flank of the worm wheel is moving during the gear mesh. The coordinates of the path of contact are defined in Figure 27 and Formulae (91) and (92):

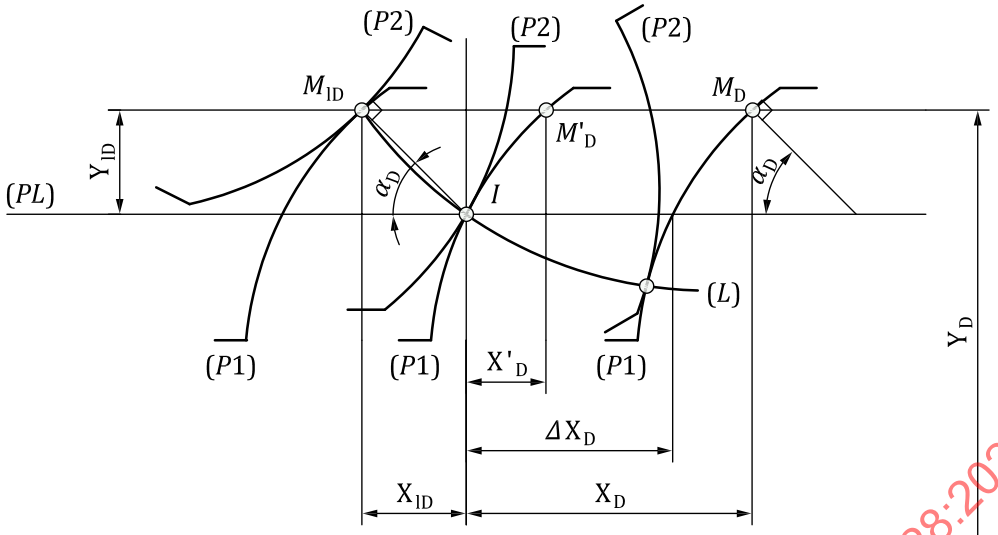

Key

(*P*1)	profile of worm
(*P*2)	profile of worm wheel
(*L*)	path of contact
(*PL*)	pitch line of worm
I	pitch point

Figure 27 — Path of contact in offset plane *D*

$$y_{lD}\left(y_p, D\right) = y_D\left(y_p, D\right) - \frac{d_{w1}}{2} \tag{91}$$

$$x_{lD}\left(y_p, D\right) = -\frac{y_{lD}\left(y_p, D\right)}{\tan\alpha_D\left(y_p, D\right)} \tag{92}$$

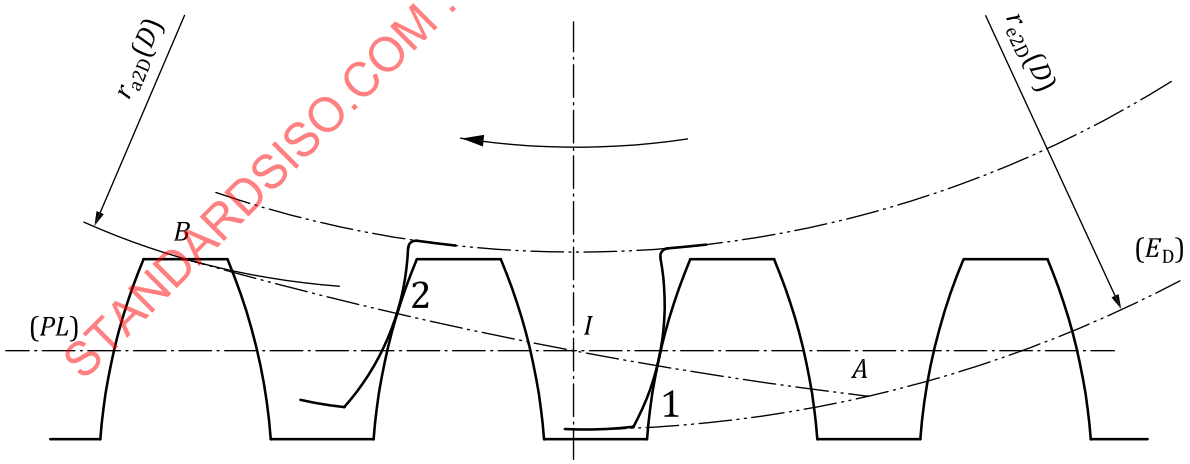

Key

1	point of contact 1
2	point of contact 2
(d_e)	external diameter
(*PL*)	pitch line
I	pitch point

Figure 28 — Path of contact

When there is no singularity (see 10.6) in the gear mesh, the active path of contact is limited:

— on one side by the outside diameter of the worm wheel to define the start of active profile (SAP) in the concerned offset plane, point A on Figure 28;

— on the other side by the active tip diameter of the worm (often equal to the outside diameter of the worm except if there is chamfering), point B on Figure 28. Point B corresponds to the end of active profile of the worm (EAP) in the concerned offset plane except if there is cusp when the worm is meshing with the worm wheel (see 10.6.2).

For the calculation of points A and B, see 11.4.

10.3 Worm wheel profile conjugate with worm profile

The worm wheel profile conjugate with the worm profile in an offset plane D is obtained in Figure 29 and Formulae (93) to (97). Each point of the worm wheel profile is obtained from a point of the path of contact. The kinematic conditions of rolling without sliding of pitch surfaces allow projecting those points in polar coordinates of the wheel defined according to the centreline crossing the pitch point of the offset plane.

Polar coordinates:

$$r_{M2D}\left(y_p, D\right) = \sqrt{\left(r_{w2} - y_{lD}\left(y_p, D\right)\right)^2 + x_{lD}\left(y_p, D\right)^2} \tag{93}$$

$$\varepsilon_D\left(y_p, D\right) = \frac{\left(x'_D\left(y_p, D\right) - x'_D\left(r_{wD}, D\right)\right) - x_{lD}\left(y_p, D\right)}{r_{w2}} \tag{94}$$

$$\theta_D\left(y_p, D\right) = \varepsilon_D\left(y_p, D\right) + \arctan\left(\frac{x_{lD}\left(y_p, D\right)}{r_{w2} - y_{lD}\left(y_p, D\right)}\right) \tag{95}$$

Cartesian coordinates with origin at the pitch point:

$$xR_D\left(y_p, D\right) = r_{M2D}\left(y_p, D\right) \cdot \sin\left(\theta_D\left(y_p, D\right)\right) \tag{96}$$

$$yR_D\left(y_p, D\right) = r_{w_2} - r_{M2D}\left(y_p, D\right) \cdot \cos\left(\theta_D\left(y_p, D\right)\right) \tag{97}$$

The angular origin of the conjugate profile with worm is on axis O_{2I} crossing the pitch point (see Figure 29).

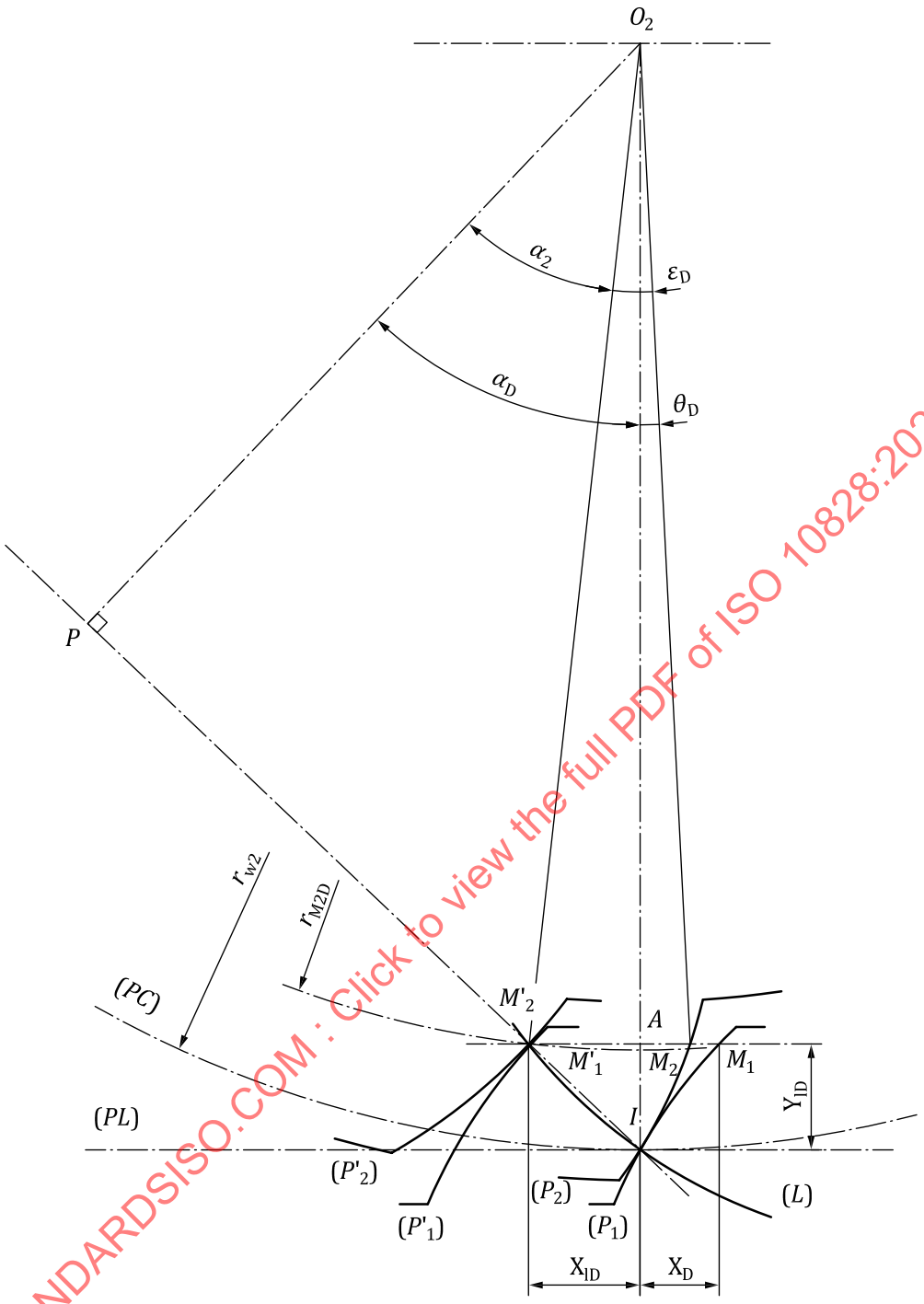

Key

(PC)	pitch circle of the worm wheel
(PL)	pitch line of worm
(L)	path of contact
I	pitch point

Figure 29 — Determination of the worm wheel profile conjugate with the worm profile in an offset plane

The outside radius of the worm wheel in the offset plane D is given by Formula (98):

$$r_{e2D}(D) = \min\left[a - \sqrt{\left(\frac{d_{f1}}{2} + c_1\right)^2 - D^2}\ ,\ 0{,}5 \cdot d_{e2}\right] \tag{98}$$

In certain cases, it is interesting to determine the point of the worm (for A, I, N profiles) or of the grinding wheel (for C and K profile) which has generated the point of the worm wheel in an offset plane r_{Wheel}. The algorithm is given in Annex C.

10.4 Trochoid (or fillet) at root of the worm wheel

The tip corner of the cutting tool, which generates the worm wheel, generates a fillet or trochoid at the root of the worm wheel tooth. The tip corner is defined in each offset plane by the coordinates (x_{a0D}, y_{a0D}) obtained by increasing the outside diameter of the worm by the value of the clearance at the root of the worm wheel teeth; this corresponds to the outside radius of the cutting tool r_{a0} (see Figure 30).

The kinematic conditions of rolling without sliding of pitch surfaces allow for the projection of those points in polar coordinates of the wheel defined according to the centreline crossing the tip corner of the offset plane.

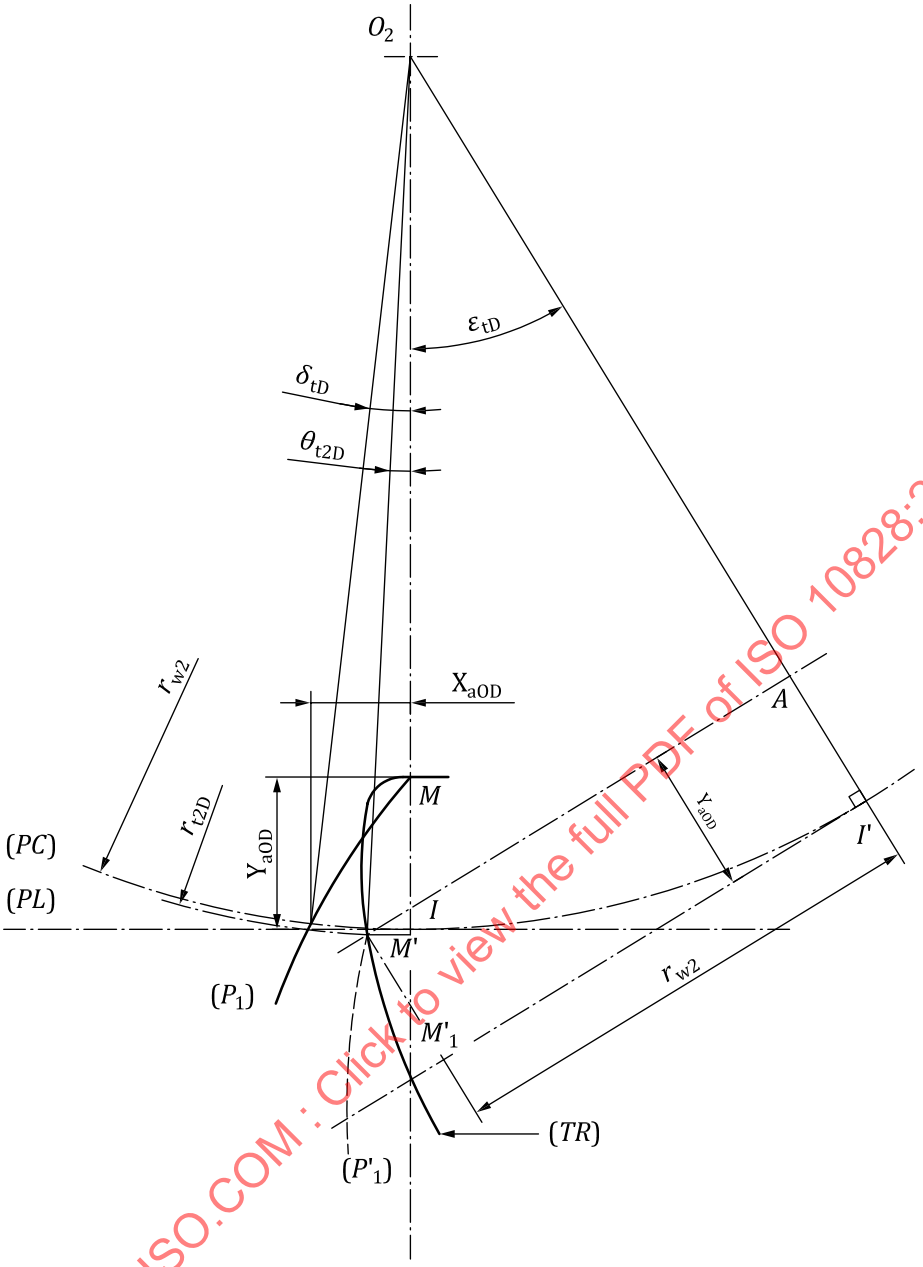

Key

(*PC*)	pitch circle of the worm wheel
(*PL*) (*P'*$_1$)	offset profile of equivalent cutting tool
(*TR*)	trochoid generated by tip corner of cutting tool
I	pitch point

Figure 30 — Trochoid (or fillet) of the worm wheel teeth

Polar coordinates (r_{t2D}, θ_{t2D}): in Formulae (99) to (100), the radius circle of the point of the fillet r_{t2D} is the parameter.

r_{t2D} shall be greater than the root radius of the worm wheel r_{f2D} given by:

$$r_{f2D}(D) = a_w - \sqrt{{r_{a0}}^2 - D^2} \tag{99}$$

and:

$$\theta_{t2D}(r_{t2D}, D) = \frac{x'_D(r_{a0}, D) - x'_D(r_{wD}, D)}{r_{w2}} - \arctan\left[\frac{\sqrt{r_{t2D}^2 - (r_{w2} - y_{lD}(r_{a0}, D))^2}}{r_{w2} - y_{lD}(r_{a0}, D)}\right] + \frac{\sqrt{r_{t2D}^2 - (r_{w2} - y_{lD}(r_{a0}, D))^2}}{r_{w2}} \tag{100}$$

Cartesian coordinates:

$$xT_D(r_{t2D}, D) = r_{t2D} \cdot \sin(\theta_{t2D}(r_{t2D}, D)) \tag{101}$$

$$yT_D(r_{t2D}, D) = r_{w2} - r_{t2D} \cdot \cos(\theta_{t2D}(r_{t2D}, D)) \tag{102}$$

The relations are obtained directly as a function of a radius of the circle crossing the point of the trochoid. In Formulae (101) and (102), θ_{t2D} is determined with the same origin axis O_2I as the conjugate profile of the worm wheel (see 10.3).

This allows to calculate, for each offset plane, the form radius of the worm wheel r_{fnD} which corresponds to the intersection of the trochoid and conjugate profile. This value is obtained when $\theta_{t2D} = \theta_D$ for $r_{t2D} = r_{M2D}$ [see Formulae (93), (95) and (102)].

10.5 Equivalent radius of curvature in an offset plane

To determine the equivalent radius of curvature the following process is used:

1) calculation of the radius of curvature of the worm at the point of contact. This calculation is made on the basis of analytical formula of the worm profile in each offset plane;

2) calculation of the radius of curvature of the conjugate profile of the worm wheel by using the Euler Savary method;

3) from those two values, it is possible to calculate an equivalent radius of curvature.

10.5.1 Curvature for the worm at a point in an offset plane

It is given by Formula (103) resulting in general mathematical formulae for a curve in two dimensions:

$$C_{\mathrm{eq1D}}\left(y_{\mathrm{p}},D\right)=\frac{1}{\rho_1\left(y_{\mathrm{p}},D\right)}=\frac{\dfrac{\mathrm{d}^2 x_{\mathrm{D}}\left(y_{\mathrm{p}},D\right)}{\mathrm{d}\,y_D^2\left(y_{\mathrm{p}},D\right)}}{\left[1+\left(\dfrac{\mathrm{d}\,x_{\mathrm{D}}\left(y_{\mathrm{p}},D\right)}{\mathrm{d}\,y_{\mathrm{D}}\left(y_{\mathrm{p}},D\right)}\right)^2\right]^{\frac{3}{2}}} \tag{103}$$

From Formula (86), the denominator can be replaced with Formula (104):

$$1+\left(\frac{\mathrm{d}\,x_{\mathrm{D}}\left(y_{\mathrm{p}},D\right)}{\mathrm{d}\,y_{\mathrm{D}}\left(y_{\mathrm{p}},D\right)}\right)^2=1+\tan^2\alpha_{\mathrm{D}}\left(y_{\mathrm{p}},D\right)=\frac{1}{\cos^2\alpha_{\mathrm{D}}\left(y_{\mathrm{p}},D\right)} \tag{104}$$

From Formula (86), the numerator can be replaced with Formula (105):

$$\frac{\mathrm{d}^2 x_{\mathrm{D}}\left(y_{\mathrm{p}},D\right)}{\mathrm{d}\,y_D^2\left(y_{\mathrm{p}},D\right)}=\frac{\mathrm{d}}{\mathrm{d}\,y_D}\left(\frac{\mathrm{d}\,x_{\mathrm{D}}\left(y_{\mathrm{p}},D\right)}{\mathrm{d}\,y_{\mathrm{D}}\left(y_{\mathrm{p}},D\right)}\right)=\frac{\mathrm{d}}{\mathrm{d}\,y_D}\left(\tan\alpha_{\mathrm{D}}\left(y_{\mathrm{p}},D\right)\right)=\frac{\mathrm{d}}{\mathrm{d}\,y_{\mathrm{p}}}\left(\tan\alpha_{\mathrm{D}}\left(y_{\mathrm{p}},D\right)\right)\frac{\mathrm{d}\,y_{\mathrm{p}}\left(y_{\mathrm{p}},D\right)}{\mathrm{d}\,y_{\mathrm{D}}\left(y_{\mathrm{p}},D\right)} \tag{105}$$

From Formula (82), Formulae (106) and (107) can be determined:

$$\frac{\mathrm{d}\,y_D\left(y_{\mathrm{p}},D\right)}{\mathrm{d}\,y_p\left(y_{\mathrm{p}},D\right)}=\frac{1}{\cos\left(\delta_{\mathrm{D}}\left(y_{\mathrm{p}},D\right)\right)}\ \text{and}\ \frac{\mathrm{d}\,y_p\left(y_{\mathrm{p}},D\right)}{\mathrm{d}\,y_D\left(y_{\mathrm{p}},D\right)}=\cos\left(\delta_{\mathrm{D}}\left(y_{\mathrm{p}},D\right)\right) \tag{106}$$

$$\text{And}\ \frac{\mathrm{d}^2 x_D\left(y_{\mathrm{p}},D\right)}{\mathrm{d}\,y_D^2\left(y_{\mathrm{p}},D\right)}=\cos\left(\delta_{\mathrm{D}}\left(y_{\mathrm{p}},D\right)\right)\cdot\frac{\mathrm{d}}{\mathrm{d}\,y_{\mathrm{p}}}\left(\tan\alpha_{\mathrm{D}}\left(y_{\mathrm{p}},D\right)\right) \tag{107}$$

With Formula (86), Formula (108) can be determined:

$$\frac{\mathrm{d}}{\mathrm{d}\,y_p}\left(\tan\alpha_{\mathrm{D}}\left(y_p,D\right)\right)=-\sin\left(\delta_{\mathrm{D}}\left(y_p,D\right)\right)\cdot\tan\alpha_{\mathrm{x}}\left(y_p\right)\cdot\mathrm{d}\,\delta_{\mathrm{D}}\left(y_p,D\right)+\cos\left(\delta_{\mathrm{D}}\left(y_p,D\right)\right)\cdot\mathrm{d}\tan\alpha_{\mathrm{x}}\left(y_p\right)+\frac{2\cdot p_{\mathrm{zu1}}\cdot D}{y_{\mathrm{x}}\left(y_{\mathrm{p}}\right)^3} \tag{108}$$

Then, Formulae (109) and (110) can be determined

$$C_{\mathrm{eq1D}}\left(y_{\mathrm{p}},D\right)=\cos^3\alpha_{\mathrm{D}}\left(y_{\mathrm{p}},D\right)\cdot\cos\left(\delta_{\mathrm{D}}\left(y_{\mathrm{p}},D\right)\right)\cdot\frac{\mathrm{d}\tan\alpha_{\mathrm{D}}\left(y_{\mathrm{G}},D\right)}{\mathrm{d}\,y_{\mathrm{x}}\left(y_{\mathrm{G}}\right)} \tag{109}$$

$$C_{\mathrm{eq1D}}\left(y_{\mathrm{p}},D\right)=\cos^3\alpha_{\mathrm{D}}\left(y_{\mathrm{p}},D\right)\cdot\cos\left(\delta_{\mathrm{D}}\left(y_{\mathrm{p}},D\right)\right)\cdot\left[-\sin\left(\delta_{\mathrm{D}}\left(y_{\mathrm{p}},D\right)\right)\cdot\tan\alpha_{\mathrm{x}}\left(y_{\mathrm{p}}\right)\cdot\mathrm{d}\,\delta_{\mathrm{D}}\left(y_{\mathrm{p}},D\right)+\cos\left(\delta_{\mathrm{D}}\left(y_{\mathrm{p}},D\right)\right)\cdot\mathrm{d}\tan\alpha_{\mathrm{x}}\left(y_{\mathrm{p}}\right)-\frac{p_{\mathrm{zu1}}\cdot D}{y_{\mathrm{x}}\left(y_{\mathrm{p}}\right)^3}\right] \tag{110}$$

For $\mathrm{d}\tan\alpha_{\mathrm{x}}\left(y_{\mathrm{p}}\right)$ see 7.8.2.

10.5.2 Curvature for the worm wheel at a point in an offset plane

To determine the radius of curvature of the worm wheel, the Euler-Savary geometric construction is used (see Figure 31).

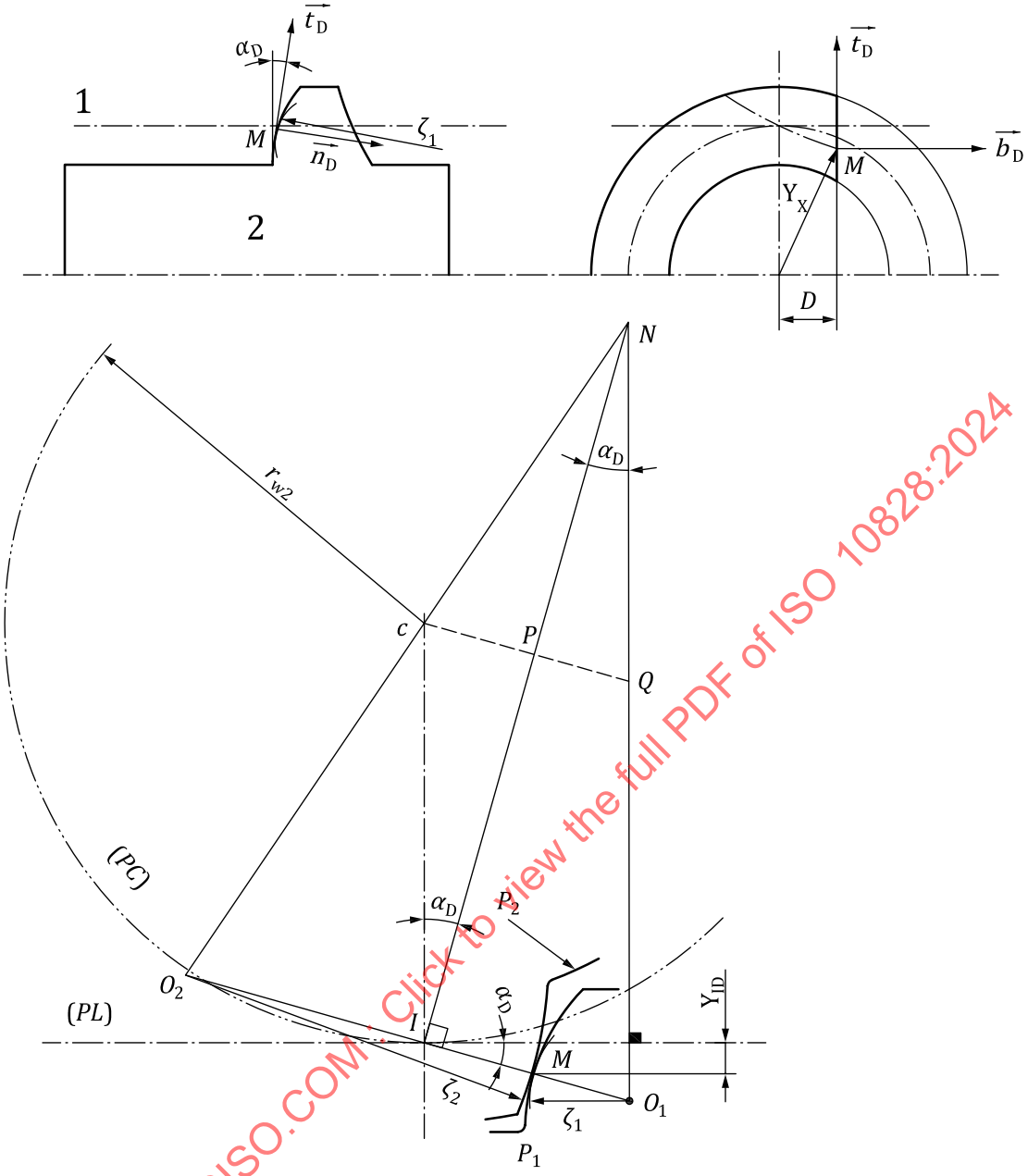

Key

(*P*1) offset profile of worm

(*P*2) worm wheel profile conjugate to the offset profile of worm

(*PC*) pitch circle of the worm wheel

(*PL*) pitch line of worm

I pitch point

Figure 31 — Radius of curvature in an offset plane

In an offset plane, at a point M of path of contact, the centre of curvature of the worm wheel profile resulting from the enveloping curve (envelope) of the worm profile, is the same as the centre of curvature 0_2 of the trajectory of the centre of curvature 0_1 of the worm profile as shown in Formulae (111) and (112).

$$C_{eq2D}\left(y_p,D\right)=\frac{1-C_{eq1D}\left(y_p,D\right)\cdot\left(\frac{y_{lD}\left(y_p,D\right)}{\sin\alpha_D\left(y_p,D\right)}+r_{w2}\cdot\sin\alpha_D\left(y_p,D\right)\right)}{r_{w2}\cdot\sin\alpha_D\left(y_p,D\right)-\frac{y_{lD}\left(y_p,D\right)}{\sin\alpha_D\left(y_p,D\right)}\cdot\left(1-\frac{y_{lD}\left(y_p,D\right)\cdot C_{eq1D}\left(y_p,D\right)}{\sin\alpha_D\left(y_p,D\right)}\right)}=\frac{1}{\rho_2\left(y_p,D\right)} \quad (111)$$

With:

$$\sin\alpha_D\left(y_p,D\right)=\sin\left(\arctan\left(\tan\alpha_D\left(y_p,D\right)\right)\right) \quad (112)$$

10.5.3 Equivalent radius of curvature in an offset plane

It is given in Formula (113):

$$R_{eqD}\left(y_p,D\right)=\frac{1}{C_{eq1D}\left(y_p,D\right)+C_{eq2D}\left(y_p,D\right)} \quad (113)$$

10.6 Singularities of worm gear mesh

10.6.1 Point of zero pressure angle

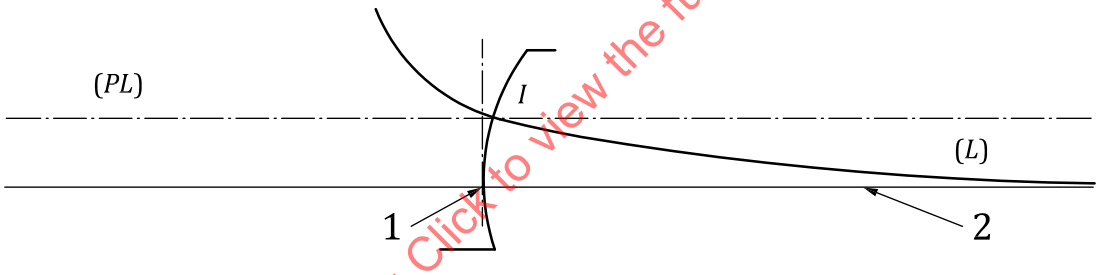

Key

(*PL*)	pitch line of worm
I	pitch point
(*L*)	path of contact
1	point of zero pressure angle
2	asymptote

Figure 32 — Point of zero pressure angle

The presence of a point of an offset profile with zero pressure angle gives a very flat path of contact as shown in Figure 32. There is an asymptotic direction above the point of zero pressure angle.

The calculation of the point of the worm in the offset plane with pressure angle equal to zero is only valid if $D > 0$.

It is based on the calculation of the point where $\tan\alpha_D\left(ynul,D\right)=0$ in each offset plane.

The algorithm is given in Table 7.

Table 7 — Algorithm for A, I, N and C and K profiles

A, I, N profiles	C and K profiles
$ZERO(y_x) =$ $D_{min} = 0$ $D_{max} = y_x$ $D_{nul} = 0{,}5 \cdot (D_{min} + D_{max})$ DO WHILE $\lvert \tan\alpha_D(y_x, D_{nul}) \rvert > 0{,}000\,000\,1$ IF $\tan\alpha_D(y_x, D_{nul}) > 0$ THEN $D_{min} = D_{nul}$ IF $\tan\alpha_D(y_x, D_{nul}) < 0$ THEN $D_{max} = D_{nul}$ $D_{nul} = \min(0{,}5 \cdot (D_{min} + D_{max}), y_x)$ END DO RETURN D_{nul}	$ZERO\_KC(y_x) =$ $D_{min} = 0$ $D_{max} = y_x$ $D_{nul} = 0{,}5 \cdot (D_{min} + D_{max})$ DO WHILE $\lvert \tan\alpha_D(y_x, D_{nul}) \rvert > 0{,}000\,000\,1$ IF $\tan\alpha_D(y_x, D_{nul}) > 0$ THEN $D_{min} = D_{nul}$ IF $\tan\alpha_D(y_x, D_{nul}) < 0$ THEN $D_{max} = D_{nul}$ $D_{nul} = \min(0{,}5 \cdot (D_{min} + D_{max}), y_x)$ END DO RETURN D_{nul}

The coordinate of the point of zero pressure angle is obtained by calculation $x'_D(ynul, D)$ and $y_D(ynul, D)$ [see Formulae (90) and (82)].

For the different offset planes (with $D > 0$), the points of zero pressure angle give the line of zero pressure angle.

For profile I the line of zero pressure angle is a horizontal line tangent to the cylinder base.

10.6.2 Loss of contact

The zero-pressure angle gives a very flat path of contact which can give a limitation of the gear mesh (see Figure 33).

This phenomenon can only appear for offset planes with $D > 0$. This can be a limitation of the active face width of worm wheel.

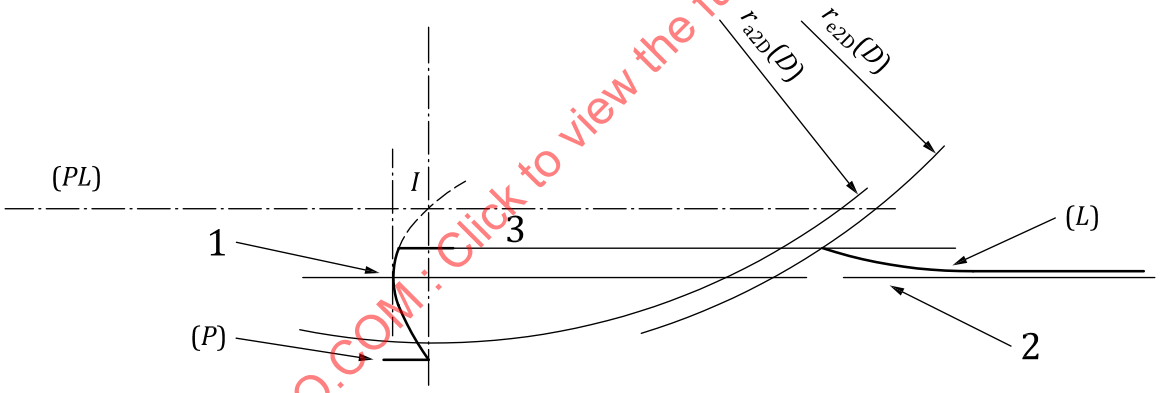

Key

(*PL*) pitch line of the worm
(*L*) path of contact
I pitch point
(*P*) offset profile of worm
3 tip circle
1 point of zero pressure angle
2 asymptote to the path of contact

Figure 33 — Limitation of gear mesh by the point of zero pressure angle

This phenomenon can appear for offset planes with $D > 0$ and close to the border of face width of the worm wheel.

The process to detect such case is as follows:

— Determine the point of path of contact for $y_p = r_{a1}$ (point B on Figure 28) with Formula (92), $x_{laD} = x_{lD}(r_{a1}, D)$;

— Calculate the radius of worm wheel conjugate to point B, tip of the worm profile in the offset plane $r_{a2D}(D) = \sqrt{(x_{lD}(r_{a1}, D))^2 + \left(r_{w2} - y_{lD}(r_{a1}, D)\right)^2}$;

— If $r_{a2D} > r_{e2D}$ there is no point of contact with the worm in the offset plane as in Figure 33, otherwise the start of active profile (point A) exists as in Figure 28.

10.6.3 Cusp

In certain circumstances, a limitation of conjugate action can appear due to the fact that the path of contact presents a cusp as shown in Figure 34.

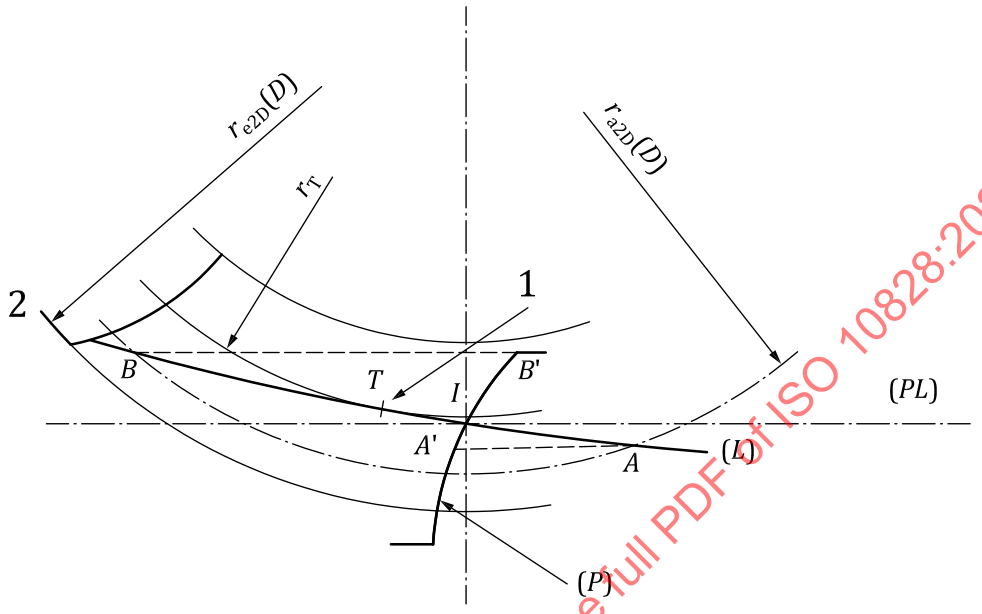

Key

1	point of tangency: cusp
2	worm wheel profile
(*PL*)	pitch line of worm
(*L*)	path of contact
I	pitch point
(*P*)	offset profile of worm (rack profile)

Figure 34 — Cusp effect

This effect can appear when the path of contact is flat; C profile is more sensitive to this effect than other profile types. It produces a limitation of the contact ratio because the path of contact is limited to the points between A and T. The potential of contact between T and B is lost.

Calculation of the cusp point of the worm wheel in the offset plane is valid for all the face width of the worm wheel. It is based on the calculation of the minimum value of the radius of the conjugate worm wheel in each offset plane.

To obtain this minimum value, it should be determined when the derivative of $r_{M2D}(y_p, D)$ (see Formula (93)) according to y_p is equal to zero as shown in Formula (114).

$$\mathrm{d}r_{M2D}(y_p,D)=\frac{1}{r_{M2D}(y_p,D)}\cdot\left[-(a_w-y_D(y_p,D))\cdot\mathrm{d}\,y_D(y_p,D)\right]+\left(\frac{y_D(y_p,D)-r_{w1}}{\tan\alpha_D(y_p,D)}\right)\cdot\frac{1}{\tan\alpha_D(y_p,D)^2}\cdot\left[\mathrm{d}\,y_D(y_p,D)\cdot\tan\alpha_D(y_p,D)-(y_D(y_p,D)-r_{w1})\cdot(1+\tan\alpha_D(y_p,D)\right] \quad (114)$$

The algorithm is given in Table 8:

Table 8 — Algorithm for A, I, N and C and K profiles

A,I,N profile types	C and K profile types
$CUSP(D)=$ $y_{min}=r_{w1}$ $y_{max}=6\cdot r_{a1}$ $y_{cusp}=0{,}5\cdot(y_{min}+y_{max})$ DO WHILE $\lvert \mathrm{d}\,r_{M2D}(y_{cusp},D)\rvert>0{,}000\,000\,1$ IF $\mathrm{d}\,r_{M2D}(y_{cusp},D)<0$ THEN $y_{min}=y_{cusp}$ IF $\mathrm{d}\,r_{M2D}(y_{cusp},D)>0$ THEN $y_{max}=y_{cusp}$ $y_{cusp}=0{,}5\cdot(y_{min}+y_{max})$ END DO RETURN y_{cusp}	$CUSP\_K(D)=$ $y_{min}=R_{GrindK}(R_{Gm},m_{x1},r_{w1})$ $y_{max}=R_{Gm}-6\cdot m_{x1}$ $y_{cusp}=0{,}5\cdot(y_{min}+y_{max})$ DO WHILE $\lvert \mathrm{d}\,r_{M2D}(y_{cusp},D)\rvert>0{,}000\,000\,1$ IF $\mathrm{d}\,r_{M2D}(y_{cusp},D)>0$ THEN $y_{min}=y_{cusp}$ IF $\mathrm{d}\,r_{M2D}(y_{cusp},D)<0$ THEN $y_{max}=y_{cusp}$ $y_{cusp}=0{,}5\cdot(y_{min}+y_{max})$ END DO RETURN y_{cusp} $CUSP\_C(D)=$ $y_{min}=R_{GrindC}(R_{Gm},m_{x1},r_{w1})$ $y_{max}=R_{Gm}-\rho\cdot\sin\alpha_{0n}$ $y_{cusp}=0{,}5\cdot(y_{min}+y_{max})$ DO WHILE $\lvert \mathrm{d}\,r_{M2D}(y_{cusp},D)\rvert>0{,}000\,000\,1$ IF $\mathrm{d}\,r_{M2D}(y_{cusp},D)>0$ THEN $y_{min}=y_{cusp}$ IF $\mathrm{d}\,r_{M2D}(y_{cusp},D)<0$ THEN $y_{max}=y_{cusp}$ $y_{cusp}=0{,}5\cdot(y_{min}+y_{max})$ END DO RETURN y_{cusp}

The coordinate of the cusp is obtained by calculation $x_D(ycusp, D)$ and $y_D(ycusp, D)$ [see Formulae (90) and (82)].

For the different offset planes, the cusps give the line of cusp points (see Figure 35). This line shall be outside of the zone of contact otherwise it limits the maximum potential contact and reduces the load capacity.

At each point of cusp, the equivalent radius of curvature is equal to zero the other reason to avoid this line in the zone of contact.

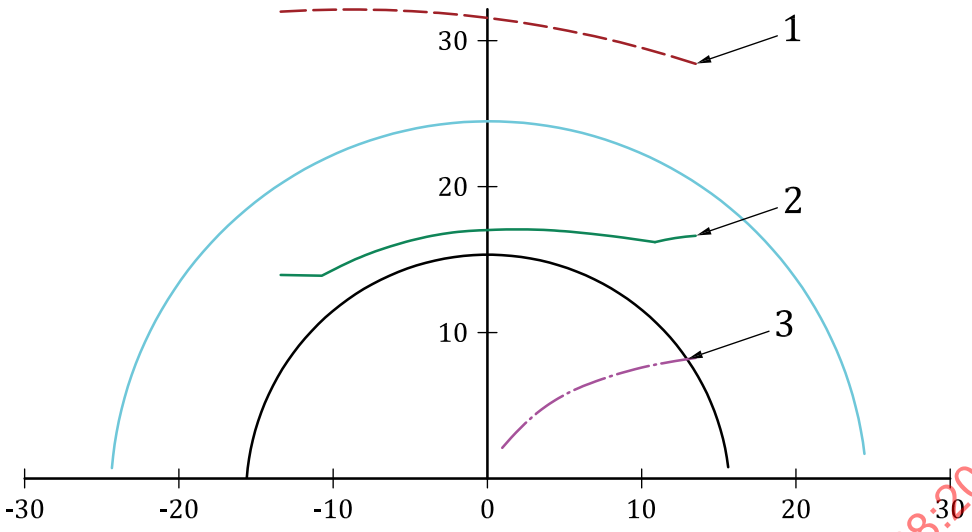

Key

1	line of cusp points
2	line of start of active profile points or start of zone of contact
3	line of zero pressure angle points
In BLACK	it is the root cylinder of the worm.
In BLUE	it is the outside cylinder of the worm.
In RED	(dashed line key 1) it is the limit given by the cusp. If this line is crossing the outside cylinder of the worm, there is a limitation of gear mesh. For the point of contact closed to the cusp line, the radius of curvature is closed to zero.
In GREEN	(continuous line key 2) it is the limit given by the root active radii on the worm. Normally the lines of contact are between that line and the outside circle of the worm in BLUE.
In MAGENTA	(dashed dot line key 3) it is the limit given by the zero-pressure angle. When this line is near root active lines, there is a limitation of gear mesh.

Figure 35 — Cusp line, zero pressure angle line, active root line for worm

The changes of line zero pressure angle and of cusp line according to profile types are shown in Annex E.

11 Geometry of contact

11.1 General

In fact, the development of the formulae for the profile of the worm is a function of two parameters y_p and D.

With the partial derivative according to these two parameters of the vector which define the coordinate vector of a point of the worm, given in Formula (115), two vectors of the tangential plane to the worm can be obtained.

$$\overrightarrow{P\left(y_p, D\right)} = \begin{pmatrix} x_D\left(y_p, D\right) \\ y_D\left(y_p, D\right) \\ D \end{pmatrix} \tag{115}$$

11.2 Tangent plane at point of contact

With the derivation according to y_p as shown in Formula (116):

$$\overrightarrow{T1(y_p,D)}=\begin{pmatrix} dx_D(y_p,D) \\ dy_D(y_p,D) \\ 0 \end{pmatrix} \tag{116}$$

And $TD1$ the normalised vector is obtained from Formula (117):

$$\overrightarrow{TD1(y_p,D)}=\frac{\overrightarrow{T1(y_p,D)}}{\left|\overrightarrow{T1(y_p,D)}\right|} \tag{117}$$

With the derivation according to D given by Formulae (118) to (120):

$$dDx_D(y_p,D)=\frac{p_{zu1}}{\cos(\delta_D(y_p,D))\cdot y_x(y_p)} \tag{118}$$

$$dDy_D(y_p,D)=-\tan(\delta_D(y_p,D)) \tag{119}$$

$$\overrightarrow{T2(y_p,D)}=\begin{pmatrix} dDx_D(y_p,D) \\ dDy_D(y_p,D) \\ 1 \end{pmatrix} \tag{120}$$

And $TD2$, the normalised vector is obtained from Formula (121):

$$\overrightarrow{TD2(y_p,D)}=\frac{\overrightarrow{T2(y_p,D)}}{\left|\overrightarrow{T2(y_p,D)}\right|} \tag{121}$$

11.3 Normal plane at point of contact

The unit normal vector to the point of contact: (orientation from the inside to the outside of the worm) is given by Formulae (122) to (124):

$$\overrightarrow{NORMAL(y_p,D)}=\frac{\overrightarrow{TD2(y_p,D)}\times\overrightarrow{TD1(y_p,D)}}{\left|\overrightarrow{TD2(y_p,D)}\times\overrightarrow{TD1(y_p,D)}\right|} \tag{122}$$

$$nNxy(y_p,D)=\sqrt{(NORMAL(y_p,D)_1)^2+(NORMAL(y_p,D)_2)^2} \tag{123}$$

$$\overrightarrow{NormalNxy(y_p,D)}=\begin{pmatrix} \frac{NORMAL(y_p,D)_1}{nNxy(y_p,D)} \\ \frac{NORMAL(y_p,D)_2}{nNxy(y_p,D)} \\ 0 \end{pmatrix} \tag{124}$$

NOTE $\overrightarrow{NormalNxy(y_p,D)}$ is the common normal vector to conjugate profiles in the offset plane at the point of contact.

11.4 Zone of contact

The zone of contact is limited in each offset plane by the active radius at the root of the worm and the tip radius of the worm or the cusp radius when there is limited conjugate contact.

In the longitudinal direction (along the face width of the worm wheel), the limitation is the face width of the worm wheel, or the tip radius of the worm (see Figures 36, 38 and 39). In case of important value of face width, the cusp line or/and the line of zero pressure angle, can be in the gear mesh area and then there is limited conjugate contact area (see Figure 40).

The zone of contact is the surface defined by all the path of contact in the different offset planes. It is limited by the tip cylinder of the worm and the external surface of the worm wheel defined by the external cylinder and external throat surface.

In the case of chamfering, those limits are respectively the addendum active cylinder of the worm and the active tip line at the tip of the worm wheel teeth.

In case of cusp in the gear mesh, the zone of contact is limited by the cusp.

In each offset plane, it can be defined as follows:

— The start of active profile for the worm by the intersection of the path of contact with the external diameter of the worm wheel in this plane (either defined by the external cylinder or the throat diameter of the worm wheel). The result is that the radius of SAP of the worm is defined by the closest point to the axis of the worm of all offset planes. See Figure 35.

— The start of active profile for the worm wheel (SAP worm wheel) by either the intersection of the path of contact with the external diameter of the worm in this plane or by the point of tangency cusp if there is a cusp (see Figure 34). The result is that for the worm wheel there is a distinct SAP in each offset plane.

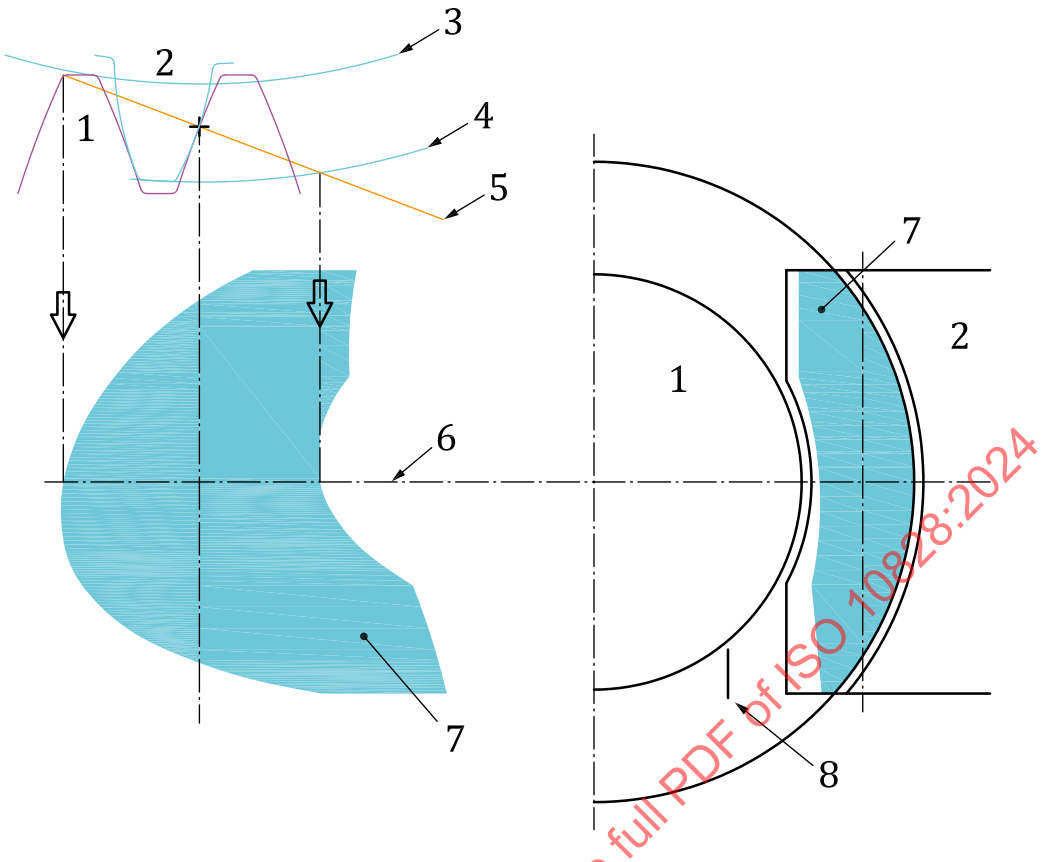

Key

1 worm
2 wheel
3 form circle
4 outside diameter
5 path contact
6 axis of worm
7 zone of contact
8 line of zero pressure angles

Figure 36 — Zone of contact

The lines of contact are moving on the surface limited by the zone of contact.

In each offset plane, the zone of contact (see Figures 36 and 40) is limited by the start of active profile (point A in Figure 28) and the end of active profile (point B in Figure 28) except if there is a cusp (point T of Figure 34). In the last case, the zone of contact is truncated as in Figure 40.

This calculation shall be done for all offset planes. It is recommended to use between 30 and 80 offset planes uniformly distributed along the worm wheel face width.

In continuation of the algorithm in 7.9, the following algorithm in Figure 37 can be executed in each offset plane D_i:

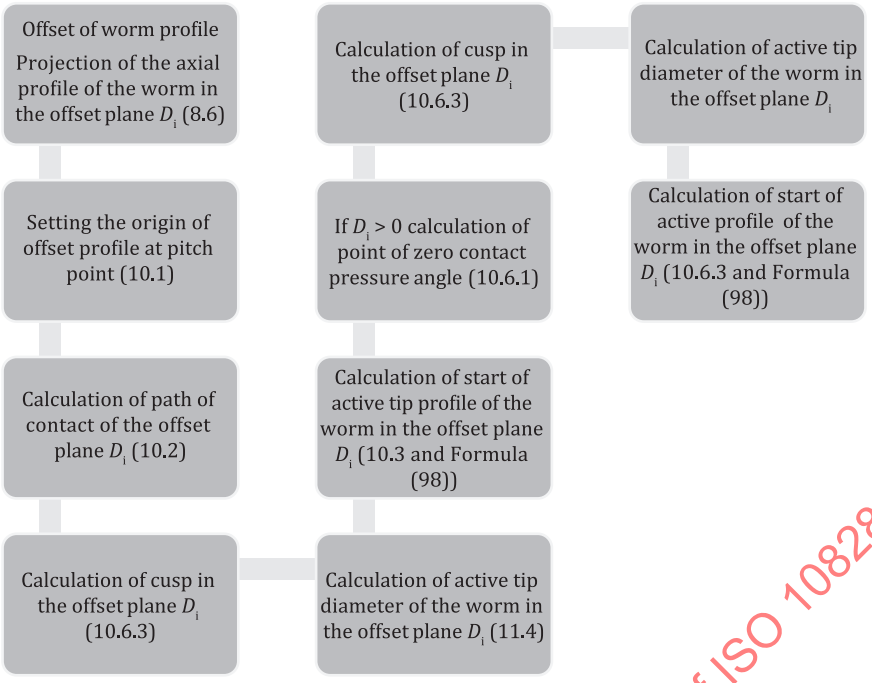

NOTE The zone of contact in an offset plane is delimited by the limit points as indicated in 11.4.

Figure 37 — Algorithm for the calculation of zone of contact

The changes of zone of contact according to profile types are shown in Annex F.

11.5 Lines of contact

A line of contact is composed of all the conjugate points between the flank of the worm and the conjugate flank of the worm wheel for a relative position of the worm gear set.

Several threads of the worm can be simultaneously in contact.

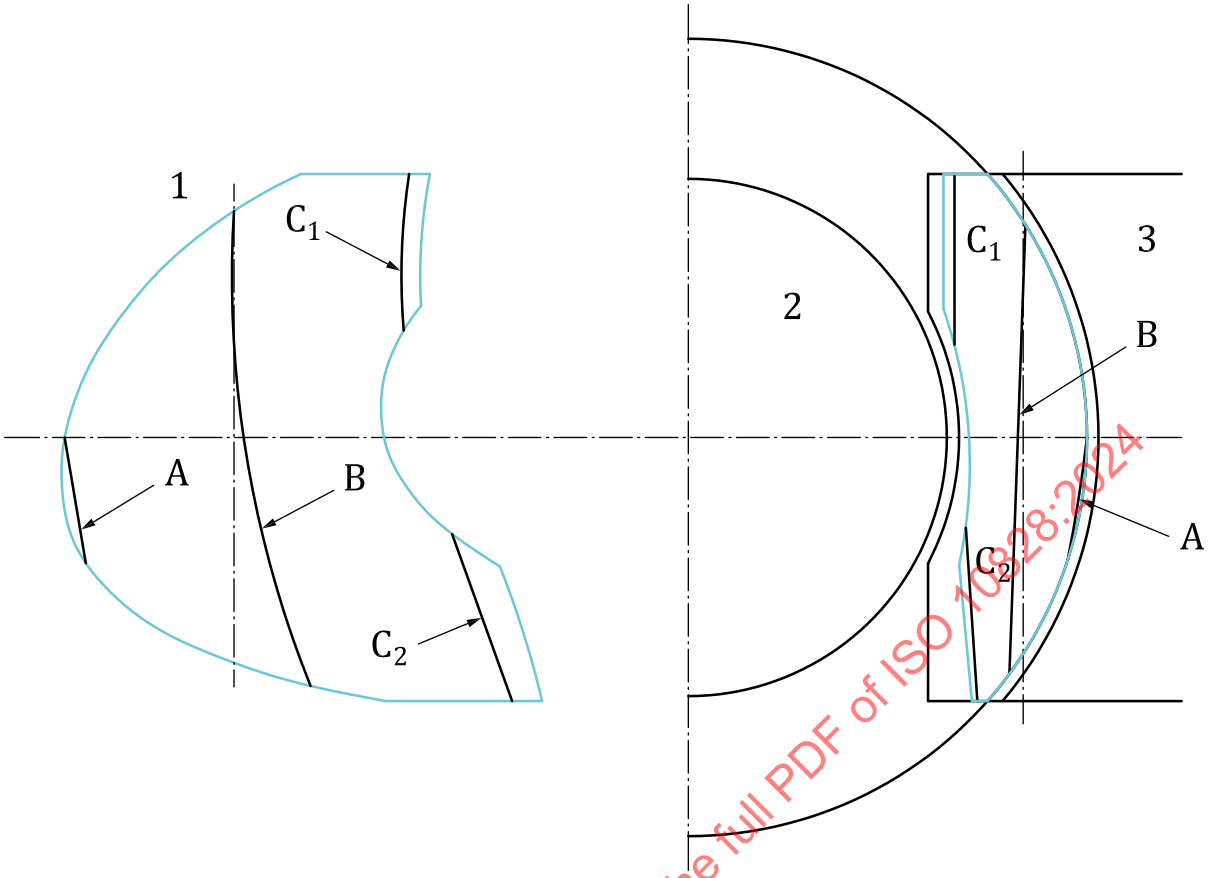

Key

1 zone of contact
2 worm
3 wheel

NOTE 1 A, B, C_1 and C_2 are instantaneous lines of contact.

NOTE 2 Three threads are in contact for this relative position.

Figure 38 — Zone of contact and lines of contact for one relative position of worm and worm wheel

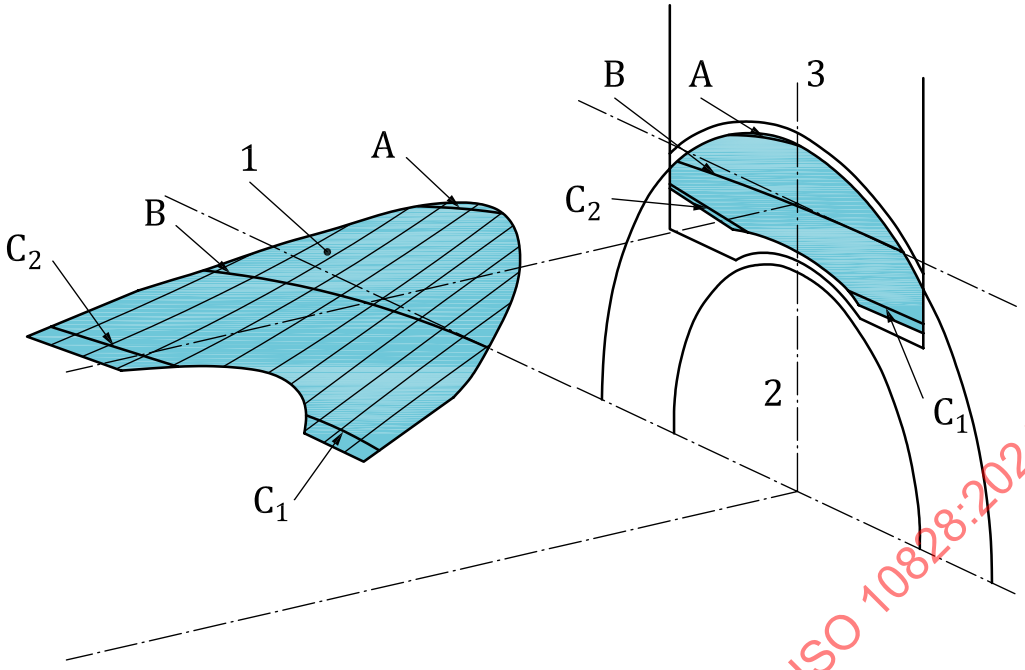

Key

1 zone of contact with path of contact in different offset planes

2 worm

3 worm wheel

NOTE A, B, C_1 and C_2 are instantaneous lines of contact.

Figure 39 — Path of contact, zone of contact and lines of contact for one relative position of worm and worm wheel

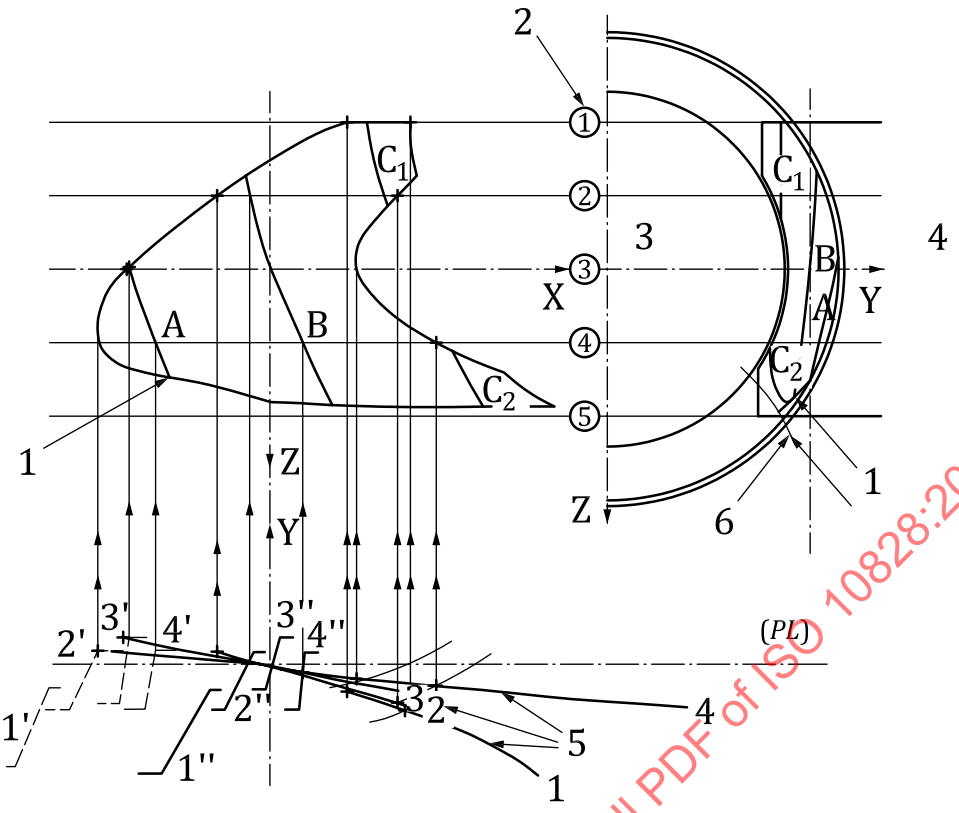

Key

1	cusp
2	offset planes
3	worm
4	worm wheel
5	path of contact
6	line of zero pressure angles
(*PL*)	pitch line

NOTE A, B, C_1 and C_2 are instantaneous lines of contact.

Figure 40 — Path of contact, zone of contact and lines of contact for one relative position of worm and worm wheel

The formula of the lines of contact $\mathrm{Fcont}\left(y_\mathrm{p}, D\right)=0$ is given by Formula (125):

$$\mathrm{Fcont}\left(y_\mathrm{p}, D\right)=x_\mathrm{lD}\left(y_\mathrm{p}, D\right)\cdot\tan\alpha_\mathrm{D}\left(y_\mathrm{p}, D\right)+y_\mathrm{D}\left(y_\mathrm{p}, D\right)-r_{w1} \tag{125}$$

For the coordinates of a point of contact, only the point along the path of contact (in fact for a relative position between the worm and the worm wheel, there are one or three points of contact) is considered.

For the worm (0M) they are given by Formula (126):

$$\overrightarrow{M_1(y_p, D)} = \begin{pmatrix} x_{lD}(y_p, D) \\ y_D(y_p, D) \\ D \end{pmatrix} \quad (126)$$

For the worm wheel (0_2M) they are given by Formula (127):

$$\overrightarrow{M_2(y_p, D)} = \begin{pmatrix} x_{lD}(y_p, D) \\ -a_w + y_D(y_p, D) \\ D \end{pmatrix} \quad (127)$$

The determination of lines of contact is done by the determination of points of contact.

First of all, the relative position of the worm is set up by the parameter $\Delta x_D(D)$ of Formula (90). This value is set up in order to obtain the first line of contact tangent to the zone of contact (see Figure 41); this is the initial value $\Delta x_{Dinit}(D)$.

To determine the first line of contact, the calculation is made in all the offset planes used to determine the zone of contact. In each offset plane, the initial value of y_p to calculate $\mathrm{Fcont}(y_p, D) = 0$ is initialized between the values obtained for the start of active profile (point A in Figure 28) and the end of active profile (point B in Figure 28) or the cusp (point T of Figure 34). So, the point of contact is obtained easily.

To obtain the next line of contact, the value of $\Delta x_{Dinit}(D)$ is decreased by the axial pitch p_{x1}, and all the points of contact are determined in each offset plane. Continue by decreasing axial position of the active worm flank by one axial pitch p_{x1} no more contact points exist in the zone of contact.

To study a second relative position of the worm and the worm wheel, the initial value $\Delta x_{Dinit}(D)$ is decreased by a portion of the axial pitch p_{x1}, p_{x1}/n where n is an integer corresponding to the number of relative positions to study (e.g. for 10 relative positions to study n=10). The process then starts again with this new initial value.

The variations of instantaneous length of contact lines and the distribution of equivalent radius of curvature according to profile types are shown in Annex F.

11.6 Contact ratio

In a worm gear, the contact ratio is obtained by the ratio of the distance between the two positions of the worm defined when the first line of contact is tangent to the zone of contact and the last line of contact is tangent to the zone of contact (see Figure 41) divided by the axial pitch.

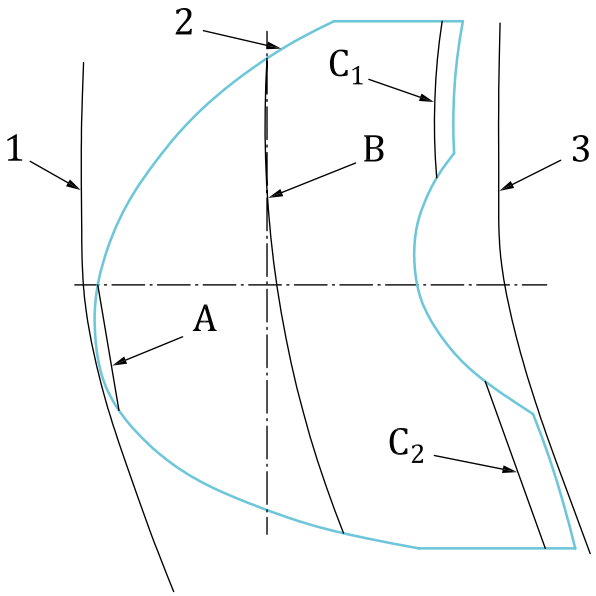

Key

1 last line in contact
2 zone of contact
3 first line in contact

NOTE A, B, C_1 and C_2 are instantaneous lines of contact.

Figure 41 — Contact ratio

11.7 Tangent vector to the line of contact

To determine the vector tangent to the line of contact, the formula of the lines of contact $\mathrm{Fcont}\left(y_p, D\right)=0$ shall be considered.

The partial derivatives of $\mathrm{Fcont}\left(y_p, D\right)$ shall be evaluated for the point the contact. It means that in the Formulae (128) to (131), $x_D\left(y_p, D\right)$ shall be replaced with $x_{1D}\left(y_p, D\right)$ which satisfies the contact formula.

$$\frac{\partial \mathrm{Fcont}\left(y_p, D\right)}{\partial y_p}=x_{1D}\left(y_p, D\right)\cdot \mathrm{d}\tan\alpha_D\left(y_p, D\right)+\mathrm{d}x_D\left(y_p, D\right)\cdot\tan\alpha_D\left(y_p, D\right)+\mathrm{d}y_D\left(y_p, D\right) \quad (128)$$

$$\frac{\partial \mathrm{Fcont}\left(y_p, D\right)}{\partial D}=x_{1D}\left(y_p, D\right)\cdot \mathrm{d}D\tan\alpha_D\left(y_p, D\right)+\mathrm{d}Dx_D\left(y_p, D\right)\cdot\tan\alpha_D\left(y_p, D\right)+\mathrm{d}Dy_D\left(y_p, D\right) \quad (129)$$

With $\mathrm{d}x_D\left(y_p, D\right)$, $\mathrm{d}y_D\left(y_p, D\right)$, $\mathrm{d}\tan\alpha_D\left(y_p, D\right)$, $\mathrm{d}Dx_D\left(y_p, D\right)$, $\mathrm{d}Dy_D\left(y_p, D\right)$ respectively given by Formulae (84), (85), (108), (118), (119) and:

$$\mathrm{d}D\delta_D\left(y_p, D\right)=\frac{1}{y_x\left(y_p\right)\cdot\cos\left(\delta_D\left(y_p, D\right)\right)} \quad (130)$$

then:

$$\mathrm{d}D\tan\alpha_{\mathrm{D}}\left(y_{\mathrm{p}},D\right)=-\sin\left(\delta_{\mathrm{D}}\left(y_{\mathrm{p}},D\right)\right)\cdot\tan\alpha_{\mathrm{x}}\left(y_{\mathrm{p}}\right)\cdot\mathrm{d}D\delta_{\mathrm{D}}\left(y_{\mathrm{p}},D\right)-\frac{p_{\mathrm{zu1}}}{y_{\mathrm{x}}\left(y_{\mathrm{p}}\right)^{2}} \tag{131}$$

This is obtained by considering the derivative of $\mathrm{Fcont}\left(y_{\mathrm{p}},D\right)=0$ at the point of contact, and it gives the relation between D and y_{p} along the line of contact as the relation of partial derivatives of $\mathrm{Fcont}\left(y_{\mathrm{p}},D\right)$ as shown in Formula (132):

$$\mathrm{d}Dym\left(y_{\mathrm{p}},D\right)=\frac{dD}{dy_{\mathrm{p}}}=-\frac{\dfrac{\partial\mathrm{Fcont}\left(y_{\mathrm{p}},D\right)}{\partial y_{\mathrm{p}}}}{\dfrac{\partial\mathrm{Fcont}\left(y_{\mathrm{p}},D\right)}{\partial D}}=-\frac{\mathrm{d}y\mathrm{Fcont}\left(y_{\mathrm{p}},D\right)}{\mathrm{d}D\mathrm{Fcont}\left(y_{\mathrm{p}},D\right)} \tag{132}$$

To obtain the tangent vector to the lines of contact, the total derivative of $\overrightarrow{P\left(y_{\mathrm{p}},D\right)}$ [see Formula (115)] according to parameter y_{p} shall be taken as shown in Formula (133):

$$\overrightarrow{Tcont\left(y_{\mathrm{p}},D\right)}=\begin{pmatrix}\dfrac{dx_{\mathrm{D}}\left(y_{\mathrm{p}},D\right)}{dy_{\mathrm{p}}}=\dfrac{\partial x_{\mathrm{D}}\left(y_{\mathrm{p}},D\right)}{\partial y_{\mathrm{p}}}+\dfrac{\partial x_{\mathrm{D}}\left(y_{\mathrm{p}},D\right)}{\partial D}\dfrac{dD}{dy_{\mathrm{p}}}\\ \dfrac{dy_{\mathrm{D}}\left(y_{\mathrm{p}},D\right)}{dy_{\mathrm{p}}}=\dfrac{\partial y_{\mathrm{D}}\left(y_{\mathrm{p}},D\right)}{\partial y_{\mathrm{p}}}+\dfrac{\partial y_{\mathrm{D}}\left(y_{\mathrm{p}},D\right)}{\partial D}\dfrac{dD}{dy_{\mathrm{p}}}\\ \dfrac{dz_{\mathrm{D}}\left(y_{\mathrm{p}},D\right)}{dy_{\mathrm{p}}}=\dfrac{\partial z_{\mathrm{D}}\left(y_{\mathrm{p}},D\right)}{\partial y_{\mathrm{p}}}+\dfrac{\partial z_{\mathrm{D}}\left(y_{\mathrm{p}},D\right)}{\partial D}\dfrac{dD}{dy_{\mathrm{p}}}\end{pmatrix}=\begin{pmatrix}\dfrac{\partial x_{\mathrm{D}}\left(y_{\mathrm{p}},D\right)}{\partial y_{\mathrm{p}}}+\dfrac{\partial x_{\mathrm{D}}\left(y_{\mathrm{p}},D\right)}{\partial D}\dfrac{dD}{dy_{\mathrm{p}}}\\ \dfrac{\partial y_{\mathrm{D}}\left(y_{\mathrm{p}},D\right)}{\partial y_{\mathrm{p}}}+\dfrac{\partial y_{\mathrm{D}}\left(y_{\mathrm{p}},D\right)}{\partial D}\dfrac{dD}{dy_{\mathrm{p}}}\\ \dfrac{dD}{dy_{\mathrm{p}}}\end{pmatrix} \tag{133}$$

$$=\begin{pmatrix}\mathrm{d}x_{\mathrm{D}}\left(y_{\mathrm{p}},D\right)+\mathrm{d}Dx_{\mathrm{D}}\left(y_{\mathrm{p}},D\right)\cdot\mathrm{d}Dym\left(y_{\mathrm{p}},D\right)\\ \mathrm{d}y_{\mathrm{D}}\left(y_{\mathrm{p}},D\right)+\mathrm{d}Dy_{\mathrm{D}}\left(y_{\mathrm{p}},D\right)\cdot\mathrm{d}Dym\left(y_{\mathrm{p}},D\right)\\ \mathrm{d}Dym\left(y_{\mathrm{p}},D\right)\end{pmatrix}$$

And the unit vector is given by Formula (134):

$$\overrightarrow{TNcont\left(y_{\mathrm{p}},D\right)}=\frac{\overrightarrow{Tcont\left(y_{\mathrm{p}},D\right)}}{\left|\overrightarrow{Tcont\left(y_{\mathrm{p}},D\right)}\right|} \tag{134}$$

Or by Formula (135) with derivatives of $\overrightarrow{P\left(y_{\mathrm{p}},D\right)}$ [see Formula (115)] according to parameter D:

$$\overrightarrow{Tcont1\left(y_{\mathrm{p}},D\right)}=\begin{pmatrix}\mathrm{d}Dx_{\mathrm{D}}\left(y_{\mathrm{p}},D\right)+\dfrac{\mathrm{d}Dx_{\mathrm{D}}\left(y_{\mathrm{p}},D\right)}{\mathrm{d}Dym\left(y_{\mathrm{p}},D\right)}\\ \mathrm{d}Dy_{\mathrm{D}}\left(y_{\mathrm{p}},D\right)+\dfrac{\mathrm{d}Dy_{\mathrm{D}}\left(y_{\mathrm{p}},D\right)}{\mathrm{d}Dym\left(y_{\mathrm{p}},D\right)}\\ 1\end{pmatrix} \tag{135}$$

And the unit vector is given by Formula (136):

$$\overrightarrow{TNcont1\left(y_{\mathrm{p}},D\right)}=\frac{\overrightarrow{Tcont1\left(y_{\mathrm{p}},D\right)}}{\left|\overrightarrow{Tcont1\left(y_{\mathrm{p}},D\right)}\right|} \tag{136}$$

NOTE $\overrightarrow{TNcont\left(y_{\mathrm{p}},D\right)}$ and $\overrightarrow{TNcont1\left(y_{\mathrm{p}},D\right)}$ are identical.

11.8 Normal plane at point of contact

As the contact is linear along the lines of contact, according to Euler's theory on curvatures of surface, the direction tangent to line of contact is one of the principal directions of curvature.

The second principal direction of curvature is normal to that one and can be obtain with the vector product between the tangent vector to the line of contact and the normal to the tangent plane of contact. Those three vectors $[\overrightarrow{TN\text{cont}(y_p,D)}, \overrightarrow{NORMAL(y_p,D)}, \overrightarrow{B(y_p,D)}]$ defines the trihedral of Darboux Ribaucour given by Formula (137):

$$\overrightarrow{B(y_p,D)} = \overrightarrow{TN\text{cont}(y_p,D)} \times \overrightarrow{\text{NORMAL}(y_p,D)} \tag{137}$$

At contact point, $\overrightarrow{B(y_p,D)}$ is normal to the line of contact in the common tangent plane to both flanks.

11.9 Principal equivalent radius of curvature

For a point of contact, the equivalent of curvature reaches minimum and maximum values called principal radii of curvature when its projection in the main planes is considered.

In a point of contact, those main planes are defined as follows:

— the maximum equivalent of curvature is always in the plane defined by the normal at the surface of the worm and the vector tangent to the instantaneous line of contact;

— the minimum equivalent of curvature is always in the plane defined by the normal at the surface of the worm and the vector normal to the instantaneous line of contact.

This equivalent radius of curvature in an offset plane (see 10.5) shall be projected in the two main planes of curvature, which are in this particular case

a) the plane normal to the instantaneous line of contact between the flanks of worm and worm wheel, crossing the studied point of contact,

b) the plane tangent to the instantaneous line of contact between the flanks of worm and worm wheel, crossing the studied point of contact, and

c) in this last plane, the curvature is zero because the contact is locally linear.

At each point of contact, three vectors can be defined in an offset plane as shown by Formulae (138) to (140):

— a tangent vector to the worm and worm wheel profile

$$\overrightarrow{t_D(y_p,D)} = \begin{pmatrix} \sin\alpha_D(y_p,D) \\ \cos(\arctan(\tan\alpha_D(y_p,D))) \\ 0 \end{pmatrix} \tag{138}$$

— a normal vector to the worm and worm wheel profile

$$\overrightarrow{n_D(y_p,D)} = \begin{pmatrix} \cos(\arctan(\tan\alpha_D(y_p,D))) \\ -\sin\alpha_D(y_p,D) \\ 0 \end{pmatrix} \tag{139}$$

— a vector normal to the offset plane

$$\overrightarrow{b_D(y_p,D)} = \begin{pmatrix} 0 \\ 0 \\ 1 \end{pmatrix} \tag{140}$$

The radius of curvature is projected along the normal to the point of contact contained in the offset plane.

First of all, the radius of curvature projected along the normal to the common tangent plane of conjugate flanks at the contact point shall be determined.

The angle of projection is obtained by the scalar product between the two normal vectors as shown in Formula (141):

$$\mathrm{Req1}\left(y_{\mathrm{p}},D\right)=\frac{\mathrm{Req}xy\left(y_{\mathrm{p}},D\right)}{\overrightarrow{\mathrm{NORMAL}\left(y_{\mathrm{p}},D\right)}\cdot\overrightarrow{\mathrm{Normal}Nxy\left(y_{\mathrm{p}},D\right)}} \tag{141}$$

Euler's formula on the radius of curvature of a surface is applicable. It gives the curvature C, as a function of the 2 principal curvatures C' and C'' and the angle ζ to direction of the curvature C' and the curvature C. The relation which classifies C' and C'' is: $C'' < C'$.

Euler's formula is Formula (142):

$$C=C^{'}\cdot\cos^{2}\left(\zeta\right)+C^{''}\cdot\sin^{2}\left(\zeta\right) \tag{142}$$

In this document, because the profiles are conjugate, there is always $C''=0$. The contact is linear and the radius of curvature along the line the contact is infinite or the curvature equal to zero as shown in Formula (143).

$$\mathrm{Req}\left(y_{\mathrm{p}},D\right)=\mathrm{Req1}\left(y_{\mathrm{p}},D\right)\cdot\left|\overrightarrow{t_{\mathrm{D}}\left(y_{\mathrm{p}},D\right)}\cdot\overrightarrow{B\left(y_{\mathrm{p}},D\right)}\right|^{2} \tag{143}$$

11.10 Calculation of the path of contact and zone of contact

The following procedure shall be applied in each offset plane D.

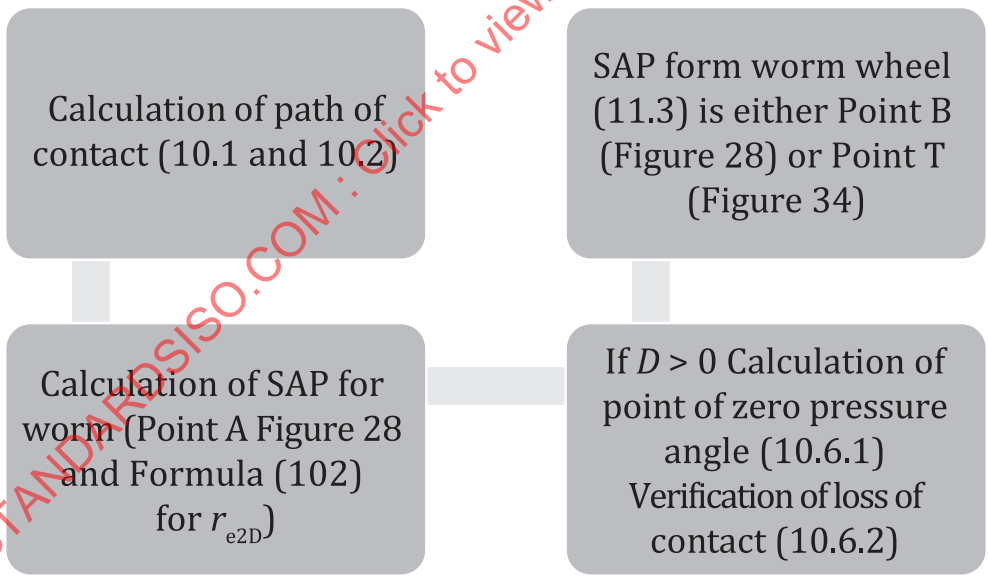

Figure 42 — Algorithm for the calculation of the path and zone of contact

SAP points are the limit of the zone of contact.

For the worm, it is possible to determine the minimum diameter for all SAP points (see 11.4).

11.11 Calculation of line of contact

For a given relative position of the worm and the worm wheel, it is possible to determine the lines of contact between the flanks of threads and worm wheel teeth.

The relative positions are initialised by the parameter $''x_{Dinit}(D)$ (see 11.5).

For the value $\Delta x_D(D)$ equal to $''x_{Dinit}(D)$ in Formula (90), the contact is just beginning in one point of SAP points of worm (see Figure 41). Then the first line of contact is obtained for the next thread. This means that $''x_{Dinit}(D)$ shall be increased by a value of axial pitch.

To determine the next line of contact $''x_{Dinit}(D)$ shall be again increased by a value of axial pitch p_{x1}. This process is carried out until the highest point of contact on a line of contact has reached the border of the zone of contact.

Then it is possible to re-initialise $\Delta x_D(D)$ to $''x_{Dinit}(D)$, increased by a $0{,}1 \cdot p_{x1}$ to set up a new relative initial position of the worm and the worm wheel and to restart the process.

In each point of contact, the followings value shall be determined:

— tangent vector to the line of contact (see 11.7);

— principal equivalent of radius of curvature (see 11.9);

— velocities at contact point (see Clause 12).

12 Velocities at contact point

12.1 Velocity of a point of worm

The angular velocity of the worm (rad/s) is given by Formula (144):

$$\omega_{w1} = \pi \cdot \frac{n_1}{30} \tag{144}$$

The angular velocity vector of the worm (rad/s) is given by Formula (145):

$$\overrightarrow{\omega_1} = \begin{pmatrix} \omega_{w1} \\ 0 \\ 0 \end{pmatrix} \tag{145}$$

Velocity of a point of the thread of the worm (in m/s) is given by Formula (146), with $\overrightarrow{M_1(y_p, D)}$ from Formula (126):

$$\overrightarrow{V_1(y_p, D)} = 10^{-3}\,\overrightarrow{\omega_1} \times \overrightarrow{M_1(y_p, D)} \tag{146}$$

12.2 Velocity of a point of worm wheel

The angular velocity of the worm wheel (rad/s) is given by Formula (147):

$$\omega_{w2} = \pi \cdot \frac{n_1}{30} \cdot \frac{z_1}{z_2} \tag{147}$$

The angular velocity vector of the worm wheel (rad/s) is given by (Formula (148):

$$\overrightarrow{\omega_2} = \begin{pmatrix} 0 \\ 0 \\ -\omega_{w2} \end{pmatrix} \tag{148}$$

The point of the worm wheel flank is given by (Formula 149):

$$\overrightarrow{M_2(y_p, D)} = \begin{pmatrix} x_{1D}(y_p, D) \\ -a_w + y_D(y_p, D) \\ D \end{pmatrix} \tag{149}$$

Velocity of a point of the tooth flank of the worm wheel (in m/s) is given by Formula (150):

$$\overrightarrow{V_2(y_p, D)} = 10^{-3}\,\overrightarrow{\omega_2} \times \overrightarrow{M_2(y_p, D)} \tag{150}$$

12.3 Relative velocity between two conjugate flanks

The relative velocity between the two flanks (in m/s) (this is the sliding velocity) is given by Formula (151) à (154):

$$\overrightarrow{V_s(y_p, D)} = \overrightarrow{V_1(y_p, D)} - \overrightarrow{V_2(y_p, D)} \tag{151}$$

This relative sliding velocity can be projected in the common tangent plane to the point of contact in two directions [Formulae (152) and (153)]:

— one normal to the line of contact, direction according to $\overrightarrow{B(y_p, D)}$;

— the second tangent to the line of contact, direction according to $\overrightarrow{TN\text{cont}(y_p, D)}$.

$$V_{1n}(y_p, D) = \overrightarrow{V_1(y_p, D)} \cdot \overrightarrow{B(y_p, D)} \tag{152}$$

$$V_{2n}(y_p, D) = \overrightarrow{V_2(y_p, D)} \cdot \overrightarrow{B(y_p, D)} \tag{153}$$

It results in the projection of these velocities on the normal to the common tangent plane at the point of contact are equal, as shown in Formula (154):

$$V_{sn}(y_p, D) = V_{1n}(y_p, D) - V_{2n}(y_p, D) = \overrightarrow{V_s(y_p, D)} \cdot \overrightarrow{B(y_p, D)} \tag{154}$$

12.4 Tangent to the path of contact

The direction of the velocity of points of contact is obtained with the determination of the tangent vector to the path of contact in an offset plane as shown in Formulae (155) and (156), with Formula (85):

$$\mathrm{d}\,y_{lD}(y_p, D) = \mathrm{d}\,y_{lD}(y_p, D) \tag{155}$$

$$\mathrm{d}x_{\mathrm{lD}}\left(y_{\mathrm{p}},D\right)=\frac{-1}{\tan\alpha_{\mathrm{D}}\left(y_{\mathrm{p}},D\right)^{2}}\cdot\left(\mathrm{d}y_{\mathrm{lD}}\left(y_{\mathrm{p}},D\right)\cdot\tan\alpha_{\mathrm{D}}\left(y_{\mathrm{p}},D\right)-y_{\mathrm{lD}}\left(y_{\mathrm{p}},D\right)\cdot\mathrm{d}\tan\alpha_{\mathrm{D}}\left(y_{\mathrm{p}},D\right)\right) \tag{156}$$

If $\psi_{D}\left(y_{p},D\right)$ is the angle between the direction of pitch line of worm and the tangent to the path of contact, Formulae (157) and (158) are applied:

$$\tan\psi_{D}\left(y_{p},D\right)=\frac{\mathrm{d}y_{\mathrm{lD}}\left(y_{\mathrm{p}},D\right)}{\mathrm{d}x_{\mathrm{lD}}\left(y_{\mathrm{p}},D\right)} \tag{157}$$

$$\mathrm{d}xD\,\mathrm{d}yD\left(y_{\mathrm{p}},D\right)=\frac{1}{\tan\psi_{\mathrm{D}}\left(y_{\mathrm{p}},D\right)} \tag{158}$$

12.5 Velocity of the contact point along the path of contact

Velocity of the contact point along the path of contact in an offset plane is given by Formulae (159):

$$\overrightarrow{V_{\mathrm{cD}}\left(y_{\mathrm{p}},D\right)}=\frac{10^{-3}\cdot\omega_{w1}.p_{\mathrm{z}2}}{\tan\alpha_{\mathrm{D}}\left(y_{\mathrm{p}},D\right)-\mathrm{d}xD\,\mathrm{d}yD\left(y_{\mathrm{p}},D\right)}\cdot\begin{pmatrix}\mathrm{d}xD\,\mathrm{d}yD\left(y_{\mathrm{p}},D\right)\\1\\0\end{pmatrix} \tag{159}$$

This velocity projected along the normal to the line of contact in the common tangent plane to flanks is given by Formula (160).

$$V_{\mathrm{cDn}}\left(y_{\mathrm{p}},D\right)=\overrightarrow{V_{\mathrm{cD}}\left(y_{\mathrm{p}},D\right)}\cdot\overrightarrow{B\left(y_{\mathrm{p}},D\right)} \tag{160}$$

12.6 Velocity of the point of contact

Velocity of the contact point on the worm is given by Formula (161):

$$V_{\mathrm{c1n}}\left(y_{\mathrm{p}},D\right)=V_{\mathrm{1n}}\left(y_{\mathrm{p}},D\right)-V_{\mathrm{cDn}}\left(y_{\mathrm{p}},D\right) \tag{161}$$

Velocity of the contact point on the worm wheel is given by Formula (162):

$$V_{\mathrm{c2n}}\left(y_{\mathrm{p}},D\right)=V_{\mathrm{2n}}\left(y_{\mathrm{p}},D\right)-V_{\mathrm{cDn}}\left(y_{\mathrm{p}},D\right) \tag{162}$$

where $V_{\mathrm{cDn}}\left(y_{\mathrm{p}},D\right)$ is the projection along the normal to the line of contact in the common tangent plane at the contact point.

The sum of velocities at contact point (in the direction normal to the line of contact in the tangent plane to tooth flanks) is given by Formula (163):

$$V_{\mathrm{SUMn}}\left(y_{\mathrm{p}},D\right)=\left|V_{\mathrm{c1n}}\left(y_{\mathrm{p}},D\right)+V_{\mathrm{c2n}}\left(y_{\mathrm{p}},D\right)\right| \tag{163}$$

Annex A
(informative)

Parameters and derivatives of formulae for A, I, N profile types

A.1 General

This annex contains details for the formula of profile in the axial plane of the worm ox X-Y plane according to the conventions of Figure 9.

A.2 Formulae of the profile in the X-Y plane for worms with A profile type

See Figures 10 to 11 and A.1 for the setting for worms with A profile type, where:

α_{0t} is the tool transverse pressure angle for A;

α_n is the normal pressure angle [see Formula (19)];

γ_{m1} is the reference lead angle of worm.

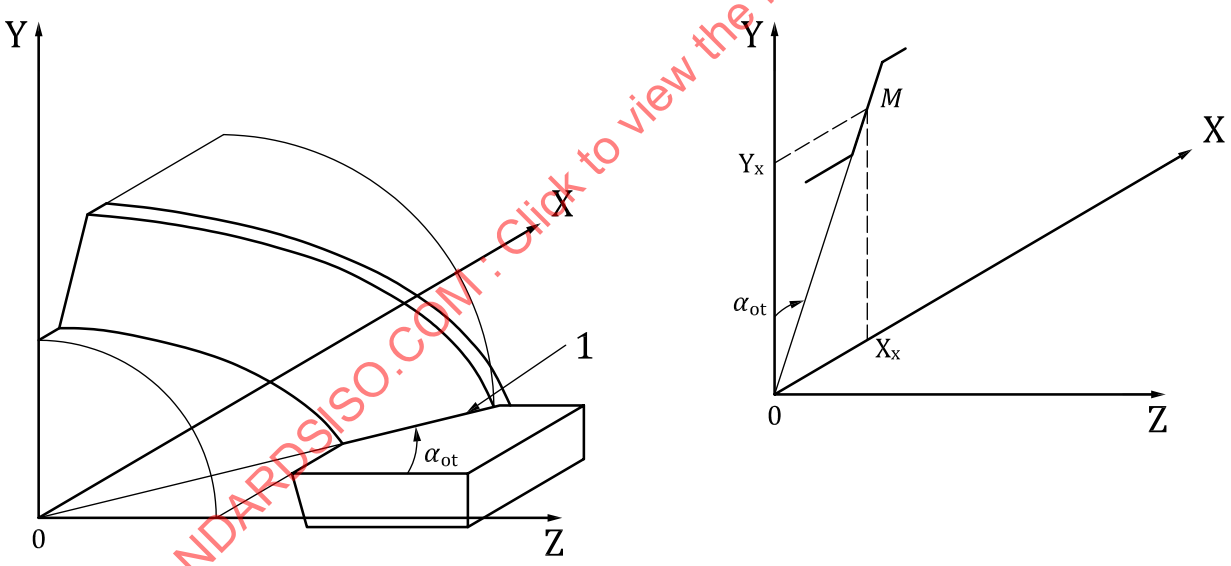

Key
1 generatrix

Figure A.1 — Generation of A profile type

For a point (x_x, y_x) at a distance y_x from the worm axis use Formula (A.1) and (A.2):

$$x_x = y_x \cdot \tan(\alpha_{0t}) = y_x \cdot \tan(\alpha_n) / \cos(\gamma_{m1}) \quad \text{(A.1)}$$

and

$$\alpha_x = \alpha_{0t} \quad \text{(A.2)}$$

A.3 Formulae of the profile in the X-Y plane for worms with I profile type

See Figures 13 to 15 and A.2 for the setting for worms with I profile type, where:

p_{z1} is the lead;

r_{b1} is the base radius of involute profile [see Formula (22)];

γ_{b1} is the base lead angle of worm thread [see Formula (21)].

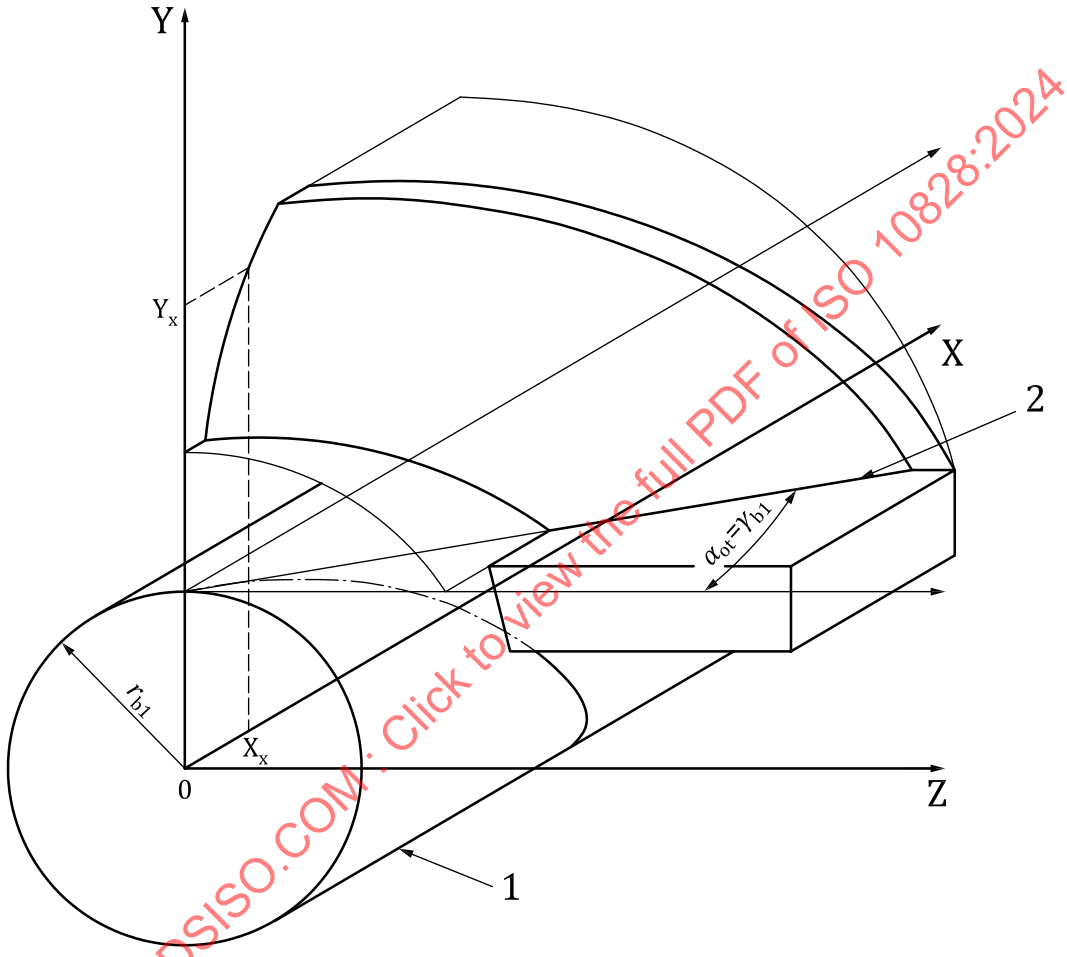

Key

1 base cylinder

2 generatrix

Figure A.2 — Generation of I profile type

For a point (x_x, y_x) at a distance y_x from the worm axis, use Formulae (A.3) and (A.4):

$$x_x = P_{z1} \arctan\frac{\sqrt{y_x^2 - r_{b1}^2}}{r_{b1}} + \sqrt{y_x^2 - r_{b1}^2}.\tan(\gamma_{b1}) \tag{A.3}$$

$$\tan(\alpha_x) = \frac{\sqrt{y_x^2 - r_{b1}^2}}{r_{b1}}.\frac{p_{zu1}}{y_x} \tag{A.4}$$

A.4 Formulae of the profiles in the X-Y plane for worms with N profile type

See Figures 16 and 17 and A.3 to A.5 for the setting for worms with N profile type, where:

p_{x1} is the axial pitch;

p_{z1} is the lead (of worm);

r'_{b1} is the base radius of a notional base circle;

γ'_{b1} is the base lead angle of the notional base helix;

A is the distance from the worm axis to virtual point of the cutter (OO_1 on Figure A.4) (see Reference [4]);

γ_{m1} is the reference lead angle of worm;

α_{0n} is the normal pressure angle;

d_{m1} is the worm reference diameter.

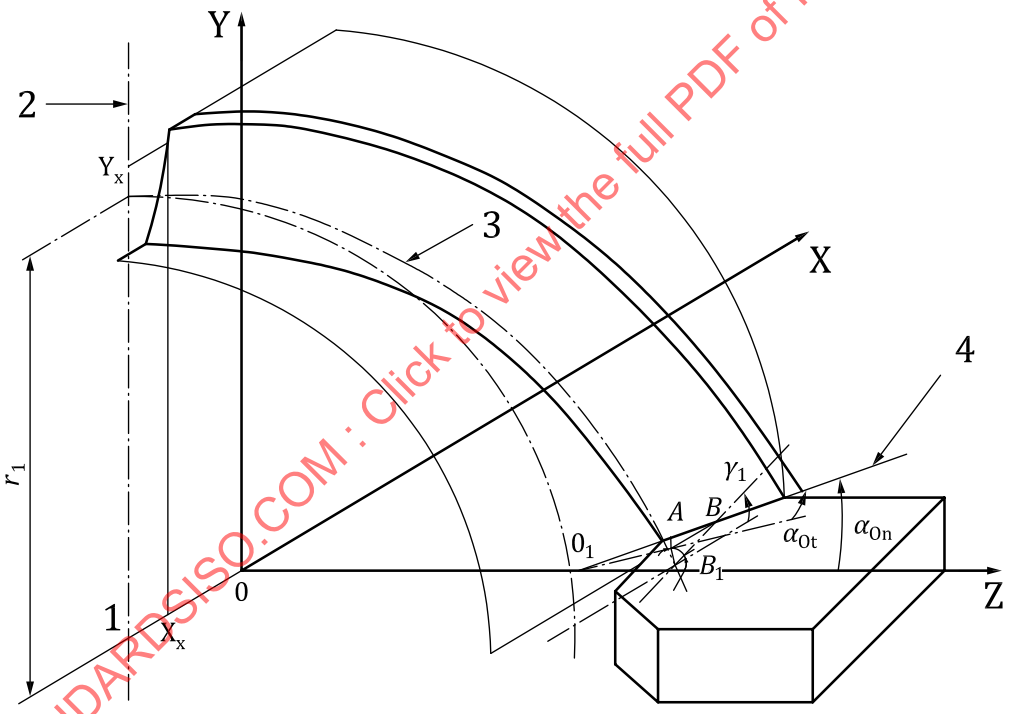

Key

1 axis of worm
2 axis of symmetry of the tooth space
3 reference helix
4 generatrix

Figure A.3 — Generation of N profile type

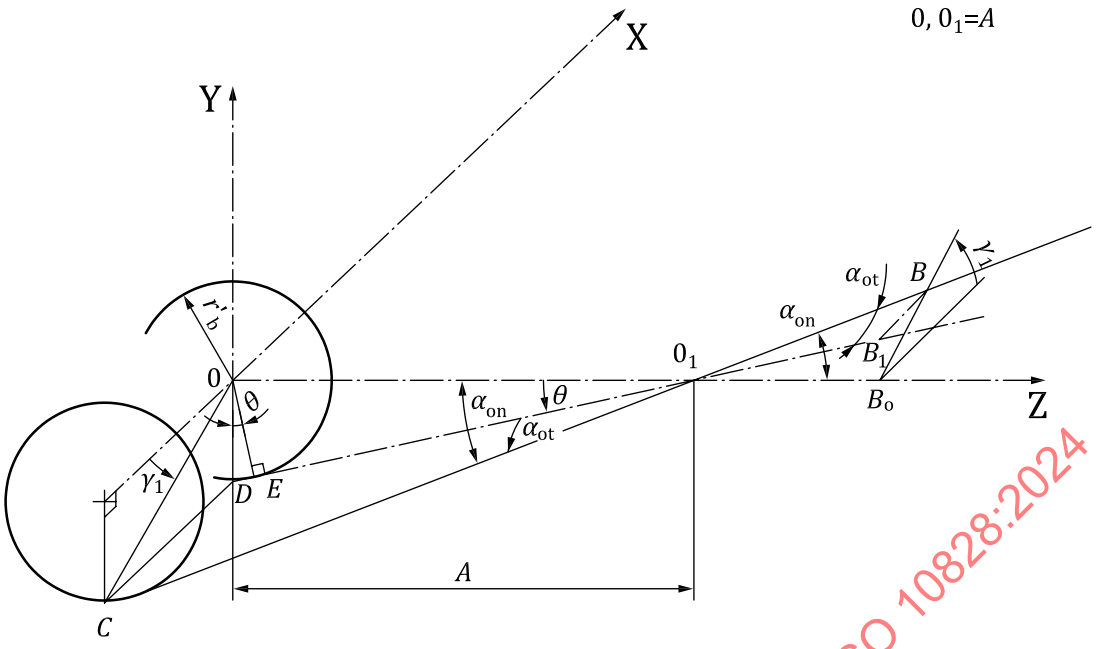

Figure A.4 — N Profile type: Convention for formulae

For a point (x_x, y_x) at radial distance y_x from the worm axis is given by Formulae (A.5) and (A.6):

$$x_x = p_{zu1} \cdot \left\{ \arctan\left(\frac{\sqrt{y_x^2 - r'^2_{b1}}}{r'_{b1}} \right) - \theta \right\} + \sqrt{y_x^2 - r'^2_{b1}} \cdot \tan(\gamma'_{b1}) \quad \text{(A.5)}$$

$$\tan(\alpha_x) = \frac{p_{z1} \cdot r'_{b1} + 2 \cdot \pi \cdot y_x \cdot \tan(\gamma'_{b1})}{2 \cdot \pi \cdot y_x \sqrt{y_x^2 - r_{x1}^2}} \quad \text{(A.6)}$$

NOTE r'_{b1} is a pseudo base radius. The profile in the plane tangent to the cylinder of radius r'_{b1} is a straight line.

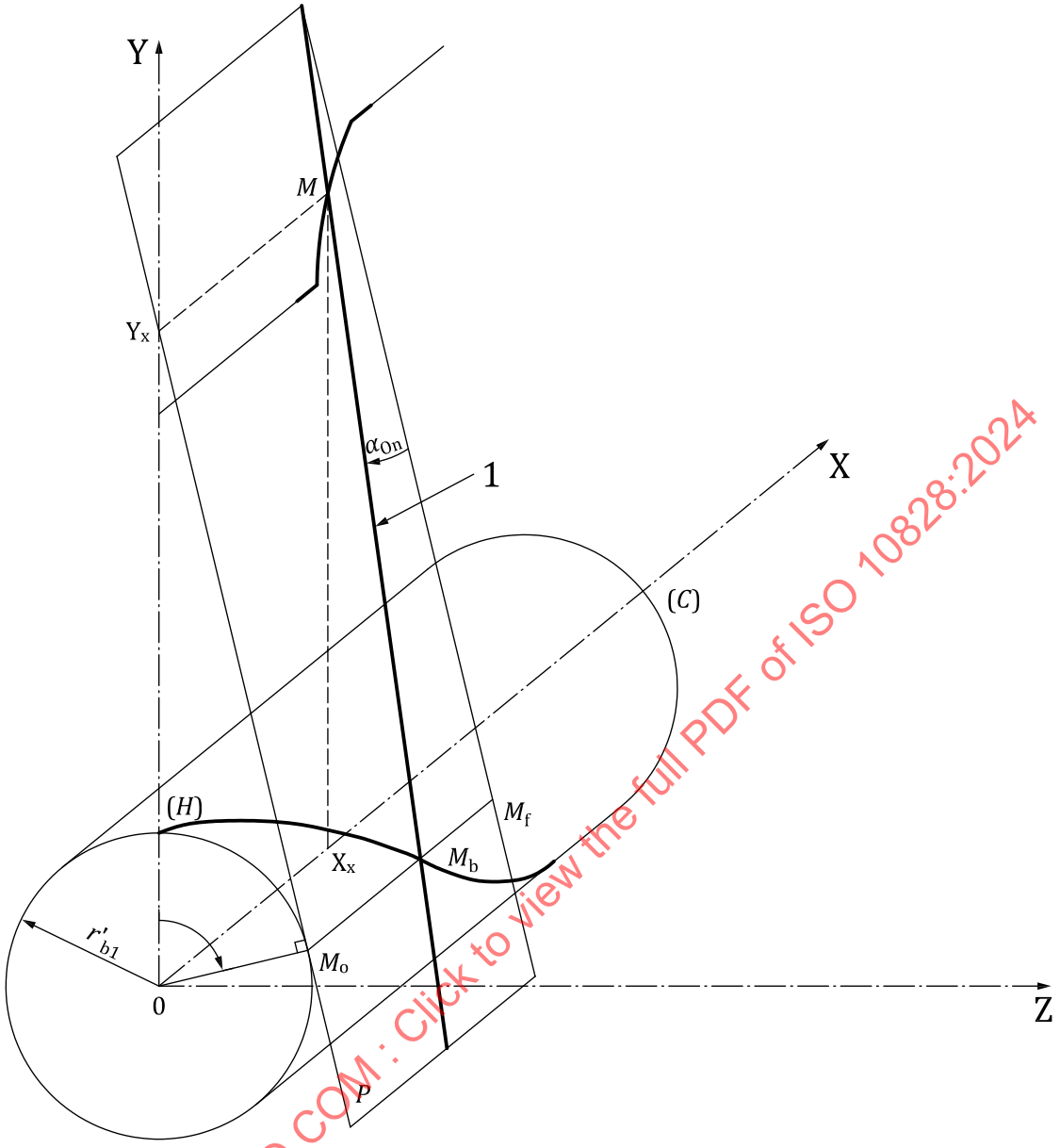

Key

1 generatrix

Figure A.5 — N profile type: Generatrix with pseudo base radius

with Formula (A.7):

$$\theta = \arctan\left(\frac{\sqrt{A - r'^{2}_{b1}}}{r'_{b1}}\right) \tag{A.7}$$

where, as in Formulae (A.8) to (A.10):

$$\gamma'_{b} = \arctan\left(\frac{r'_{b1}}{A \cdot \tan(\gamma_{m1})}\right) \tag{A.8}$$

$$r'_{b1} = \frac{A \cdot \sin(\gamma_{m1}) \cdot \tan(\alpha_{0n})}{\sqrt{1 - (\sin(\gamma_{m1}) \cdot \tan(\alpha_{0n}))^{2}}} \tag{A.9}$$

$$A = r_{ml} - \frac{s_{mx1} \cdot \cos(\gamma_{m1})}{2 \cdot \tan(\alpha_{0n})} \tag{A.10}$$

A.5 Second derivative of axial profile formula

From Formula (49), Formulae (A.11) and (A.12) are given:

$$d2x_x(y_p) = \left[-a_1 \cdot a_2 \cdot \left[2 - \left(\frac{a_2}{y_p} \right)^2 \right] - a_3 \cdot {a_2}^2 \right] \cdot \frac{1}{\left({y_p}^2 - {a_2}^2 \right)^{\frac{3}{2}}} \tag{A.11}$$

$$d2y_x(y_p) = 0 \tag{A.12}$$

Annex B
(informative)

Parameters and derivatives of formulae for K and C profile types

B.1 Formulae for worms with K profile type

Where

a_0	is the cutter spindle/worm centre distance;
γ_{m1}	is the reference lead angle of worm;
p_{z1}	is the lead;
$(y_G, x_G(y_G))$	are the coordinates of a point on the tool flank when the origin is at the point of intersection of the tool axis and the tool median plane, with the x-axis as the tool spindle axis and the abscissa on the trace of the median plane;
d_{m1}	worm reference diameter;
p_{x1}	axial pitch;
α_{0n}	normal pressure angle of the tool.

The profile of a bi-conical grinding wheel is shown in Figure B.1, is given by Formulae (B.1) to (B.5).

Like I profile type, K profile type is convex in axial planes.

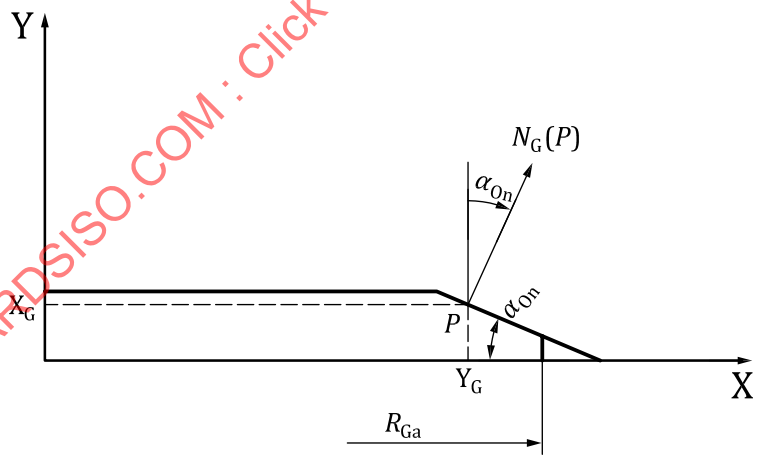

Figure B.1 — K profile type - Grinding wheel profile

One of the advantages of this profile type is that the two flanks of a thread space can be machined simultaneously.

A disadvantage is that the form of the thread flanks varies with the tool diameter, so the reproducibility is approximated.

NOTE 1 The smaller the diameter of the tool, the more nearly the normal profiles of the thread spaces approach those of worms with N profile type, and the larger the tool diameter, the more nearly the forms of the thread flanks approach those of worms with I profile type.

NOTE 2 It is possible to machine worms with K profile type with conical milling cutter. The flank surfaces have facets resulting of the cutting discontinuity caused by cutting tooth pitch.

$$x_w(y_G) = x_{ms} - \tan(\alpha_{0n}) \cdot (y_G - R_{Ga}) \quad \text{(B.1)}$$

$$\alpha_G(y_G) = \alpha_{0n} \quad \text{(B.2)}$$

where

y_G is the radius of grinding wheel which generates the point on the worm as shown in Formulae (B.3) to (B.5):

$$a_0 = R_{Ga} + \frac{d_{f1}}{2} \quad \text{(B.3)}$$

$$R_w = a_0 - \frac{d_{m1}}{2} \quad \text{(B.4)}$$

$$x_{ms} = \frac{(\pi \cdot m_{x1} - s_{x1}) \cdot \cos(\gamma_{m1})}{2} \quad \text{(B.5)}$$

B.2 Formulae for worms with C profile type

With the basic data of the tool indicated in Figure B.2, the parameters y_G, x_G and α_G can be derived for any point *G* of the tool profile.

On the basis of these three parameters and with the Formulae (B.6) to (B.11) giving the profile of the grinding wheel, the coordinates *x*, *r*, of an axial profile and the angle α of the tangent can be determined for any point P of the profile of a worm.

Where:

a_0 is the worm/tool centre distance (length of the common perpendicular to the worm/tool axes);

p_{z1} is the lead (of worm);

γ_{m1} is the lead angle of worm;

R_{Gm}, x_{Gm}, α_{0n} see Figure B.2;

$$\alpha_G(y_G) = \arcsin\left(\sin(\alpha_{0n}) - \frac{R_{Gm} - y_G}{\rho_{Gm}}\right) \quad \text{(B.6)}$$

$$x_G(y_G) = x_{Gm} + \rho_{Gm} \cdot (\cos(\alpha_G(y_G)) - \cos(\alpha_{0n})) \quad \text{(B.7)}$$

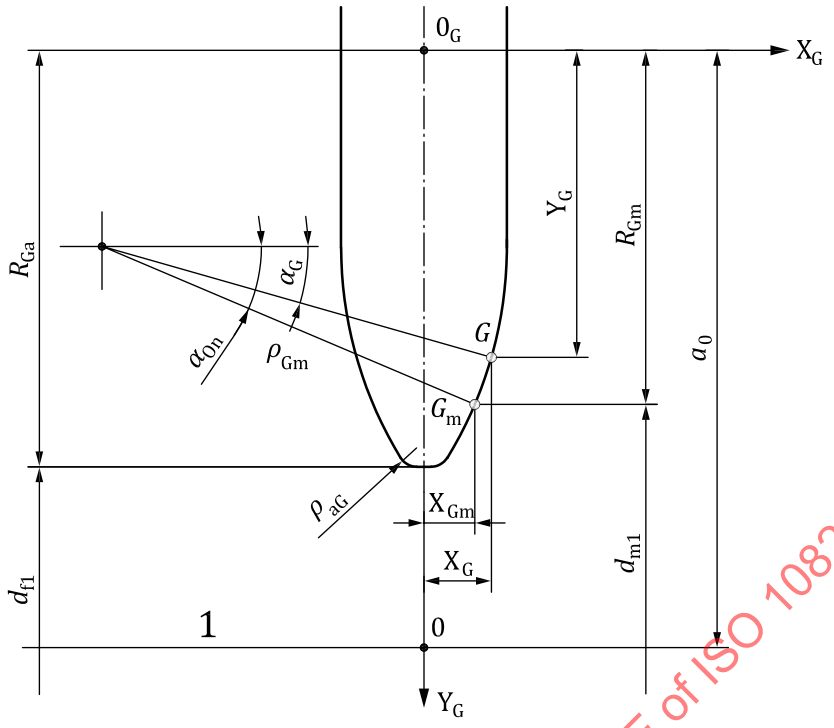

Key

1 axis of the grinding wheel

Figure B.2 — C profile type - Axial section of the tool

$$y_G(y_G) = y_G \tag{B.8}$$

with

$$x_{Gm} = \frac{(\pi \cdot m_{x1} - s_{mx1}) \cdot \cos(\gamma_{m1})}{2} \tag{B.9}$$

$$a_0 = R_{Ga} + \frac{d_{f1}}{2} \tag{B.10}$$

$$R_{Gm} = a_0 - \frac{d_{m1}}{2} \tag{B.11}$$

B.3 Derivatives for K profile type

B.3.1 First derivative of K profile type

First derivatives of K profile type are given by Formulae (B.12) and (B.13):

$$d\alpha_G(y_G) = 0 \tag{B.12}$$

$$dx_G(y_G) = -\tan(\alpha_{0n}) \tag{B.13}$$

B.3.2 Second derivative of K profile type

Second derivatives of K profile type are given by Formulae (B.14) and (B.15):

$$d2\alpha_G(y_G)=0 \tag{B.14}$$

$$d2x_G(y_G)=0 \tag{B.15}$$

B.3.3 Third derivative of K profile type

Third derivatives of K profile type are given by Formulae (B.16) and (B.17):

$$d3\alpha_G(y_G)=0 \tag{B.16}$$

$$d3x_G(y_G)=0 \tag{B.17}$$

B.4 Derivatives for C profile type

B.4.1 First derivative of C profile type

First derivatives of C profile type are given by Formulae (B.18) and (B.19):

$$d\alpha_G(y_G) = \frac{1}{\rho_{Gm} \cdot \left[1 - \left(\sin(\alpha_{0n}) - \frac{R_{Gm} - y_G}{\rho_{Gm}}\right)^2\right]^{\frac{1}{2}}} \tag{B.18}$$

$$dx_G(y_G) = -\rho_{Gm} \cdot \sin(\alpha_G(y_G)) \cdot d\alpha_G(y_G) \tag{B.19}$$

B.4.2 Second derivative of C profile type

Second derivatives of C profile type are given by Formulae (B.20) and (B.21):

$$d2\alpha_G(y_G) = \frac{1}{{\rho_{Gm}}^2 \cdot \left[1 - \left(\sin(\alpha_{0n}) - \frac{R_{Gm} - y_G}{\rho_{Gm}}\right)^2\right]^{\frac{3}{2}}} \cdot \left(\sin(\alpha_{0n}) - \frac{R_{Gm} - y_G}{\rho_{Gm}}\right) \tag{B.20}$$

$$d2x_G(y_G) = -\rho_{Gm} \cdot \left[\cos(\alpha_G(y_G)) \cdot d\alpha_G(y_G)^2 + \sin(\alpha_G(y_G)) \cdot d2\alpha_G(y_G)\right] \tag{B.21}$$

B.4.3 Third derivative of C profile type

Third derivatives of C profile type are given by Formulae (B.22) and (B.23):

$$\begin{aligned} d3\alpha_G(y_G) = {} & \frac{3}{{\rho_{Gm}}^3 \cdot \left[1 - \left(\sin(\alpha_{0n}) - \frac{R_{Gm} - y_G}{\rho_{Gm}}\right)^2\right]^{\frac{5}{2}}} \cdot \left(\sin(\alpha_{0n}) - \frac{R_{Gm} - y_G}{\rho_{Gm}}\right)^2 \\ & + \frac{1}{{\rho_{Gm}}^3 \cdot \left[1 - \left(\sin(\alpha_{0n}) - \frac{R_{Gm} - y_G}{\rho_{Gm}}\right)^2\right]^{\frac{3}{2}}} \end{aligned} \tag{B.22}$$

$$\begin{aligned} d3x_G(y_G) = {} & \rho_{Gm} \cdot \sin(\alpha_G(y_G)) \cdot d\alpha_G(y_G)^3 \\ & - 3\rho_{Gm} \cdot \cos(\alpha_G(y_G)) \cdot d\alpha_G(y_G) \cdot d2\alpha_G(y_G) \\ & - \rho_{Gm} \cdot \sin(\alpha_G(y_G)) \cdot d3\alpha_G(y_G) \end{aligned} \tag{B.23}$$

B.5 Second derivative for K/C profile types for $c2(y_G)$ and $c3(y_G)$

Second derivatives for K/C profile types for $c2(y_G)$ and $c3(y_G)$ are given by Formulae (B.24) and (B.25):

$$d2c2(y_G) = \left(d2x_G(y_G) - \frac{2 \cdot d2x_G(y_G)}{dx_G(y_G)^2} + \frac{2 \cdot y_G}{dx_G(y_G)^3} \cdot d2x_G(y_G)^2 - \frac{y_G}{dx_G(y_G)^2} \cdot d3x_G(y_G)\right) \cdot \sin(\gamma_{m1}) \tag{B.24}$$

$$\begin{aligned} d2c3(y_G) = {} & 2\left(\frac{a_0 \cdot \sin(\gamma_{m1}) - p_{zu1} \cdot \cos(\gamma_{m1})}{dx_G(y_G)^3} \cdot d2x_G(y_G)^2\right) \\ & - \frac{a_0 \cdot \sin(\gamma_{m1}) - p_{zu1} \cdot \cos(\gamma_{m1})}{dx_G(y_G)^2} \cdot d3x_G(y_G) \end{aligned} \tag{B.25}$$

B.6 Second derivative for K/C profile for $\varepsilon_G(y_G)$

B.6.1 First derivation of the first term of $d\varepsilon_G(y_G)$

First derivation of the first term of $d\varepsilon_G(y_G)$ is given by Formula (B.26).

NOTE For $\varepsilon_w(y_G)$ and $d\varepsilon_w(y_G)$, see 7.7.2.1 and 7.7.2.3.2.

$$dA\varepsilon_G(y_G)=\frac{d2c_3(y_G)}{\left(c_1{}^2+c_2(y_G)^2-c_3(y_G)^2\right)^{\frac{1}{2}}}-\frac{dc_3(y_G)\cdot(c_2(y_G)\cdot dc_2(y_G)-c_3(y_G)\cdot dc_3(y_G))}{\left(c_1{}^2+c_2(y_G)^2-c_3(y_G)^2\right)^{\frac{3}{2}}} \quad (B.26)$$

B.6.2 First derivation of the numerator of the 2nd term of $d\varepsilon_G(y_G)$

First derivation of the numerator of the 2nd term of $d\varepsilon_G(y_G)$ is given by Formulae (B.27) and (B.28):

$$BN\varepsilon_G(y_G)=-c_3(y_G)\cdot c_2(y_G)\cdot dc_2(y_G) \quad (B.27)$$

and

$$dBN\varepsilon_G(y_G)=-dc_3(y_G)\cdot c_2(y_G)\cdot dc_2(y_G)-c_3(y_G)\cdot dc_2(y_G)^2-c_3(y_G)\cdot c_2(y_G)\cdot d2c_2(y_G) \quad (B.28)$$

B.6.3 First derivation of the 3rd term of $d\varepsilon_G(y_G)$

First derivation of the 3rd term of $d\varepsilon_G(y_G)$ is given by Formula (B.29):

$$dC\varepsilon_G(y_G)=\left(-d2c_2(y_G)+\frac{2dc_2(y_G)^2\cdot c_2(y_G)}{c_1{}^2+c_2(y_G)^2}\right)\cdot\frac{c_1}{c_1{}^2+c_2(y_G)^2} \quad (B.29)$$

B.6.4 First derivation of the denominator of the 2nd term of $d\varepsilon_G(y_G)$

First derivation of the denominator of the 2nd term of $d\varepsilon_G(y_G)$ is given by Formulae (B.30) to (B.32):

$$BD\varepsilon_G(y_G)=\left(c_1{}^2+c_2(y_G)^2\right)\cdot\left(c_1{}^2+c_2(y_G)^2-c_3(y_G)^2\right)^{\frac{1}{2}} \quad (B.30)$$

$$dB\varepsilon_G(y_G)=2c_2(y_G)\cdot dc_2(y_G)\cdot\left(c_1{}^2+c_2(y_G)^2-c_3(y_G)^2\right)^{\frac{1}{2}}+\left(c_1{}^2+c_2(y_G)^2\right)\cdot\left(c_1{}^2+c_2(y_G)^2-c_3(y_G)^2\right)^{\frac{-1}{2}}\cdot(c_2(y_G)\cdot dc_2(y_G)-c_3(y_G)\cdot dc_3(y_G)) \quad (B.31)$$

$$dB\varepsilon_G(y_G)=\frac{dBN\varepsilon_G(y_G)\cdot BD\varepsilon_G(y_G)-dBD\varepsilon_G(y_G)\cdot BN\varepsilon_G(y_G)}{BD\varepsilon_G(y_G)^2} \quad (B.32)$$

B.6.5 Second derivative for K/C profile for $\varepsilon_G(y_G)$

Second derivative for K/C profile for $\varepsilon_G(y_G)$ is given by Formula (B.33):

$$d2\varepsilon_G(y_G)=dA\varepsilon_G(y_G)+dB\varepsilon_G(y_G)+dC\varepsilon_G(y_G) \quad (B.33)$$

B.7 Second derivative of point generated by the grinding wheel

Second derivatives of point generated by the grinding wheel are given by Formulae (B.34) to (B.36):

$$\begin{aligned} \mathrm{d}2xc_{\mathrm{uw}}(y_{\mathrm{G}}) = {} & \mathrm{d}2xc_{\mathrm{G}}(y_{\mathrm{G}})\cdot\cos(\gamma_{\mathrm{m1}}) - \\ & (2\cos(\varepsilon_{\mathrm{w}}(y_{\mathrm{G}}))\cdot d\varepsilon_{\mathrm{w}}(y_{\mathrm{G}}) - y_{\mathrm{G}}\cdot\sin(\varepsilon_{\mathrm{w}}(y_{\mathrm{G}}))\cdot\mathrm{d}\varepsilon_{\mathrm{w}}(y_{\mathrm{G}})^2 + \\ & y_{\mathrm{G}}\cdot\cos(\varepsilon_{\mathrm{w}}(y_{\mathrm{G}}))\cdot\mathrm{d}2\varepsilon_{\mathrm{w}}(y_{\mathrm{G}}))\cdot\sin(\gamma_{\mathrm{m1}}) \end{aligned} \tag{B.34}$$

$$\begin{aligned} \mathrm{d}2yc_{\mathrm{uw}}(y_{\mathrm{G}}) = {} & 2\sin(\varepsilon_{\mathrm{w}}(y_{\mathrm{G}}))\cdot\mathrm{d}\varepsilon_{\mathrm{w}}(y_{\mathrm{G}}) + \\ & y_{\mathrm{G}}\cdot\cos(\varepsilon_{\mathrm{w}}(y_{\mathrm{G}}))\cdot\mathrm{d}\varepsilon_{\mathrm{w}}(y_{\mathrm{G}})^2 + y_{\mathrm{G}}\cdot\sin(\varepsilon_{\mathrm{w}}(y_{\mathrm{G}}))\cdot\mathrm{d}2\varepsilon_{\mathrm{w}}(y_{\mathrm{G}})) \end{aligned} \tag{B.35}$$

$$\begin{aligned} \mathrm{d}2zc_{\mathrm{uw}}(y_{\mathrm{G}}) = {} & -\mathrm{d}2x_{\mathrm{G}}(y_{\mathrm{G}})\cdot\sin(\gamma_{\mathrm{m1}}) - \\ & \left(2\cos(\varepsilon_{\mathrm{w}}(y_{\mathrm{G}}))\cdot\mathrm{d}\varepsilon_{\mathrm{w}}(y_{\mathrm{G}}) - y_{\mathrm{G}}\cdot\sin\left(\varepsilon_{\mathbf{w}}(y_{\mathrm{G}})\right)\cdot\mathrm{d}\varepsilon_{\mathrm{w}}(y_{\mathrm{G}})^2 + y_{\mathrm{G}}\cdot\cos(\varepsilon_{\mathrm{w}}(y_{\mathrm{G}}))\cdot\mathrm{d}2\varepsilon_{\mathrm{w}}(y_{\mathrm{G}})\right)\cdot\cos(\gamma_{\mathrm{m1}}) \end{aligned} \tag{B.36}$$

B.8 Second derivative of point generated by the grinding wheel projected in the axial plane of worm

Second derivative of point generated by the grinding wheel projected in the axial plane of worm is given by Formulae (B.37) to (B.40):

$$\begin{aligned} \mathrm{d}2\varphi_{\mathrm{x}}(y_{\mathrm{G}}) = {} & \frac{\mathrm{d}2zc_{\mathrm{uw}}(y_{\mathrm{G}})\cdot yc_{\mathrm{uw}}(y_{\mathrm{G}}) - zc_{\mathrm{uw}}(y_{\mathrm{G}})\cdot\mathrm{d}2yc_{\mathrm{uw}}(y_{\mathrm{G}})}{yc_{\mathrm{uw}}(y_{\mathrm{G}})^2 + zc_{\mathrm{uw}}(y_{\mathrm{G}})^2} - \\ & 2(\mathrm{d}zc_{\mathrm{uw}}(y_{\mathrm{G}})\cdot yc_{\mathrm{uw}}(y_{\mathrm{G}}) - zc_{\mathrm{uw}}(y_{\mathrm{G}})\cdot\mathrm{d}yc_{\mathrm{uw}}(y_{\mathrm{G}}))\cdot\frac{yc_{\mathrm{uw}}(y_{\mathrm{G}})\cdot\mathrm{d}yc_{\mathrm{uw}}yc_{\mathrm{uw}}(y_{\mathrm{G}}) + zc_{\mathrm{uw}}yc_{\mathrm{uw}}(y_{\mathrm{G}})\cdot\mathrm{d}zc_{\mathrm{uw}}}{\left(yc_{\mathrm{uw}}(y_{\mathrm{G}})^2 + zc_{\mathrm{uw}}(y_{\mathrm{G}})^2\right)^2} \end{aligned} \tag{B.37}$$

$$\mathrm{d}2x_{\mathrm{x}}(y_{\mathrm{G}}) = \mathrm{d}2xc_{\mathrm{uw}}(y_{\mathrm{G}}) - p_{\mathrm{zu1}}\cdot\mathrm{d}2\varphi_{\mathrm{x}}(y_{\mathrm{G}}) \tag{B.38}$$

$$\begin{aligned} d2y_x(y_{\mathrm{G}}) = {} & \frac{d2yc_{uw}(y_{\mathrm{G}})}{\cos(\varphi_x(y_{\mathrm{G}}))} + \frac{2d2yc_{uw}(y_{\mathrm{G}})}{\cos(\varphi_x(y_{\mathrm{G}}))^2}\cdot\sin(\varphi_x(y_{\mathrm{G}}))\cdot d\varphi_x(y_{\mathrm{G}}) + \\ & \left(\frac{2\cdot\sin(\varphi_x(y_{\mathrm{G}}))^2}{\cos(\varphi_x(y_{\mathrm{G}}))^3} + \frac{1}{\cos(\varphi_x(y_{\mathrm{G}}))}\right)\cdot yc_{uw}(y_{\mathrm{G}})\cdot d\varphi_x(y_{\mathrm{G}})^2 + \\ & \frac{yc_{uw}(y_{\mathrm{G}})}{\cos(\varphi_x(y_{\mathrm{G}}))^2}\cdot\sin(\varphi_x(y_{\mathrm{G}}))\cdot d2\varphi_x(y_{\mathrm{G}}) \end{aligned} \tag{B.39}$$

$$d\tan\alpha_c(y_{\mathrm{G}}) = \frac{d2x_x(y_{\mathrm{G}})}{dy_x(y_{\mathrm{G}})} - \frac{dx_x(y_{\mathrm{G}})\cdot d2y_x(y_{\mathrm{G}})}{dy_x(y_{\mathrm{G}})^2} \tag{B.40}$$

B.9 Tangent vector to a helicoidal motion

Considering a point M in an helicoidal motion, the point located on cylinder of radius *r,* is defined in a reference frame (0, X, Y, Z), OX on the axis of rotation, by Formulae (B.41) and (B.42):

$$\overrightarrow{OM} = \begin{pmatrix} x \\ y \\ z \end{pmatrix} = \begin{pmatrix} z_O + \frac{p_{z1}}{2\pi}\omega \cdot t \\ r \cdot \cos(\omega \cdot t) \\ r \cdot \sin(\omega \cdot t) \end{pmatrix} \tag{B.41}$$

with

p_{z1} lead of the helicoidal motion

ω rotational speed in rad/s

z_O origin of point O

t time parameter

The speed vector at point M is obtained by the derivative $\frac{d}{dt}\overrightarrow{OM}$:

$$\frac{d}{dt}\overrightarrow{OM} = \omega \cdot \begin{pmatrix} \frac{p_{z1}}{2\pi} \\ -r \cdot \sin(\omega \cdot t) \\ r \cdot \cos(\omega \cdot t) \end{pmatrix} = \omega \cdot \begin{pmatrix} \frac{p_{z1}}{2\pi} \\ -z \\ y \end{pmatrix} \tag{B.42}$$

Therefore, the speed vector to helicoidal motion at point M is colinear to the tangent vector: $\begin{pmatrix} \frac{p_{z1}}{2\pi} \\ -z \\ y \end{pmatrix}$

B.10 Development of formulae for the point generated on the worm

The following conventions are used: the profile of the grinding wheel is defined in the right-handed frame $R_G(O_G, X_G, Y_G, Z_G)$ with:

— 0_G, origin crossing the axis of rotation and the mid plane of the grinding wheel;

— X_G, corresponding to axis of rotation of the grinding wheel;

— Y_G, in radial direction;

— Z_G, complete the frame (see Figure B.3).

The outside radius of the grinding wheel is R_{Ga}. The grinding wheel can have eventually a cylindrical external surface on a length of $2E_{aPG}$.

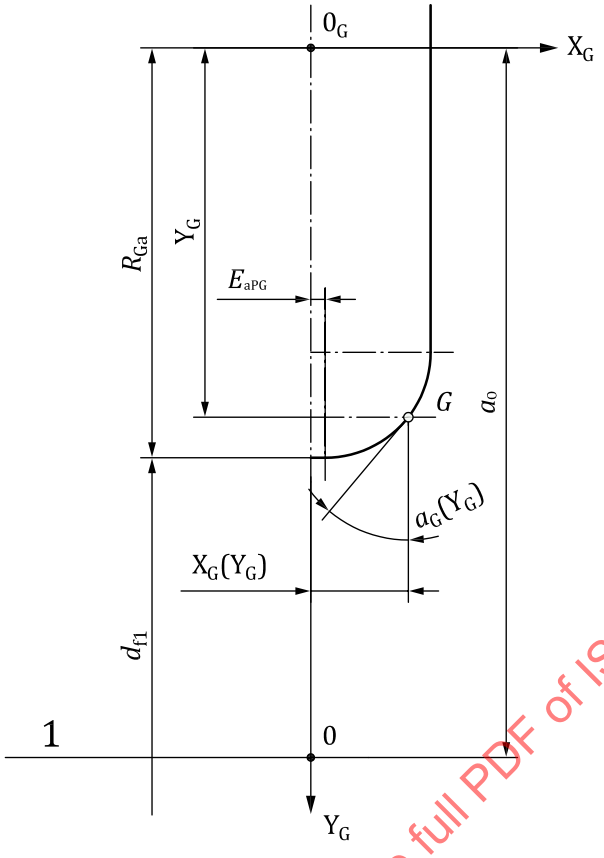

Figure B.3 — Generic grinding wheel

The main parameter is the radius y_G. A point G of the profile of the grinding wheel is defined in frame $R_G(O_G, X_G, Y_G, Z_G)$ by Formulae (B.43) to (B.61):

$$\overrightarrow{O_G G} = \begin{pmatrix} x_G(y_G) \\ y_G \\ 0 \end{pmatrix} \tag{B.43}$$

The pressure angle at point G is obtained by the derivate of $x_G(y_G)$:

$$\tan(\alpha_G(y_G)) = \frac{d}{dy_G}(x_G(y_G)) \tag{B.44}$$

And

$$\alpha_G(y_G) = \tan^{-1}\left(\frac{d}{dy_G}(x_G(y_G))\right) \tag{B.45}$$

The normal vector to grinding wheel profile is:

$$\overrightarrow{N_G} = \begin{pmatrix} \cos(\alpha_G(y_G)) \\ \sin(\alpha_G(y_G)) \\ 0 \end{pmatrix} \tag{B.46}$$

The common centre distance normal to the worm axis and the grinding wheel axis is $\overrightarrow{OO_G} = a_0$

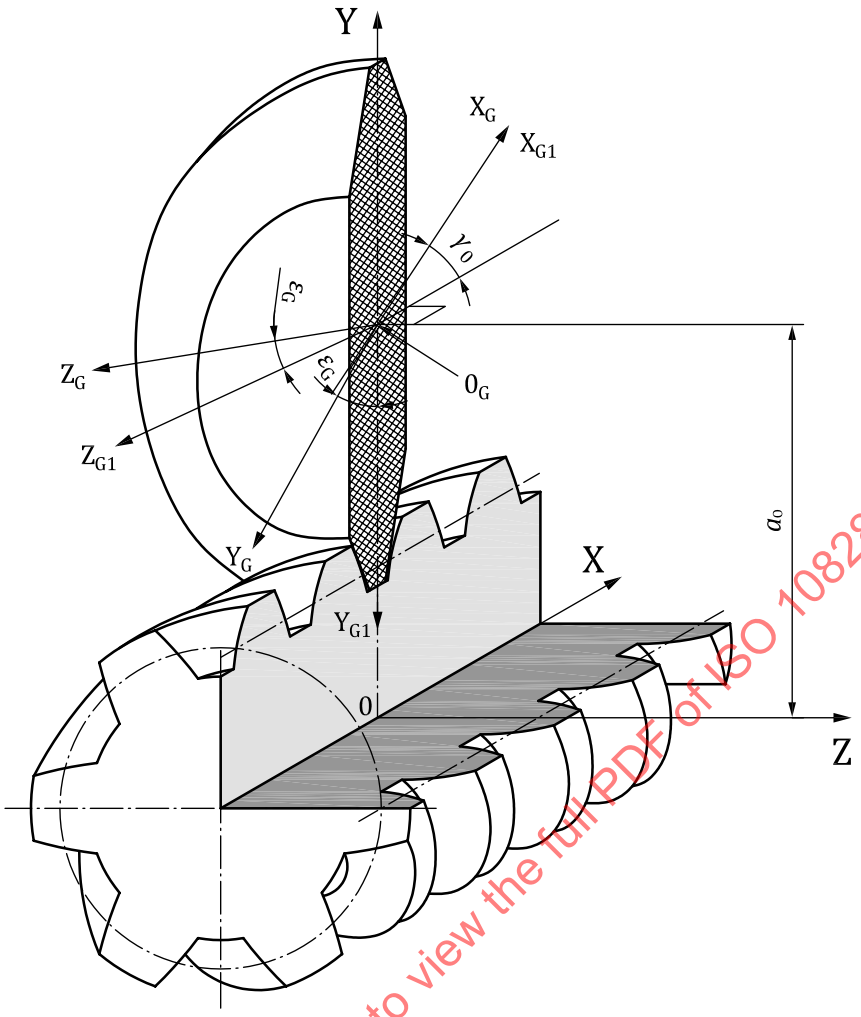

Figure B.4 — Definition of considered frames

The right-handed frame reference to the worm is R(0, X, Y, Z) is defined by:

— 0 on the axis of the worm crossing the axis of symmetry of the considered space-width;

— OX, axis of rotation of the worm;

— OY, radial axis crossing the centre of the grinding wheel O_G;

— OZ, complete the frame (see Figure B.4).

The axis of rotation of the grinding wheel is inclined according to the axis of the worm by an angle γ_0 A fixed frame $R_{G1}(O_G, X_{G1}, Y_{G1}, Z_{G1})$ linked to the reference frame is defined axis Y_{G1} on axis OY. The grinding wheel is rotating around axis X_G. The frame $R_G(O_G, X_G, Y_G, Z_G)$ is linked to this rotation, relative to axis OY_G and the angle of rotation is $\varepsilon_G(y_G)$ function of the radius y_G.

The coordinates point *G* of the grinding wheel in the frame $R_{G1}(O_G, X_{G1}, Y_{G1}, Z_{G1})$ are:

$$\overrightarrow{O_G G}_{R_G} = \begin{pmatrix} 1 & 0 & 0 \\ 0 & \cos\varepsilon_G(y_G) & -\sin\varepsilon_G(y_G) \\ 0 & \sin\varepsilon_G(y_G) & \cos\varepsilon_G(y_G) \end{pmatrix} \begin{pmatrix} x_G(y_G) \\ y_G \\ 0 \end{pmatrix} = \begin{pmatrix} x_G(y_G) \\ y_G \cdot \cos\varepsilon_G(y_G) \\ y_G \cdot \sin\varepsilon_G(y_G) \end{pmatrix} \quad \text{(B.47)}$$

This point *G* in the reference frame *R* is:

$$\overrightarrow{OG}_R = \overrightarrow{OO_G}_R + \overrightarrow{O_G O}_R$$

$$\overrightarrow{OG}_R = \begin{pmatrix} x \\ y \\ z \end{pmatrix} = \begin{pmatrix} 0 \\ a_0 \\ 0 \end{pmatrix} + \begin{pmatrix} \cos\gamma_0 & 0 & -\sin\gamma_0 \\ 0 & -1 & 0 \\ -\sin\gamma_0 & 0 & -\cos\gamma_0 \end{pmatrix} \begin{pmatrix} x_G(y_G) \\ y_G \cdot \cos\varepsilon_G(y_G) \\ y_G \cdot \sin\varepsilon_G(y_G) \end{pmatrix} = \begin{pmatrix} x_G(y_G)\cdot\cos\gamma_0 - y_G \cdot \sin\varepsilon_G(y_G)\cdot\sin\gamma_0 \\ a_0 - y_G \cdot \cos\varepsilon_G(y_G) \\ -x_G(y_G)\cdot\sin\gamma_0 - y_G \cdot \sin\varepsilon_G(y_G)\cdot\cos\gamma_0 \end{pmatrix} \quad \text{(B.48)}$$

For a point of the flank of the worm, the speed vector to the helicoidal motion at the coincident point in contact with the grinding wheel is:

$$\vec{V}_R = \begin{pmatrix} \frac{p_{z1}}{2\pi} \\ -z \\ y \end{pmatrix} = \begin{pmatrix} \frac{p_{z1}}{2\pi} \\ x_G(y_G)\cdot\sin\gamma_0 + y_G \cdot \sin\varepsilon_G(y_G)\cdot\cos\gamma_0 \\ a_0 - y_G \cdot \cos\varepsilon_G(y_G) \end{pmatrix} \quad \text{(B.49)}$$

The normal vector to grinding wheel profile is:

$$\overrightarrow{N_G}_R = \begin{pmatrix} \cos\gamma_0 & 0 & -\sin\gamma_0 \\ 0 & -1 & 0 \\ -\sin\gamma_0 & 0 & -\cos\gamma_0 \end{pmatrix} \begin{pmatrix} 1 & 0 & 0 \\ 0 & \cos\varepsilon_G(y_G) & -\sin\varepsilon_G(y_G) \\ 0 & \sin\varepsilon_G(y_G) & \cos\varepsilon_G(y_G) \end{pmatrix} \begin{pmatrix} \cos(\alpha_G(y_G)) \\ \sin(\alpha_G(y_G)) \\ 0 \end{pmatrix} \quad \text{(B.50)}$$

$$\overrightarrow{N_G}_R = \begin{pmatrix} \cos(\alpha_G(y_G))\cdot\cos\gamma_0 - \sin(\alpha_G(y_G))\cdot\sin\gamma_0\cdot\sin\varepsilon_G(y_G) \\ -\sin(\alpha_G(y_G))\cdot\cos\varepsilon_G(y_G) \\ -\cos(\alpha_G(y_G))\cdot\sin\gamma_0 - \sin(\alpha_G(y_G))\cdot\cos\gamma_0\cdot\sin\varepsilon_G(y_G)_G \end{pmatrix} \quad \text{(B.51)}$$

In each point of worm profile generated by the point G of the grinding wheel, the speed vector of the worm shall be perpendicular to the coincident normal vector of the grinding wheel. So, the dot product $\vec{V}_R \bullet \overrightarrow{N_G}_R = 0$ shall be zero.

From Formula (4), the unit lead is $p_{zu1} = \frac{p_{z1}}{2\grave{A}}$, and it results in:

$$\begin{aligned} & p_{zu1}\cdot[\cos(\alpha_G(y_G))\cdot\cos\gamma_0 - \sin(\alpha_G(y_G))\cdot\sin\gamma_0\cdot\sin\varepsilon_G(y_G)] \\ & -[x_G(y_G)\cdot\sin\gamma_0 + y_G\cdot\sin\varepsilon_G(y_G)\cdot\cos\gamma_0]\cdot\sin(\alpha_G(y_G))\cdot\cos\varepsilon_G(y_G) \\ & -(a_0 - y_G\cdot\cos\varepsilon_G(y_G))\cdot[\cos(\alpha_G(y_G))\cdot\sin\gamma_0 + \sin(\alpha_G(y_G))\cdot\cos\gamma_0\cdot\sin\varepsilon_G(y_G)] = 0 \end{aligned} \quad \text{(B.52)}$$

Isolating terms with $\varepsilon_G(y_G)$:

$$\begin{aligned} & [-p_{zu1}\cdot\sin\gamma_0 - a_0\cdot\cos\gamma_0]\cdot\sin(\alpha_G(y_G))\cdot\sin\varepsilon_G(y_G) \\ & +[-x_G(y_G)\cdot\sin(\alpha_G(y_G)) + y_G\cdot\cos(\alpha_G(y_G))]\cdot\sin\gamma_0\cdot\cos\varepsilon_G(y_G) \\ & +[p_{zu}\cdot\cos\gamma_0 - a_0\cdot\sin\gamma_0]\cdot\cos(\alpha_G(y_G)) = 0 \end{aligned} \quad \text{(B.53)}$$

After multiplication by $\frac{1}{\sin(\alpha_G(y_G))}$ it becomes:

$$[p_{zu1}\cdot\sin\gamma_0 + a_0\cdot\cos\gamma_0]\cdot\sin\varepsilon_G(y_G) + \left[x_G(y_G) - \frac{y_G}{\tan(\alpha_G(y_G))}\right]\cdot\sin\gamma_0\cdot\cos\varepsilon_G(y_G) - \frac{p_{zu1}\cdot\cos\gamma_0 - a_0\cdot\sin\gamma_0}{\tan(\alpha_G(y_G))} = 0 \quad \text{(B.54)}$$

Which can be written as: $c_1\cdot\sin\varepsilon_G(y_G) + c_2(y_G)\cdot\cos\varepsilon_G(y_G) - c_3(y_G) = 0$ which corresponds to Formula (58).

$$c_1 = p_{zu1} \cdot \sin\gamma_0 + a_0 \cdot \cos\gamma_0$$

With: $c_2(y_G) = \left[x_G(y_G) - \frac{y_G}{\tan(\alpha_G(y_G))} \right] \cdot \sin\gamma_0$, which correspond to Formulae (59) to (61). (B.55)

$$c_3(y_G) = \frac{p_{zu1} \cdot \cos\gamma_0 - a_0 \cdot \sin\gamma_0}{\tan(\alpha_G(y_G))}$$

To solve the equation in $\varepsilon_G(y_G)$ it can be written as:

$$\frac{c_1}{\sqrt{{c_1}^2 + c_2(y_G)^2}} \cdot \sin\varepsilon_G(y_G) + \frac{c_2(y_G)}{\sqrt{{c_1}^2 + c_2(y_G)^2}} \cdot \cos\varepsilon_G(y_G) - \frac{c_3(y_G)}{\sqrt{{c_1}^2 + c_2(y_G)^2}} = 0 \quad \text{(B.56)}$$

And with

$$\tan w(y_G) = \frac{c_1}{c_2(y_G)} \text{ then: } \cos w(y_G) = \frac{c_1}{\sqrt{{c_1}^2 + c_2(y_G)^2}} \sin w(y_G) = \frac{c_2(y_G)}{\sqrt{{c_1}^2 + c_2(y_G)^2}} \quad \text{(B.57)}$$

$$\text{So: } \cos w(y_G) \cdot \sin\varepsilon_G(y_G) + \sin w(y_G) \cdot \cos\varepsilon_G(y_G) = \frac{c_3(y_G)}{\sqrt{{c_1}^2 + c_2(y_G)^2}} \quad \text{(B.58)}$$

$$\text{Equivalent to: } \sin(w(y_G) + \varepsilon_G(y_G)) = \frac{c_3(y_G)}{\sqrt{{c_1}^2 + c_2(y_G)^2}} \quad \text{(B.59)}$$

$$\text{And } \varepsilon_G(y_G) = \sin^{-1} \frac{c_3(y_G)}{\sqrt{{c_1}^2 + c_2(y_G)^2}} - w(y_G) \quad \text{(B.60)}$$

$$\varepsilon_G(y_G) = \sin^{-1} \frac{c_3(y_G)}{\sqrt{{c_1}^2 + c_2(y_G)^2}} - \tan^{-1} \frac{c_1}{c_2(y_G)} \text{, which corresponds to Formula (62).} \quad \text{(B.61)}$$

NOTE For standard worm grinding, the setting helix angle of grinding wheel γ_0 is identical to the reference lead angle of worm γ_{m1}.